University of Strathclyde

Modelling the aerodynamics of wind turbines

Wind Panel Manual

Alexander Duncan Giles

supervised by

Prof. William Leithead & Prof. Mike Graham

October 20, 2017

Contents

List of Figures

Acknowledgements

This piece of work would not have been possible without the help and support of friends and colleagues to whom I am extremely grateful. These are Wang Yue (Susan), Professor Mike Graham, Dr Carlos Simao-Ferreira, Professor William Leithead, Dr James Carroll, Edward Corr, and Andrew Smith.

Summary

Wind Panel is a multi-body free-wake panel method. That is, in its 'purest' form, it is assumed that the flow field (with the exception of vortex cores) is inviscid. Specifically, the boundary layers on the bodies are assumed to be infinitely thin. In addition, the flow field is assumed to be incompressible and irrotational. By this, it follows that the velocity field of the fluid satisfies the following equations:

$$\nabla.\boldsymbol{u} = 0 \tag{1}$$

$$\nabla \times \boldsymbol{u} = 0 \tag{2}$$

where $\boldsymbol{u}$ is the fluid velocity. Given that the curl of the gradient of **any** scalar field is zero, it is possible to express the velocity in terms of a velocity potential, Φ:

$$\nabla \times \nabla\Phi = 0 \rightarrow \boldsymbol{u} = \nabla\Phi \tag{3}$$

Inserting this expression into equation 1 yields Laplace's equation:

$$\nabla^2\Phi = 0 \tag{4}$$

That is, 'pure' panel methods are looking for solutions to Laplace's equation [1].

Laplace's equation is appealing because of its linearity. That is, the scalar field Φ could be expressed as a linear sum of appropriately weighted scalar fields, ϕ_i so long as those scalar fields are themselves solutions to Laplace's equation. That is,

$$\Phi = \sum_i C_i\phi_i \tag{5}$$

with the requirement that

$$\nabla^2\phi_i = 0 \tag{6}$$

C_i is the weighting factor.

This linearity allows a potentially complicated scalar field Φ to be built up from a linear combination of simple scalar fields, ϕ_i. Sources, sinks, doublets and point vortices are examples of point objects which are solutions to Laplace's equation; vortex blobs are strictly reserved to two-dimensional simulations. Irrotational vortex segments are also solutions to Laplace's equation; however, the vortex segment is somewhat different to the previous solutions since it is not a point object. However, they are extremely useful just like the point objects. The general term for these solutions are singularity elements. Full details of each one may be found in part I.

A panel is a line in two dimensions or a surface in three dimensions which contains a continuous distribution of point objects. The net effect of an individual panel at some point of interest is found by integrating the influence of the point objects across the space that the panel occupies on the point of interest. As the net effect of a panel is a linear summation of the effects of the individual point objects that it comprises, it follows that these panels are also solutions to Laplace's equation. Bodies and wakes (to at least some extent) are represented by panels which feature one or a combination of the singularity elements.

The aim of the panel method is to determine the weighting factors associated with each panel, from which the forces acting on the body can ultimately be determined. In addition to the panels on the bodies, newly shed wake panels have unknown strengths which need determining also. The additional unknowns can be expressed in terms of the unknown strengths of the body panels by employing the Kutta condition at all trailing edges. Thus, a system comprising 'j' body panels effectively has 'j' unknowns. In order to determine the strengths, 'j' simultaneous equations are required. The 'j' equations are developed by having 'j' control, or collocation, points where the velocity or velocity potential is to be evaluated. Since flow cannot pass through a solid surface, the control points are chosen as the midpoints of the body panels (one control point for each panel).

[1] A standard solution of Laplace's equation can be based on Green's identity, details of which may be found in Katz & Plotkin

If a velocity formulation of the panel method is adopted (Neumann), at each control point the normal (to the relevant panel surface) component of the net velocity induced by all panels must balance the normal (again to the relevant panel surface) component of the free stream wind velocity. If a velocity potential formulation of the panel method is adopted (Dirichlet), at each control point the net potential due to all the panels must be equal to the internal potential of the body.

The default representation for the bodies is the source-doublet approach using the Dirichlet (velocity potential) boundary condition. The wake is modelled initially as a doublet system before being converted to a vortex lattice. Vortex core models are implemented to minimise occurrences of numerical instability. Full details can be found in part I.

Part I

Theory manual

Chapter 1

Aerodynamic theory of panel methods

In this chapter, the basic assumptions behind panel methods are introduced along with their mathematical implications. Fundamental building blocks of two- and three-dimensional panel methods (called point objects) are introduced. Furthermore, Kelvin's circulation theorem is introduced. Finally, for completeness, a brief revision of vector calculus in different coordinate systems in presented.

1.1 Coordinate system definitions and fundamental vector calculus

In two dimensions, the velocity vector, $\boldsymbol{u}$, adopts the following notation in Cartesian coordinates:

$$\boldsymbol{u} = \begin{bmatrix} u & v \end{bmatrix}^{\mathrm{T}} \tag{1.1}$$

where u and v are the x- and y-components of the fluid velocity respectively. In three dimensions, $\boldsymbol{u}$ adopts the following notation in Cartesian coordinates:

$$\boldsymbol{u} = \begin{bmatrix} u & v & w \end{bmatrix}^{\mathrm{T}} \tag{1.2}$$

where w is the z-component of the fluid velocity.

In some situations, it is preferable to adopt one of the spherical or cylindrical polar coordinate systems. Notation for the spherical polar coordinate system in this text is as follows:

$$\boldsymbol{u} = \begin{bmatrix} u_r & u_\theta & u_\psi \end{bmatrix}^{\mathrm{T}} \tag{1.3}$$

where u_r is the radial component of the fluid velocity, u_θ is the polar component of the fluid velocity, and u_ψ is the azimuth component. That is, the 'physics' convention has been adopted as opposed to 'mathematics' convention.

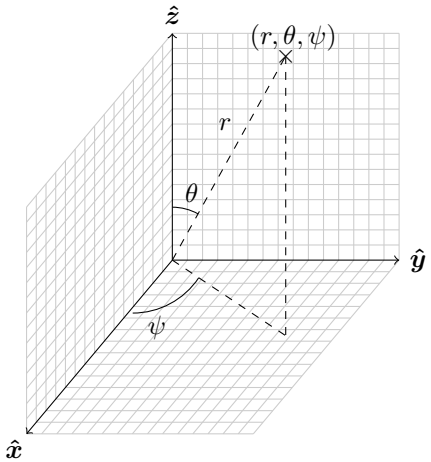

Figure 1.1: Illustration of the spherical polar coordinate system and its relation to the Cartesian coordinate system.

Notation for the cylindrical polar coordinate system in this text is as follows:

$$\boldsymbol{u} = \begin{bmatrix} u_{\mathrm{r}} & u_\theta & u_z \end{bmatrix}^{\mathrm{T}} \tag{1.4}$$

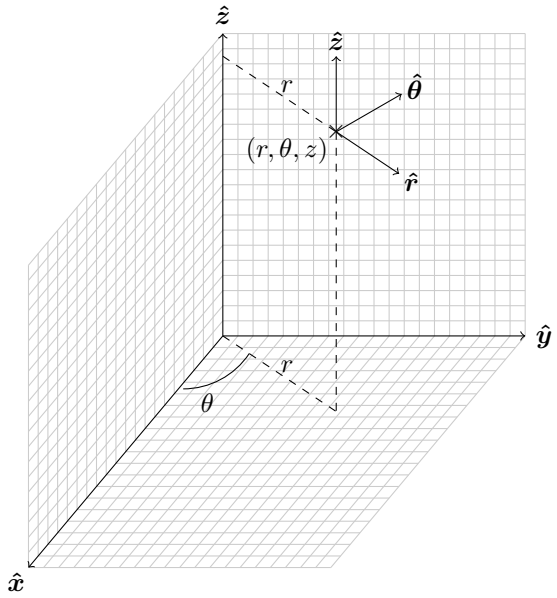

Figure 1.2: Illustration of the cylindrical polar coordinate system and its relation to the Cartesian coordinate system.

1.1.1 The del operator in two dimensions

For two dimensional studies, the Cartesian and 'condensed' cylindrical polar coordinate systems will be used.

The gradient of some scalar field, ϕ, as expressed in the Cartesian coordinate system is as follows:

$$\nabla\phi = \left(\frac{\partial\phi}{\partial x}\right)\hat{\boldsymbol{x}} + \left(\frac{\partial\phi}{\partial y}\right)\hat{\boldsymbol{y}} \tag{1.5}$$

The equivalent operation in the condensed cylindrical polar coordinate system is

$$\nabla\phi = \left(\frac{\partial\phi}{\partial r}\right)\hat{\boldsymbol{r}} + \left(\frac{1}{r}\frac{\partial\phi}{\partial\theta}\right)\hat{\boldsymbol{\theta}} \tag{1.6}$$

The divergence of some vector field, $\boldsymbol{u}$, as expressed in the Cartesian coordinate system is as follows:

$$\nabla.\boldsymbol{u} = \frac{\partial u_{\mathrm{x}}}{\partial x} + \frac{\partial u_{\mathrm{y}}}{\partial y} \tag{1.7}$$

The equivalent operation in the condensed cylindrical polar coordinate system is

$$\nabla.\boldsymbol{u} = \frac{1}{r}\frac{\partial(ru_{\mathrm{r}})}{\partial r} + \frac{1}{r}\frac{\partial u_\theta}{\partial\theta} \tag{1.8}$$

The curl of some vector field, $\boldsymbol{u}$, as expressed in the Cartesian coordinate system is as follows:

$$\nabla\times\boldsymbol{u} = \left(\frac{\partial u_{\mathrm{y}}}{\partial x} - \frac{\partial u_{\mathrm{x}}}{\partial y}\right) \tag{1.9}$$

The equivalent operation in the condensed cylindrical polar coordinate system is

$$\nabla\times\boldsymbol{u} = \frac{1}{r}\left(\frac{\partial(ru_\theta)}{\partial r} - \frac{\partial u_{\mathrm{r}}}{\partial\theta}\right) \tag{1.10}$$

Note, no unit vector is given on the right hand side of the previous two expressions. This is because the curl of a 2D vector is a rank-0 tensor.

Finally, the Laplace operator in the Cartesian coordinate system is

$$\nabla^2\phi = \frac{\partial^2\phi}{\partial x^2} + \frac{\partial^2\phi}{\partial y^2} \tag{1.11}$$

The equivalent operation in the condensed cylindrical polar coordinate system is

$$\nabla^2\phi = \frac{1}{r}\frac{\partial}{\partial r}\left(r\frac{\partial\phi}{\partial r}\right) + \frac{1}{r^2}\frac{\partial^2\phi}{\partial\theta^2} \tag{1.12}$$

1.1.2 The del operator in three dimensions

For three dimensional studies, the Cartesian and spherical polar coordinate systems will be used.

The gradient of some scalar field, ϕ, as expressed in the Cartesian coordinate system is as follows:

$$\nabla\phi = \left(\frac{\partial\phi}{\partial x}\right)\hat{\boldsymbol{x}} + \left(\frac{\partial\phi}{\partial y}\right)\hat{\boldsymbol{y}} + \left(\frac{\partial\phi}{\partial z}\right)\hat{\boldsymbol{z}} \tag{1.13}$$

The equivalent operation in the spherical polar coordinate system is

$$\nabla\phi = \left(\frac{\partial\phi}{\partial r}\right)\hat{\boldsymbol{r}} + \left(\frac{1}{r}\frac{\partial\phi}{\partial\theta}\right)\hat{\boldsymbol{\theta}} + \frac{1}{r\sin\theta}\frac{\partial\phi}{\partial\psi}\hat{\boldsymbol{\psi}} \tag{1.14}$$

The divergence of some vector field, $\boldsymbol{u}$, as expressed in the Cartesian coordinate system is as follows:

$$\nabla.\boldsymbol{u} = \frac{\partial u_{\mathrm{x}}}{\partial x} + \frac{\partial u_{\mathrm{y}}}{\partial y} + \frac{\partial u_{\mathrm{z}}}{\partial z} \tag{1.15}$$

The equivalent operation in the spherical polar coordinate system is

$$\nabla.\boldsymbol{u} = \frac{1}{r^2}\frac{\partial(r^2u_{\mathrm{r}})}{\partial r} + \frac{1}{r\sin\theta}\frac{\partial u_\theta\sin\theta}{\partial\theta} + \frac{1}{r\sin\theta}\frac{\partial u_\psi}{\partial\psi} \tag{1.16}$$

The curl of some vector field, $\boldsymbol{u}$, as expressed in the Cartesian coordinate system is as follows:

$$\nabla\times\boldsymbol{u} = \left(\frac{\partial u_{\mathrm{y}}}{\partial x} - \frac{\partial u_{\mathrm{x}}}{\partial y}\right) \tag{1.17}$$

The equivalent operation in the spherical polar coordinate system is

$$\nabla\times\boldsymbol{u} = \frac{1}{r\sin\theta}\left(\frac{\partial(u_\psi\sin\theta)}{\partial\theta} - \frac{\partial u_\theta}{\partial\psi}\right)\hat{\boldsymbol{r}} + \frac{1}{r}\left(\frac{1}{\sin\theta}\frac{\partial u_{\mathrm{r}}}{\partial\psi} - \frac{\partial(ru_\psi)}{\partial r}\right)\hat{\boldsymbol{\theta}} + \frac{1}{r}\left(\frac{\partial(ru_\theta)}{\partial r} - \frac{\partial u_{\mathrm{r}}}{\partial\theta}\right)\hat{\boldsymbol{\psi}} \tag{1.18}$$

Finally, the Laplace operator in the Cartesian coordinate system is

$$\nabla^2\phi = \frac{\partial^2\phi}{\partial x^2} + \frac{\partial^2\phi}{\partial y^2} + \frac{\partial^2\phi}{\partial z^2} \tag{1.19}$$

The equivalent operation in the condensed cylindrical polar coordinate system is

$$\nabla^2\phi = \frac{1}{r^2}\frac{\partial}{\partial r}\left(r^2\frac{\partial\phi}{\partial r}\right) + \frac{1}{r^2\sin\theta}\frac{\partial}{\partial\theta}\left(\sin\theta\frac{\partial\phi}{\partial\theta}\right) + \frac{1}{r^2\sin^2\theta}\frac{\partial^2\phi}{\partial\psi^2} \tag{1.20}$$

1.2 Potential flow & Laplace's equation

In its 'purest' form, a panel method assumes that the entire flow field is inviscid. That is to say, the boundary layers on the bodies are assumed to be infinitely thin. In addition, viscous effects in the wake and general flow field are assumed to be confined to small regions such as vortex cores. The flow field is also assumed to be incompressible and irrotational. By these statements, it is meant that the velocity field of the fluid satisfies the following equations:

$$\nabla . \boldsymbol{u} = 0 \tag{1.21}$$

$$\nabla \times \boldsymbol{u} = 0 \tag{1.22}$$

Given that the curl of the gradient of **any** scalar field is zero, it is possible to express the velocity in terms of a velocity potential, Φ:

$$\nabla \times \nabla \Phi = 0 \rightarrow \boldsymbol{u} = \nabla \Phi \tag{1.23}$$

Inserting this expression into equation 1.21 yields Laplace's equation:

$$\nabla^2 \Phi = 0 \tag{1.24}$$

That is, 'pure' panel methods are looking for solutions to Laplace's equation.

Laplace's equation is appealing because of its linearity. That is, the scalar field Φ could be expressed as a linear sum of appropriately weighted scalar fields, ϕ_i so long as those scalar fields are themselves solutions to Laplace's equation. That is,

$$\Phi = \sum_i C_i \phi_i \tag{1.25}$$

with the requirement that

$$\nabla^2 \phi_i = 0 \tag{1.26}$$

This linearity allows a potentially complicated scalar field Φ to be built up from a linear combination of simple scalar fields, ϕ_i.

1.3 Fundamental solutions to Laplace's equation

In this section, point objects which satisfy Laplace's equation will be developed.

The point source/sink

Let us consider a solution in two dimensions. Furthermore, let us adopt a polar coordinate system centred on the point object whose potential we are trying to deduce.

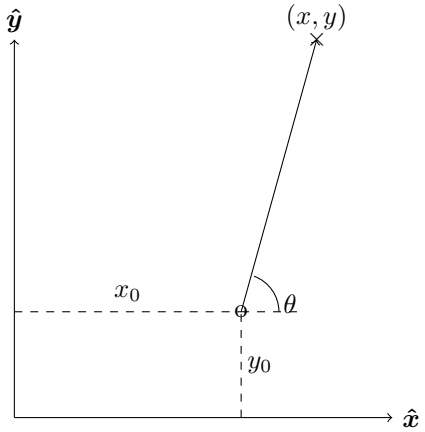

Figure 1.3: Illustration of the polar coordinate system used in this derivation and its relation to the Cartesian coordinate system

The mathematical statement of irrotational flow is one where the curl is zero; that is,

$$\begin{aligned}\nabla \times \boldsymbol{u} &= \frac{1}{r}\left(\frac{\partial(ru_\theta)}{\partial r} - \frac{\partial u_\mathrm{r}}{\partial \theta}\right)\hat{\boldsymbol{z}} \\ &= 0\end{aligned} \tag{1.27}$$

Let us assume that one of our fundamental solutions in only has a radial velocity component; that is,

$$u_\theta = 0 \tag{1.28}$$

Hence,

$$\frac{\partial u_\mathrm{r}}{\partial \theta} = 0 \tag{1.29}$$

That is to say, u_r is not a function of θ i.e. $u_\mathrm{r} = u_\mathrm{r}(r)$.

The mathematical statement of incompressible flow is one where the divergence is zero; that is, by equation 1.8

$$\frac{1}{r}\frac{\partial(ru_\mathrm{r})}{\partial r} = 0 \tag{1.30}$$

Here only the first term in $\nabla.\boldsymbol{u}$ has been considered since $u_\theta = 0$.

In order for equation 1.30 to be satisfied, it follows that $u_\mathrm{r} \propto 1/r$; that is,

$$u_\mathrm{r} = \frac{k}{r} \tag{1.31}$$

where k is some constant of proportionality.

The velocity potential may be deduced by considering its relation to velocity; that is,

$$\nabla\phi = \left(\frac{\partial\phi}{\partial r}\right)\hat{\boldsymbol{r}} + \left(\frac{1}{r}\frac{\partial\Phi}{\partial\theta}\right)\hat{\boldsymbol{\theta}} \tag{1.32}$$

Considering equations 1.28 and 1.31,

$$\frac{\partial\phi}{\partial r} = \frac{k}{r} \tag{1.33}$$

$$\frac{\partial\phi}{\partial\theta} = 0 \tag{1.34}$$

The second expression tells us that ϕ is not a function of θ. Consequently, the velocity potential may be obtained by simply integrating equation 1.34 with respect to r.

$$\phi = k\log r \tag{1.35}$$

The constant of integration has been neglected for simplicity.

Let the constant be proportional to the 'strength' of the singularity element. Defining the strength of this solution to be σ, it follows that $k \propto \sigma$.

In order for the flux to be σ, it follows that $k \propto 1/(2\pi)$. This can be observed by taking the generic expression for flux in two dimensions:

$$\begin{aligned}\text{Flux} &= \int \boldsymbol{u}.\mathrm{d}\boldsymbol{A} \\ &= \int \boldsymbol{u}.(r\mathrm{d}\theta\hat{\boldsymbol{r}}) \\ &= \int_0^{2\pi} \frac{k'\sigma}{r} r\mathrm{d}\theta \\ &= 2\pi k'\sigma\end{aligned} \tag{1.36}$$

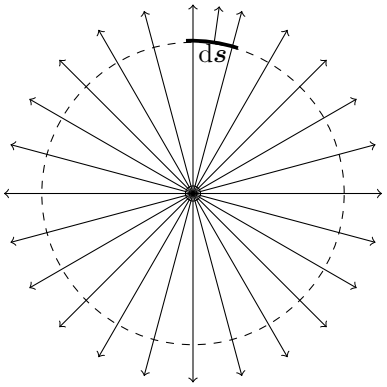

Figure 1.4: Calculation of flux of the velocity through a closed space (dashed line). A segment of this enclosure, d$\boldsymbol{s}$ is shown with its associated normal vector.

One could confirm that this is a valid solution, let us insert our expression for ϕ into the Laplace operator:

$$\begin{aligned}\nabla^2\phi &= \frac{1}{r}\frac{\partial}{\partial r}\left(r\frac{\partial}{\partial r}\left(\frac{\sigma}{2\pi}\log r\right)\right)\\ &= \frac{1}{r}\frac{\partial}{\partial r}\left(\frac{\sigma}{2\pi}\right)\\ &= 0\end{aligned} \tag{1.37}$$

Thus, equation 1.36 is indeed a solution. In reality, this stage is not required because implicit in the previous steps is the fact that Laplace's equation has been satisfied (that is, writing the velocity as the gradient of a scalar field and enforcing the incompressibility condition).

The velocity components are as follows:

$$u_{\mathrm{r}} = \frac{\sigma}{2\pi r},\ u_\theta = 0 \tag{1.38}$$

or, in a Cartesian coordinate system:

$$\begin{aligned}u &= \frac{\sigma(x-x_0)}{2\pi((x-x_0)^2+(y-y_0)^2)}\\ v &= \frac{\sigma(y-y_0)}{2\pi((x-x_0)^2+(y-y_0)^2)}\end{aligned} \tag{1.39}$$

Streamlines and equipotential lines due to the point source are shown in figure 1.5.

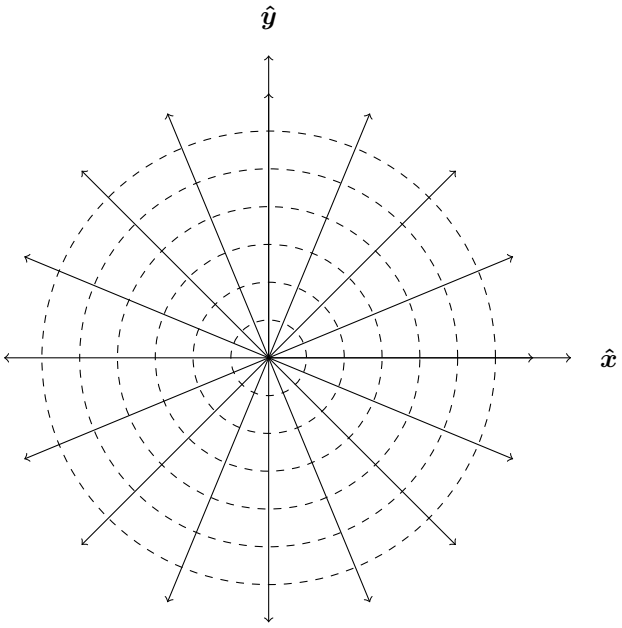

Figure 1.5: Illustration of the streamlines arising from a point source.

It can be seen that the streamlines extend outwards from a point. Accordingly, this type of singularity element is called a source. When the sign is the opposite, the streamlines are directed inwards towards the singularity element; such an element is called a sink.

Now let us develop the three-dimensional equivalent singularity element. Hence our objective is to develop a solution where the velocity induced by a point element is purely radial. Since the singularity element is a point object, let us use the spherical polar coordinate whose origin coincides with the point object.

Starting with the curl in three dimensions,

$$\begin{aligned}\nabla \times \boldsymbol{u} &= \frac{1}{r\sin\theta}\left(\frac{\partial}{\partial\theta}(u_\psi \sin\theta) - \frac{\partial u_\theta}{\partial\psi}\right)\hat{\boldsymbol{r}} + \frac{1}{r}\left(\frac{1}{\sin\theta}\frac{\partial u_\mathrm{r}}{\partial\psi} - \frac{\partial(r u_\psi)}{\partial r}\right)\hat{\boldsymbol{\theta}} + \frac{1}{r}\left(\frac{\partial(r u_\theta)}{\partial r} - \frac{\partial u_\mathrm{r}}{\partial\theta}\right)\hat{\boldsymbol{\psi}} \\ &= 0 \end{aligned} \tag{1.40}$$

Given that the aim is to develop an equivalent to the two-dimensional solution just developed, it follows that $u_\theta = u_\psi = 0$. Hence, considering the $\hat{\boldsymbol{\theta}}$ and $\hat{\boldsymbol{\psi}}$ terms, it follows that

$$\frac{\partial u_\mathrm{r}}{\partial\psi} = 0, \ \frac{\partial u_\mathrm{r}}{\partial\theta} = 0 \tag{1.41}$$

Just like the two-dimensional case, the solution is centred around an element which induces radial velocity only and that radial velocity component has no dependence on θ or ψ.

considering equation 1.21, it follows that

$$\frac{1}{r^2}\frac{\partial(r^2 u_\mathrm{r})}{\partial r} = 0 \tag{1.42}$$

Here only the first term of equation 1.16 has been considered since $u_\theta = u_\psi = 0$.

In order to satisfy equation 1.42, it follows that $u_\mathrm{r} \propto 1/r^2$; that is,

$$u_\mathrm{r} = \frac{k}{r^2} \tag{1.43}$$

The velocity potential may be deduced from

$$\nabla\phi = \left(\frac{\partial\phi}{\partial r}\right)\hat{\boldsymbol{r}} + \left(\frac{1}{r}\frac{\partial\phi}{\partial\theta}\right)\hat{\boldsymbol{\theta}} + \left(\frac{1}{r\sin\theta}\frac{\partial\phi}{\partial\psi}\right)\hat{\boldsymbol{\psi}} \tag{1.44}$$

Specifically,

$$\frac{\partial \phi}{\partial r} = \frac{k}{r^2}, \ \frac{1}{r}\frac{\partial \phi}{\partial \theta} = 0, \ \frac{\partial \phi}{\partial \psi} = 0 \tag{1.45}$$

Hence,

$$\phi = -\frac{k}{r} \tag{1.46}$$

The constant of integration has been neglected; this is equivalent to stating that as $r \to \infty$ the velocity potential due to the point object tends to zero, which is a desirable characteristic in a fundamental solution.

Applying the same logic as was done in the two dimensional case, it is shown that $k = \sigma/4\pi$ if σ is to be the interpreted as the flux.

Hence,

$$\phi = \frac{\sigma}{4\pi r} \tag{1.47}$$

The point doublet

Let us consider the potential due to a source-sink pair (equal and opposite in strength) at some point in two-dimensional space:

$$\phi = \frac{\sigma}{2\pi}(\log|\boldsymbol{r}| - \log|\boldsymbol{r} - \boldsymbol{l}|) \tag{1.48}$$

where $\boldsymbol{r}$ is the vector spanning from the point source to the point of interest, P, and $\boldsymbol{l}$ is the vector spanning from the point source to the point sink.

By the laws of logs, equation 1.48 may be formulated as follows:

$$\phi = \frac{\sigma}{2\pi}\log\left(\frac{|\boldsymbol{r}|}{|\boldsymbol{r} - \boldsymbol{l}|}\right) \tag{1.49}$$

Note, as the separation of the source and sink tends to zero, the expression inside of the log tends to one; this means that the potential due to the source-sink pair tends to zero when the two are brought infinitely close. In order for there to be a non-zero potential arising from the combination, let $\sigma \to \infty$ as $l \to 0$. Ultimately, the aim is for the product σl to be non-zero but finite. Let us define this product to be μ.

Focusing on the denominator inside the logarithm,

$$\begin{aligned} |\boldsymbol{r} - \boldsymbol{l}| &= \sqrt{r^2 + l^2 - 2\boldsymbol{r}.\boldsymbol{l}} \\ &= r\sqrt{1 + \frac{l^2}{r^2} - \frac{2\boldsymbol{r}.\boldsymbol{l}}{r^2}} \end{aligned} \tag{1.50}$$

Hence,

$$\begin{aligned} \phi &= \frac{\sigma}{2\pi}\log\left(\frac{|\boldsymbol{r}|}{r\sqrt{1 + \frac{l^2}{r^2} - \frac{2\boldsymbol{r}.\boldsymbol{l}}{r^2}}}\right) \\ &= \frac{\sigma}{2\pi}\log\left(\sqrt{\frac{1}{1 + \frac{l^2}{r^2} - \frac{2\boldsymbol{r}.\boldsymbol{l}}{r^2}}}\right) \\ &= -\frac{\sigma}{4\pi}\log\left(1 + \frac{l^2}{r^2} - \frac{2\boldsymbol{r}.\boldsymbol{l}}{r^2}\right) \end{aligned} \tag{1.51}$$

Noting that the dot product of two vectors $\boldsymbol{a}$ and $\boldsymbol{b}$ is $\boldsymbol{a}.\boldsymbol{b} = |\boldsymbol{a}||\boldsymbol{b}|\cos\delta$, it follows that

$$\phi = -\frac{\sigma}{4\pi}\log\left(1 + \frac{l^2}{r^2} - \frac{2l\cos\delta}{r}\right) \tag{1.52}$$

In the limit of $l \to 0$, the second term in the logarithm becomes vanishingly small. In this event, the velocity potential can be expressed as follows:

$$\phi = -\frac{\sigma}{4\pi}\log\left(1 - \frac{2l\cos\delta}{r}\right) \tag{1.53}$$

Applying a Taylor series expansion in l and neglecting high order terms (since $l \to 0$), it follows that

$$\phi = -\frac{\sigma l\cos\delta}{2\pi r} \tag{1.54}$$

Using the previous definition of μ, it follows that

$$\phi = -\frac{\mu\cos\delta}{2\pi r} \tag{1.55}$$

Let us define a vector, $\boldsymbol{\mu}$, that satisfies

$$\boldsymbol{\mu}.\boldsymbol{r} = \mu r\cos\delta \tag{1.56}$$

With this vector, we may write

$$\phi = -\frac{\boldsymbol{\mu}.\boldsymbol{r}}{2\pi r^2} \tag{1.57}$$

Equation 1.57 defines a doublet, sometimes referred to as a dipole.

If $\boldsymbol{\mu} = \mu\hat{\boldsymbol{x}}$, then

$$\phi = -\frac{\mu\cos\theta}{2\pi r} \tag{1.58}$$

Again, it is possible to check that this is indeed a solution to Laplace's equation:

$$\begin{aligned}\nabla^2\phi &= \frac{1}{r}\frac{\partial}{\partial r}\left(r\frac{\partial}{\partial r}\left(-\frac{\mu\cos\theta}{2\pi r}\right)\right) + \frac{1}{r^2}\frac{\partial^2}{\partial\theta^2}\left(-\frac{\mu\cos\theta}{2\pi r}\right)\\ &= -\frac{\mu\cos\theta}{2\pi r^3} + \frac{\mu\cos\theta}{2\pi r^3}\\ &= 0\end{aligned} \tag{1.59}$$

In Cartesian coordinates, the solution is expressed as follows:

$$\phi = -\frac{\mu}{2\pi}\frac{x - x_0}{(x - x_0)^2 + (y - y_0)^2} \tag{1.60}$$

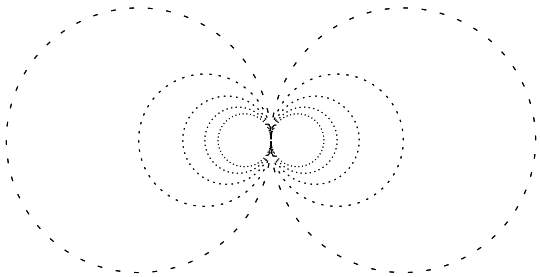

Figure 1.6: Lines of constant potential due to a point doublet in two dimensions when $\boldsymbol{\mu} = \mu\hat{\boldsymbol{x}}$

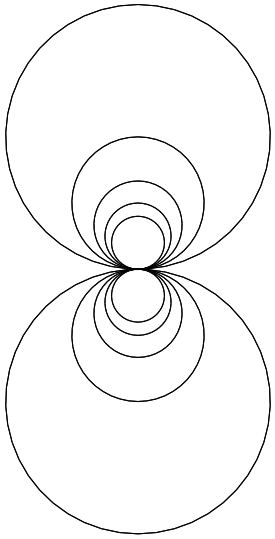

Figure 1.7: Streamlines due to a point doublet in two dimensions when $\boldsymbol{\mu} = \mu\hat{\boldsymbol{x}}$

It should be noted that changing the definition of $\boldsymbol{\mu}$ such that its orientation is different will cause a rotation of the equipotential lines and streamlines.

For three dimensions, the process is almost identical.

$$\Phi = \frac{\sigma}{4\pi}\left(\frac{1}{|\boldsymbol{r}|} - \frac{1}{|\boldsymbol{r}-\boldsymbol{l}|}\right) \tag{1.61}$$

The two fractions can be expressed using one common denominator:

$$\Phi = \frac{\sigma}{4\pi}\left(\frac{|\boldsymbol{r}-\boldsymbol{l}| - |\boldsymbol{r}|}{|\boldsymbol{r}||\boldsymbol{r}-\boldsymbol{l}|}\right) \tag{1.62}$$

In the limit of $|\boldsymbol{l}| \to 0$, the source-sink pair virtually overlap. In that case,

$$|\boldsymbol{r}||\boldsymbol{r}-\boldsymbol{l}| \to r^2 \tag{1.63}$$

Furthermore,

$$\begin{aligned} |\boldsymbol{r}-\boldsymbol{l}| &= \sqrt{r^2 + l^2 - 2\boldsymbol{r}.\boldsymbol{l}} \\ &= r\sqrt{1 + \frac{l^2}{r^2} - \frac{2\boldsymbol{r}.\boldsymbol{l}}{r^2}} \end{aligned} \tag{1.64}$$

Hence, in the limit of $l \to 0$, the l^2 term vanishes. Applying a binomial expansion to equation 1.64, it follows that

$$\begin{aligned} |\boldsymbol{r}-\boldsymbol{l}| &= r\left(1 - \frac{\boldsymbol{r}.\boldsymbol{l}}{r^2}\right) \\ &= r - l\cos\theta \end{aligned} \tag{1.65}$$

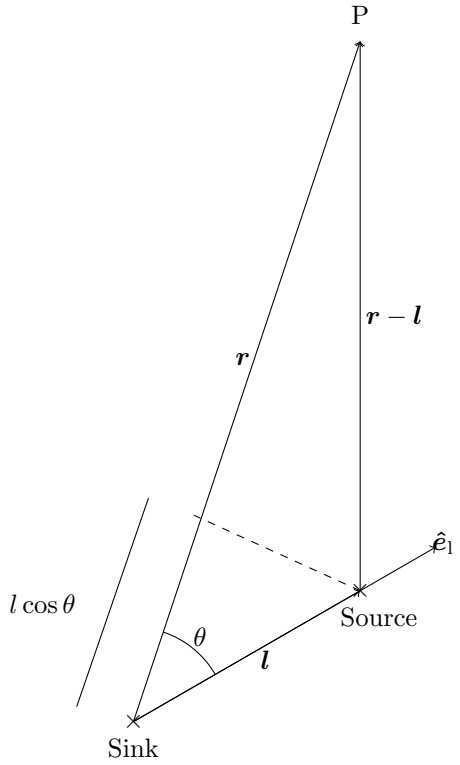

Figure 1.8: Influence of a source-sink pair at some point, P

Hence,

$$\phi = -\frac{\sigma l \cos\theta}{4\pi r^2} \tag{1.66}$$

By letting $\sigma \to \infty$ such that $l\sigma$ is defined to be μ and μ is finite, it follows that

$$\phi = -\frac{\mu \cos\theta}{4\pi r^2} \tag{1.67}$$

From inspection of figure 1.8, it may be noted that $\cos\theta = \boldsymbol{r}.\hat{\boldsymbol{e}}_\mathrm{l}/r$; hence, writing $\boldsymbol{\mu} = \mu\hat{\boldsymbol{e}}_\mathrm{l}$, it follows that

$$\phi = -\frac{\boldsymbol{\mu}.\boldsymbol{r}}{4\pi r^3} \tag{1.68}$$

If $\hat{\boldsymbol{e}}_\mathrm{l}.\boldsymbol{n} = 1$ i.e. the two vectors are parallel, then equation 1.68 is equivalent

$$\begin{aligned}\phi &= -\frac{1}{4\pi}\frac{\hat{\boldsymbol{e}}_\mathrm{l}.\boldsymbol{r}}{r^3} \\ &= -\hat{\boldsymbol{e}}_\mathrm{l}.\nabla\left(-\frac{1}{4\pi r}\right) \\ &= -\frac{\partial \Phi_\mathrm{source}}{\partial n}\end{aligned} \tag{1.69}$$

The vortex blob

As with the previous point singularity elements, let us start by considering the curl in two dimensions. In this case, let us impose the condition that the velocity arising from the point object will be constrained to the polar axis (in a cylindrical polar coordinate system); that is,

$$u_\mathrm{r} = 0 \tag{1.70}$$

Hence, the condition of a zero curl of the velocity vector (irrotational flow) gives rise to the following result:

$$\frac{\partial(ru_\theta)}{\partial r} = 0 \tag{1.71}$$

Referring to the result of the divergence of velocity vector being zero (incompressible), it also follows that

$$\frac{\partial u_\theta}{\partial \theta} = 0 \tag{1.72}$$

where only the second term has been considered since $u_\mathrm{r} = 0$. As a result, it follows that u_θ is a function of r only. Therefore, returning to the curl result, it follows that

$$u_\theta = \frac{k}{r} \tag{1.73}$$

Let the variable Γ be defined mathematically to be

$$\Gamma = \oint \boldsymbol{u}.\mathrm{d}\boldsymbol{l} \tag{1.74}$$

If the closed line integral traces out a circle, then

$$\begin{aligned}\Gamma &= \int_0^{2\pi} \boldsymbol{u}.(r\mathrm{d}\boldsymbol{\theta}) \\ &= \int_0^{2\pi} \frac{k}{r}(r\mathrm{d}\theta) \\ &= 2\pi k\end{aligned} \tag{1.75}$$

That is,

$$k = \frac{\Gamma}{2\pi} \tag{1.76}$$

Hence,

$$u_\theta = \frac{\Gamma}{2\pi r} \tag{1.77}$$

Owing to its mathematical definition, Γ is referred to as the circulation.

The velocity potential may be deduced from

$$\begin{aligned}\frac{\partial \phi}{\partial r} &= 0 \\ \frac{1}{r}\frac{\partial \phi}{\partial \psi} &= \frac{\Gamma}{2\pi r}\end{aligned} \tag{1.78}$$

Hence,

$$\phi = -\frac{\Gamma\theta}{2\pi} \tag{1.79}$$

where the constant of integration has been set to zero for convenience.

In a Cartesian coordinate system, the velocity potential and velocity components are given by equations 1.80 and 1.81 respectively:

$$\Phi = -\frac{\Gamma}{2\pi}\tan^{-1}\left(\frac{y-y_0}{x-x_0}\right) \tag{1.80}$$

$$\begin{aligned}u &= \frac{\Gamma}{2\pi}\frac{y-y_0}{(x-x_0)^2+(y-y_0)^2} \\ v &= -\frac{\Gamma}{2\pi}\frac{x-x_0}{(x-x_0)^2+(y-y_0)^2}\end{aligned} \tag{1.81}$$

The resulting streamlines and equipotential lines are shown in figure 1.9:

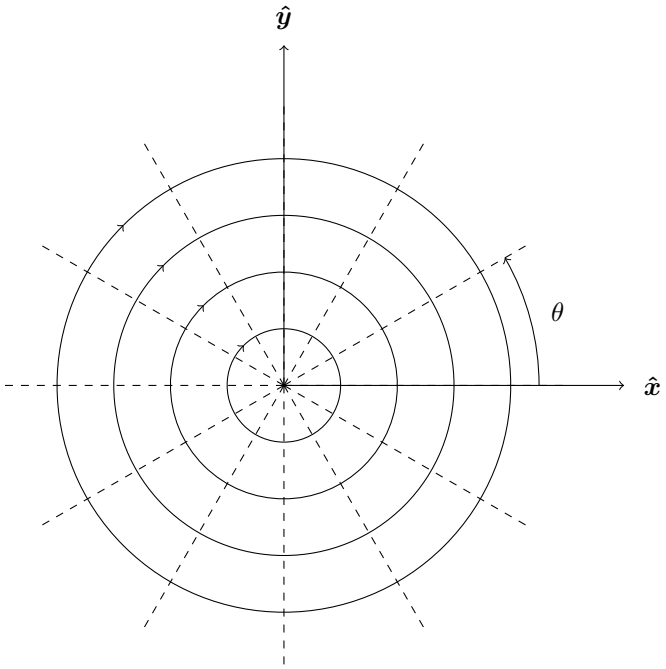

Figure 1.9: Streamlines and equipotential lines for a two-dimensional irrotational vortex located at the origin.

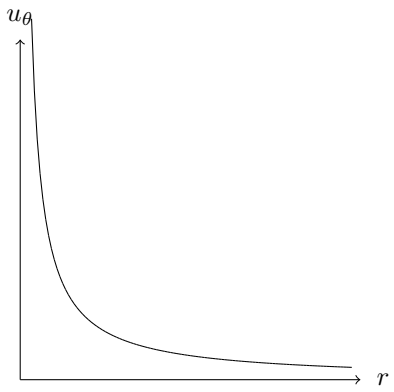

Figure 1.10: Plot of u_θ against r for an irrotational vortex blob

From figure 1.10, it can be noted that $u_\theta \to \infty$ as $r \to 0$. This singularity poses numerical stability issues. Moreover, in reality, vortices have viscous cores.

There are multiple approaches to modelling the effects of a vortex core. The simplest approach would be to introduce a cutoff radius, below which the velocity induced by the vortex blob is assumed to be zero. A plot showing the tangential velocity profile (as a function of radius) is presented in figure 1.11:

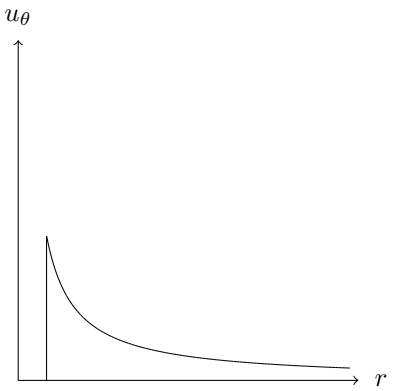

Figure 1.11: Plot of u_θ against r for an irrotational vortex blob with a simple cut-off radius

The Rankine vortex core model is an alternative to the aforementioned approach. In this model, the velocity induced by the vortex blob is calculated by the following process:

$$u_\theta = \begin{cases} \Gamma r/(2\pi R^2) & \text{if } r \leq R \\ \Gamma/(2\pi r) & \text{if } r > R \end{cases}$$

where R is the radius of the vortex core. The resulting velocity distribution is shown in figure 1.12:

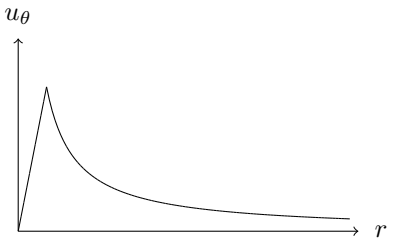

Figure 1.12: Plot of u_θ against r for a Rankine vortex blob

A third approach is the Lamb-Oseen model

$$u_\theta(r,t) = \frac{\Gamma}{2\pi r}\left(1 - \exp\left(-\frac{r^2}{r_c^2(t)}\right)\right) \tag{1.82}$$

where

$$r_c(t) = \sqrt{4\nu t + r_c(0)^2} \tag{1.83}$$

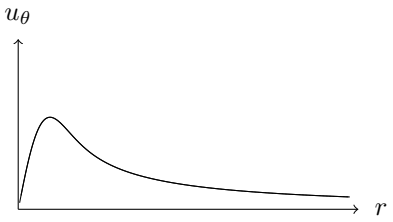

Figure 1.13: Plot of u_θ against r for a Lamb-Oseen vortex blob

1.4 Kelvin's circulation theorem

In Newtonian mechanics, there exists conservation laws, one of which is the conversation of angular momentum. Since the Navier-Stokes equations are Newton's second law applied to a fluid continuum, one would expect to see an equivalent of the conservation of angular momentum in fluids.

Let us begin by considering the material derivative of a generic vector field, $\mathbf{A}$:

$$\frac{\mathrm{D}\mathbf{A}}{\mathrm{D}t} = \frac{\partial \mathbf{A}}{\partial t} + \mathbf{u}.\nabla\mathbf{A} \tag{1.84}$$

where $\mathbf{u}$ is the flow velocity. Hence, Euler may be expressed as follows:

$$\rho\frac{\mathrm{D}\mathbf{u}}{\mathrm{D}t} = -\nabla P + \nabla\Phi \tag{1.85}$$

Again, it is worth stressing that this version of Euler is strictly only applicable to cases where the fluid is not subject to non-conservative forces.

In addition, the time-derivative of circulation may be expressed as follows:

$$\begin{aligned}\frac{\mathrm{D}\Gamma}{\mathrm{D}t} &= \frac{\mathrm{D}}{\mathrm{D}t}\left\{\oint \mathbf{u}.\mathrm{d}\mathbf{l}\right\} \\ &= \oint \frac{\mathrm{D}}{\mathrm{D}t}\{\mathbf{u}.\mathrm{d}\mathbf{l}\} \\ &= \oint \left\{\frac{\mathrm{D}\mathbf{u}}{\mathrm{D}t}.\mathrm{d}\mathbf{l} + \mathbf{u}.\frac{\mathrm{D}\mathrm{d}\mathbf{l}}{\mathrm{D}t}\right\}\end{aligned} \tag{1.86}$$

The first expression can be replaced by Euler:

$$\frac{\mathrm{D}\Gamma}{\mathrm{D}t} = \oint \left\{\frac{1}{\rho}(-\nabla P + \nabla\Phi)\,.\mathrm{d}\mathbf{l} + \mathbf{u}.\frac{\mathrm{D}\mathrm{d}\mathbf{l}}{\mathrm{D}t}\right\} \tag{1.87}$$

Using Stokes' theorem,

$$\frac{\mathrm{D}\Gamma}{\mathrm{D}t} = \iint \left\{\nabla \times \left(\frac{1}{\rho}(-\nabla P + \nabla\Phi)\right).\mathrm{d}\mathbf{S}\right\} + \oint \left\{\mathbf{u}.\frac{\mathrm{D}\mathrm{d}\mathbf{l}}{\mathrm{D}t}\right\} \tag{1.88}$$

A general result from vector calculus is that the curl of any gradient of a scalar field, f, is zero:

$$\nabla \times \nabla f = 0 \tag{1.89}$$

As ρ is a constant and both pressure and potential are scalar fields, hence,

$$\frac{\mathrm{D}\Gamma}{\mathrm{D}t} = \oint \left\{\mathbf{u}.\frac{\mathrm{D}\mathrm{d}\mathbf{l}}{\mathrm{D}t}\right\} \tag{1.90}$$

Recalling the definition of the material derivative,

$$\begin{aligned}\frac{\mathrm{D}\Gamma}{\mathrm{D}t} &= \oint \{\mathbf{u}.[(\mathrm{d}\mathbf{l}.\nabla)\mathbf{u}]\} \\ &= \oint [(\mathbf{u}.\nabla)\mathbf{u}].\mathrm{d}\mathbf{l}\end{aligned} \tag{1.91}$$

Noting that

$$\nabla(\mathbf{u}.\mathbf{u}) = 2(\mathbf{u}.\nabla)\mathbf{u} \tag{1.92}$$

Hence, equation 1.91 may be expressed as follows:

$$\frac{\mathrm{D}\Gamma}{\mathrm{D}t} = \frac{1}{2}\oint \{\nabla(\mathbf{u}.\mathbf{u}).\mathrm{d}\mathbf{l}\} \tag{1.93}$$

The term $\mathbf{u}.\mathbf{u}$ is a scalar. Thus, utilising Stokes' theorem again

$$\begin{aligned}\frac{\mathrm{D}\Gamma}{\mathrm{D}t} &= \frac{1}{2}\oint \{\nabla(\mathbf{u}.\mathbf{u}).\mathrm{d}\mathbf{l}\} \\ &= \frac{1}{2}\iint \{\nabla \times \nabla(\mathbf{u}.\mathbf{u}).\mathrm{d}\mathbf{S}\} \\ &= 0 \end{aligned} \tag{1.94}$$

If the fluid is inviscid, then equation 1.94 states that any creation of vorticity is accompanied by the creation of equal and opposite vorticity somewhere else in the system. This is Kelvin's circulation theorem.

Chapter 2

Influence coefficients for two dimensional simulations

In this chapter, the influence coefficients for panels of different types of singularity element are derived. It is noted that the influence coefficient calculations are done in a panel reference frame; that is, one in which the panel is aligned with $\hat{\boldsymbol{x}}_{\mathrm{p}}$ and start at the origin. Accordingly, in the panel reference frame, all along the length of the panel, the value of the y_{p} coordinate is zero. The notation for the panel reference frame in this text is subscript p.

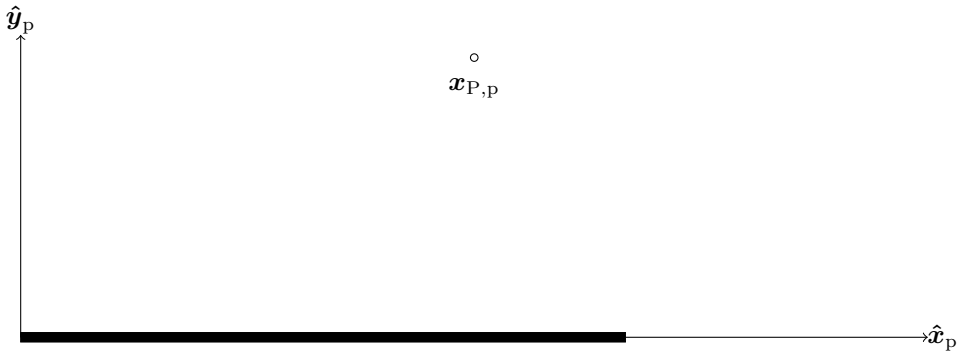

Figure 2.1: Illustration of the panel reference frame.

2.1 From the body reference frame to the panel reference frame

For a system containing N panels, there will be N independent panel reference frames. Given that panel and collocation coordinates are conventionally expressed in a common reference frame called the body reference frame (defined to be a frame in which a 'rigid' object appears stationary as it traverses through the fluid[1]), it is necessary to establish expressions to convert from the body reference frame to a panel reference frame before applying any panel influence calculations.

[1]By rigid, it is also meant that the aerofoil/aerofoils does/do not pitch.

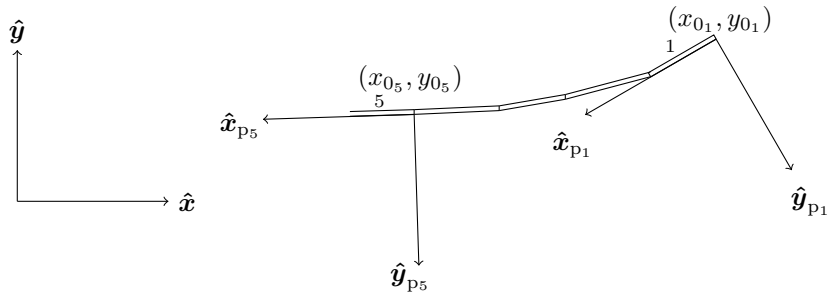

Figure 2.2: Illustration of the panel reference frames. Only the first five panels of the 'k$^{\mathrm{th}}$' object are shown. Note whilst the panel is shown as a two dimensional object in 2D space, it is actually a one dimensional object in 2D space i.e. it is a line segment. The thickness is included for visualisation purposes only.

Let us consider a generic panel, 'i'. The orientation of the panel is measured as the angle (clockwise from the perspective of the body reference frame) from $\hat{\boldsymbol{x}}_{\mathbf{p_i}}$ to $\hat{\boldsymbol{x}}$ as shown:

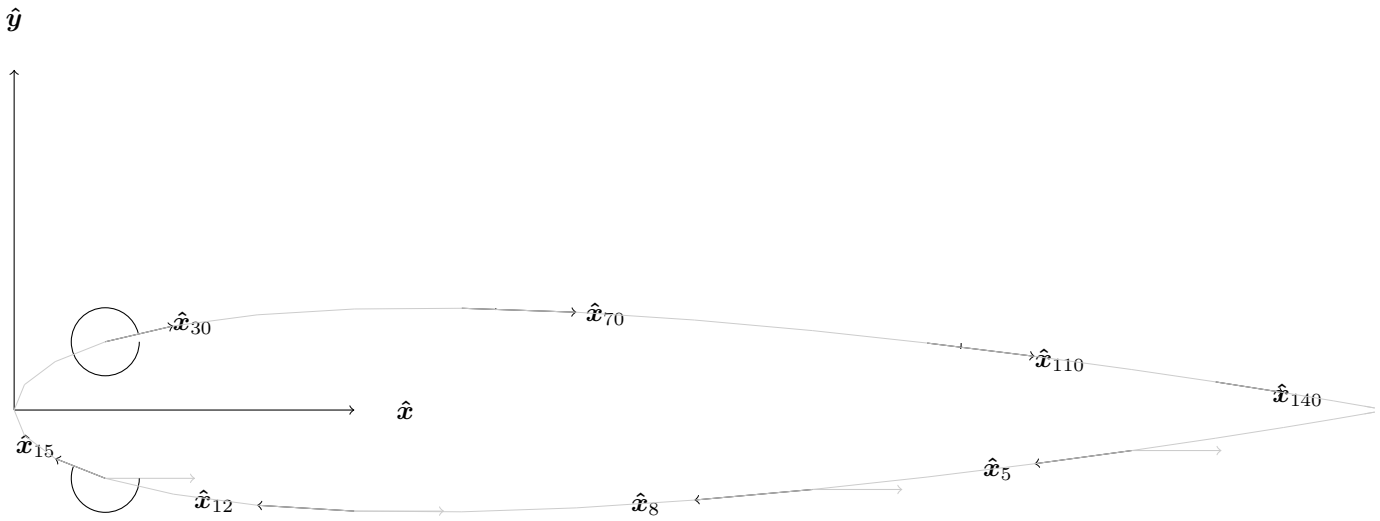

Figure 2.3: Definition of the angle convention used in this work for connecting a panel reference frame to the body reference frame. Only a few panels have been shown for illustrative purposes. Note, generally speaking $\hat{\boldsymbol{x}}$ is not parallel to the chord line (even for systems containing symmetric aerofoils).

The origin of panel 'i' as expressed in the body reference frame is $\begin{bmatrix} x_{0_\mathrm{i}} & y_{0_\mathrm{i}} \end{bmatrix}$. This corresponds to one of the corner points of the panel.

The panel orientation can be found by simple trigonometry using the panel end points. That is, if the panel end points, as expressed in the body reference frame, are $\begin{bmatrix} x_{0_\mathrm{i}} & y_{0_\mathrm{i}} \end{bmatrix}$ and $\begin{bmatrix} x_{0_{\mathrm{i}+1}} & y_{0_{\mathrm{i}+1}} \end{bmatrix}$, it follows that the orientation, θ_i, is found through the following expression:

$$\tan\theta_\mathrm{i} = \frac{y_{0_{\mathrm{i}+1}} - y_{0_\mathrm{i}}}{x_{0_{\mathrm{i}+1}} - x_{0_\mathrm{i}}} \tag{2.1}$$

The above expression does not work for the final panel on an object since there is no subsequent panel i.e. the coordinates $\begin{bmatrix} \end{bmatrix}$ do not exist. Typically, the panelling scheme is such that an object's final panel joins with the first panel as shown in figure 2.4.

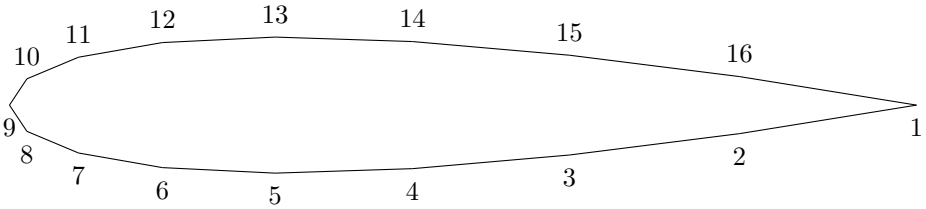

Figure 2.4: Panel numbering scheme for an aerofoil. The numbers coincide with the panel origins.

Thus, for the final panel on an aerofoil, assuming conventional panelling has been implemented, the orientation is found through

$$\tan\theta_{\mathrm{i}=\mathrm{N_p}} = \frac{y_{0_1} - y_{0_{\mathrm{N_p}}}}{x_{0_1} - x_{0_{\mathrm{N_p}}}} \tag{2.2}$$

For both equations, it can be noted that the tangent of the angle is given. The basic atan functions in most libraries yields angles that are bound between $-\pi/2$ and $\pi/2$. However, as can be seen from figure 2.3., the angle can lie anywhere between 0 and 2π (or $-\pi$ and π depending on the convention). For this reason, atan2 functions should be used; these can be found in MATLAB, standard C++ libraries, standard FORTRAN libraries etc.

It is important to choose a function which covers a full 2π range to avoid errors. This is because the basic atan functions introduce errors/ambiguities which reveal themselves when the angles are subsequently used in sine and cosine calculations. This can be seen from noting that

$$\begin{aligned}\tan\zeta &= \frac{\sin\zeta}{\cos\zeta} \\ &= \frac{\sin(\zeta+\pi)}{\cos(\zeta+\pi)}\end{aligned} \tag{2.3}$$

However, $\sin\zeta \neq \sin(\zeta+\pi)$ and $\cos\zeta \neq \cos(\zeta+\pi)$ generally speaking[2], errors can arise from basic atan functions.

To express the coordinates of some point of interest $P = \begin{bmatrix} x_{\mathrm{P}} & y_{\mathrm{P}} \end{bmatrix}$ (originally in the body reference frame) in the reference frame of panel 'i', the following operation should be carried out:

$$\begin{bmatrix} x_{\mathrm{P,p}} \\ y_{\mathrm{P,p}} \end{bmatrix} = \begin{bmatrix} \cos\theta_{\mathrm{i}} & \sin\theta_{\mathrm{i}} \\ -\sin\theta_{\mathrm{i}} & \cos\theta_{\mathrm{i}} \end{bmatrix} \begin{bmatrix} x_{\mathrm{P}} - x_{0_{\mathrm{i}}} \\ y_{\mathrm{P}} - y_{0_{\mathrm{i}}} \end{bmatrix} \tag{2.4}$$

2.2 The constant-strength vortex panel

A constant-strength vortex panel is shown in figure 2.5:

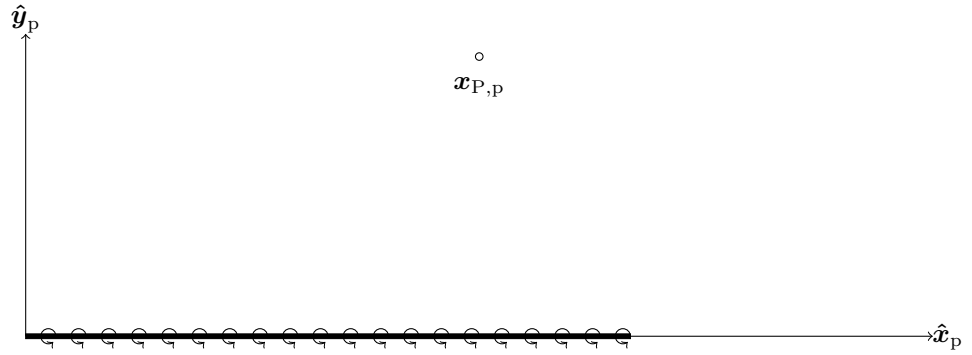

Figure 2.5: Illustration of the panel reference frame.

[2]the only exceptions for the sine term are when $\zeta = 0,\ 2\pi$; the exceptions for the cosine term are when $\zeta = \pi/2,\ 3\pi/2$; even in these cases, it can be seen that there is no value of ζ for which *both* $\sin\zeta = \sin(\zeta+\pi)$ and $\cos\zeta = \cos(\zeta+\pi)$

It comprises an infinite set of equal-strength vortex blob singularity elements spanning from $\begin{bmatrix}0 & 0\end{bmatrix}$ to $\begin{bmatrix}l_\mathrm{p} & 0\end{bmatrix}$ where lp is the length of the panel. In this derivation, the panel reference frame is defined such that its origin coincides with the start of the panel.

Since the panel is aligned with $\hat{\boldsymbol{x}}_\mathrm{p}$, the net influence of the panel at a point $\boldsymbol{x}_{\mathrm{P,p}}$ (whose coordinates have also been expressed in the panel reference frame for these calculations) is an integral spanning from $x_{0,\mathrm{p}} = 0$ to $x_{0,\mathrm{p}} = l_\mathrm{p}$, covering the inuences of all the individual point singularity elements that make up the panel. That is,

$$\Phi = -\frac{\gamma}{2\pi}\int_0^{l_\mathrm{p}} \tan^{-1}\left(\frac{y_{\mathrm{P,p}}}{x_{\mathrm{P,p}} - x_{0,\mathrm{p}}}\right)\mathrm{d}x_{0,\mathrm{p}} \tag{2.5}$$

where $\mathrm{d}x_{0,\mathrm{p}}$ is an incremental segment of the panel length, which starts at $\begin{bmatrix}x_{0,\mathrm{p}} & 0\end{bmatrix}$. γ is the 'strength' density of the panel.

Let $X = y_{\mathrm{P,p}}/(x_{\mathrm{P,p}} - x_{0,\mathrm{p}})$; thus,

$$\mathrm{d}x_{0,\mathrm{p}} = \frac{y_{\mathrm{P,p}}\mathrm{d}X}{X^2} \tag{2.6}$$

Hence,

$$\phi = -\frac{\gamma y_{\mathrm{P,p}}}{2\pi}\int_{y_{\mathrm{P,p}}/x_{\mathrm{P,p}}}^{y_{\mathrm{P,p}}/(x_{\mathrm{P,p}}-l_\mathrm{p})} \frac{\tan^{-1} X}{X^2}\mathrm{d}X \tag{2.7}$$

Let us note the following integral:

$$\int x^m \tan^{-1}(ax)\mathrm{d}x = \frac{x^{m+1}\tan^{-1}(ax)}{m+1} - \frac{a}{m+1}\int \frac{x^{m+1}}{a^2x^2+1}\mathrm{d}x \quad (m \neq -1) \tag{2.8}$$

In this case, $a = 1$ and $m = -2$. Hence,

$$\phi = -\frac{\gamma y_{\mathrm{P,p}}}{2\pi}\left[\frac{\tan^{-1} X}{X}\right]_{y_{\mathrm{P,p}}/x_{\mathrm{P,p}}}^{y_{\mathrm{P,p}}/(x_{\mathrm{P,p}}-l_\mathrm{p})} - \frac{\gamma y_{\mathrm{P,p}}}{2\pi}\int_{y_{\mathrm{P,p}}/x_{\mathrm{P,p}}}^{y_{\mathrm{P,p}}/(x_{\mathrm{P,p}}-l_\mathrm{p})} \frac{\mathrm{d}X}{X(1+X^2)} \tag{2.9}$$

Let us note that the integrand on the right hand side of equation 2.9 may be expressed as follows:

$$\begin{aligned}
-\frac{1}{X(1+X^2)} &= \left[\frac{X^2-(1+X^2)}{X(1+X^2)}\right] \\
&= \left[\frac{X}{1+X^2} - \frac{1}{X}\right] \\
&= \frac{X}{1+X^2}\left[1 - \frac{1+X^2}{X^2}\right] \\
&= \frac{1}{X\left(\frac{1+X^2}{X^2}\right)}\left[1 - \frac{1+X^2}{X^2}\right]
\end{aligned} \tag{2.10}$$

Let $u = (1+X^2)/X^2$; hence,

$$\begin{aligned}
\frac{\mathrm{d}u}{\mathrm{d}X} &= -\frac{2(1+X^2)}{X^3} + \frac{2X}{X^2} \\
&= \frac{2}{X}[1-u]
\end{aligned} \tag{2.11}$$

Hence,

$$\begin{aligned}
\int \frac{1}{X(1+X^2)}\mathrm{d}X &= \int \frac{1}{X\left(\frac{1+X^2}{X^2}\right)}\left[1 - \frac{1+X^2}{X^2}\right]\mathrm{d}X \\
&= \int \frac{1}{Xu}[1-u]\,\frac{\mathrm{d}u}{\frac{2}{X}[1-u]} \\
&= \frac{1}{2}\int \frac{\mathrm{d}u}{u} \\
&= \frac{1}{2}\log u
\end{aligned} \tag{2.12}$$

Hence,

$$\int_{y_{\mathrm{P,p}}/x_{\mathrm{P,p}}}^{y_{\mathrm{P,p}}/(x_{\mathrm{P,p}}-l_{\mathrm{p}})} \frac{\tan^{-1} X}{X^2}\mathrm{d}X = \left[\frac{\tan^{-1} X}{X} + \log\left(\frac{1+X^2}{X^2}\right)\right]_{y_{\mathrm{P,p}}/x_{\mathrm{P,p}}}^{y_{\mathrm{P,p}}/(x_{\mathrm{P,p}}-l_{\mathrm{p}})} \tag{2.13}$$

That is,

$$\phi = -\frac{\gamma}{2\pi}\left[(x_{\mathrm{P,p}})\theta_1 - (x_{\mathrm{P,p}} - l_{\mathrm{p}})\theta_2 + \frac{z_{\mathrm{P,p}}}{2}\log\left(\frac{r_1^2}{r_2^2}\right)\right] \tag{2.14}$$

where

$$\begin{aligned} \theta_1 = \tan^{-1}\left(\frac{y_{\mathrm{P,p}}}{x_{\mathrm{P,p}}}\right);\quad \theta_2 = \tan^{-1}\left(\frac{y_{\mathrm{P,p}}}{x_{\mathrm{P,p}} - l_{\mathrm{P,p}}}\right) \\ r_1^2 = x_{\mathrm{P,p}}^2 + y_{\mathrm{P,p}}^2;\ r_2^2 = (x_{\mathrm{P,p}} - l_{\mathrm{p}})^2 + y_{\mathrm{P,p}}^2 \end{aligned} \tag{2.15}$$

2.3 The constant-strength source panel

A constant-strength source panel is shown in figure 2.6:

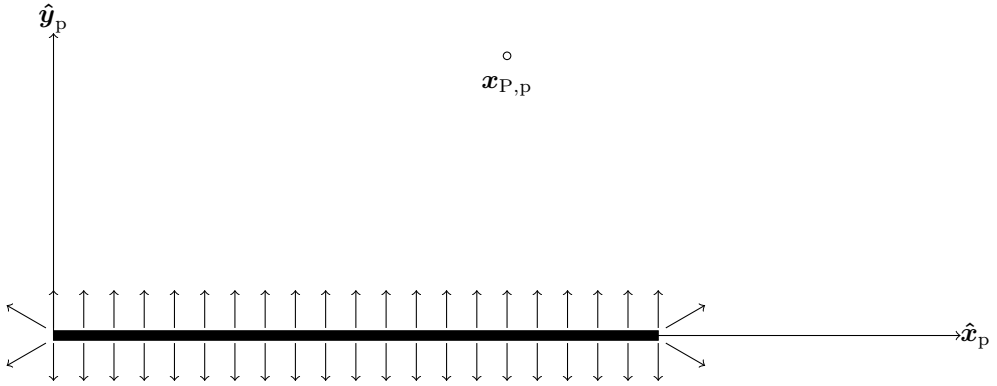

Figure 2.6: Illustration of a constant-strength source panel in two dimensional space.

It comprises an infinite set of equal-strength source singularity elements spanning from [0; 0] to $\begin{bmatrix} l_{\mathrm{p}} & 0 \end{bmatrix}$ where lp is the length of the panel. In this derivation, the panel reference frame is defined such that its origin coincides with the start of the panel. Furthermore, in the panel reference frame, the y-coordinates of all sections of the panel are zero.

The net influence of the panel at a point $\boldsymbol{x}_{\mathrm{P,p}}$ is an integral spanning from $x_{0,\mathrm{p}} = 0$ to $x_{0,\mathrm{p}} = l_{\mathrm{p}}$, covering the influences of all the individual point singularity elements that make up the panel. That is,

$$\begin{aligned} \Phi &= \frac{\sigma}{2\pi}\int_{x_{1,\mathrm{p}}}^{x_{2,\mathrm{p}}} \log\left[\sqrt{(x_{\mathrm{P,p}} - x_{0,\mathrm{p}})^2 + y_{\mathrm{P,p}}^2}\right]\mathrm{d}x_{0,\mathrm{p}} \\ &= \frac{\sigma}{4\pi}\int_0^{l_{\mathrm{p}}} \log\left[(x_{\mathrm{P,p}} - x_{0,\mathrm{p}})^2 + y_{\mathrm{P,p}}^2\right]\mathrm{d}x_{0,\mathrm{p}} \end{aligned} \tag{2.16}$$

where $\boldsymbol{x}_{\mathrm{P,p}} = \begin{bmatrix} x_{\mathrm{P,p}} & y_{\mathrm{P,p}} \end{bmatrix}^{\mathrm{T}}$, and x_0 is the variable name given to represent the location of the segment of the panel ($\mathrm{d}x_{0,\mathrm{p}}$) whose influence on $\boldsymbol{x}_{\mathrm{P,p}}$ is being evaluated. Note - as this derivation is performed in the panel reference frame, $y_{0,\mathrm{p}} = 0$.

Let $X = x_{\mathrm{P,p}} - x_{0,\mathrm{p}}$. Hence, $\mathrm{d}X = -\mathrm{d}x_{0,\mathrm{p}}$ and

$$\Phi = -\frac{\sigma}{4\pi}\int_{x_{\mathrm{P,p}}}^{x_{\mathrm{P,p}}-l_{\mathrm{p}}} \log\left[X^2 + y_{\mathrm{P,p}}^2\right]\mathrm{d}X \tag{2.17}$$

This integral is a standard integral, whose result is known to be

$$\Phi = \frac{\sigma}{4\pi}\left[x_\mathrm{p}\log r_1^2 - (x_\mathrm{p}-l_\mathrm{p})\ln r_2^2 + 2y_\mathrm{p}(\theta_2-\theta_1)\right] \tag{2.18}$$

where

$$\begin{aligned}\theta_1 &= \tan^{-1}\left(\frac{y_\mathrm{p}}{x_\mathrm{p}}\right); \quad \theta_2 = \tan^{-1}\left(\frac{y_\mathrm{p}}{x_\mathrm{p}-l_\mathrm{p}}\right)\\ r_1^2 &= x_\mathrm{p}^2 + y_\mathrm{p}^2; \quad r_2^2 = (x_\mathrm{p}-l_\mathrm{p})^2 + y_\mathrm{p}^2\end{aligned} \tag{2.19}$$

Differentiating equation 2.19 with respect to x_p and y_p yields the u and v velocity components respectively:

$$\begin{aligned}u_{\mathrm{P,p}} &= \frac{\sigma}{4\pi}\ln\left(\frac{x_{\mathrm{P,p}}^2 + y_{\mathrm{P,p}}^2}{(x_{\mathrm{P,p}}-l_\mathrm{p})^2 + y_{\mathrm{P,p}}^2}\right)\\ v_{\mathrm{P,p}} &= \frac{\sigma}{2\pi}\left[\tan^{-1}\left(\frac{y_{\mathrm{P,p}}}{x_{\mathrm{P,p}}-l_\mathrm{p}}\right) - \tan^{-1}\left(\frac{y_{\mathrm{P,p}}}{x_{\mathrm{P,p}}}\right)\right]\end{aligned} \tag{2.20}$$

2.4 The constant-strength doublet panel

A constant-strength doublet panel is shown in figure 2.7:

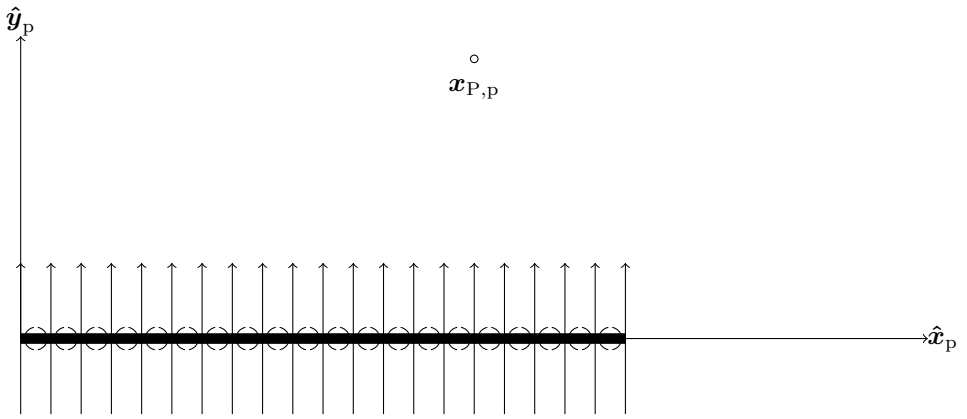

Figure 2.7: Illustration of a doublet panel in two dimensional space. The

It comprises an infinite set of equal-strength doublet singularity elements spanning from $[0,0]$ to $[l_\mathrm{p},0]$ where l_p is the length of the panel. Note - the panel reference frame is defined such that its origin coincides with the start of the panel. Furthermore, in the panel reference frame, the y-coordinates of all sections of the panel are zero.

Since the panel is aligned with $\hat{\boldsymbol{x}}_\mathrm{p}$, the net influence of the panel at a point $\boldsymbol{x}_{\mathrm{P,p}}$ (whose coordinates have also been expressed in the panel reference frame) is an integral spanning from $x_{0,\mathrm{p}} = 0$ to $x_{0,\mathrm{p}} = l_\mathrm{p}$, covering the influences of all the individual point singularity elements that make up the panel. That is,

$$\Phi = \frac{\mu}{2\pi}\int_0^{l_\mathrm{p}}\left[\frac{y_{\mathrm{P,p}}}{(x_{\mathrm{P,p}}-x_{0,\mathrm{p}})^2 + y_{\mathrm{P,p}}^2}\right]\mathrm{d}x_{0,\mathrm{p}} \tag{2.21}$$

where $\boldsymbol{x}_{\mathrm{P,p}} = \begin{bmatrix}x_{\mathrm{P,p}} & y_{\mathrm{P,p}}\end{bmatrix}^\mathrm{T}$, and $x_{0,\mathrm{p}}$ is denotes the distance along the length of the panel as measured from the start of the panel.

Let

$$r\cos\theta = x_{\mathrm{P,p}} - x_{0,\mathrm{p}} \tag{2.22}$$

$$r\sin\theta = y_{\mathrm{P,p}} \tag{2.23}$$

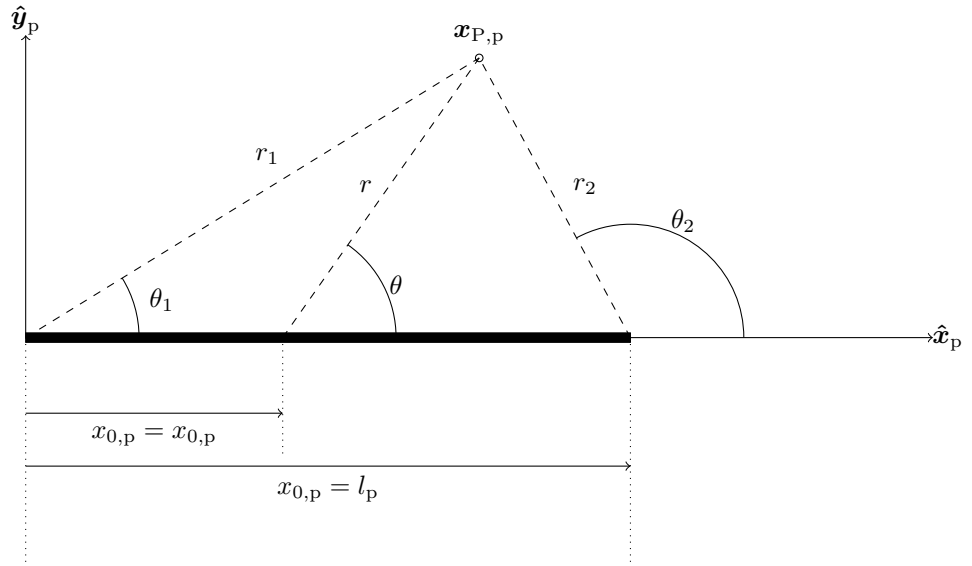

Figure 2.8: Illustration of the change in coordinate system. The points $x_0 = 0$ and $x_0 = l_\mathrm{p}$ have been shown in addition to an arbitrary point on the panel.

By dividing equation 2.23 by 2.22 and substituting $x_{0,\mathrm{p}} = 0$ and $x_{0,\mathrm{p}} = l_\mathrm{p}$, the integral limits can be expressed as follows:

$$0 \to \theta_1 = \tan^{-1}\left(\frac{y_{\mathrm{P,p}}}{x_{\mathrm{P,p}}}\right),\ l_\mathrm{p} \to \theta_2 = \tan^{-1}\left(\frac{y_{\mathrm{P,p}}}{x_{\mathrm{P,p}} - l_\mathrm{p}}\right) \tag{2.24}$$

The variables $x_{\mathrm{P,p}}$ and $y_{\mathrm{P,p}}$ are constants in this equation. Hence, we can write

$$\cos\theta \mathrm{d}r - r\sin\theta \mathrm{d}\theta = -\mathrm{d}x_{0,\mathrm{p}} \tag{2.25}$$
$$\sin\theta \mathrm{d}r + r\cos\theta \mathrm{d}\theta = 0 \tag{2.26}$$

Hence,

$$\cos\theta \frac{r\cos\theta \mathrm{d}\theta}{-\sin\theta} - r\sin\theta \mathrm{d}\theta = -\mathrm{d}x_{0,\mathrm{p}}$$
$$r\mathrm{d}\theta = \sin\theta \mathrm{d}x_{0,\mathrm{p}} \tag{2.27}$$

By substitution, equation 2.21 may be expressed as follows:

$$\begin{aligned}\Phi &= \frac{\mu}{2\pi}\int_{\theta_1}^{\theta_2} \frac{r\sin\theta}{r^2}\frac{r\mathrm{d}\theta}{\sin\theta} \\ &= \frac{\mu}{2\pi}\int_{\theta_1}^{\theta_2} \sin\theta \mathrm{d}\theta \\ &= \frac{\mu}{2\pi}[\theta]_{\theta_1}^{\theta_2}\end{aligned} \tag{2.28}$$

Hence,

$$\Phi = \frac{\mu}{2\pi}\left[\tan^{-1}\left(\frac{y_{\mathrm{P,p}}}{x_{\mathrm{P,p}}}\right) - \tan^{-1}\left(\frac{y_{\mathrm{P,p}}}{x_{\mathrm{P,p}} - l_\mathrm{p}}\right)\right] \tag{2.29}$$

The corresponding velocity induced by the panel is given as follows:

$$u_{\mathrm{P,p}} = -\frac{\mu}{2\pi}\left[\frac{y_{\mathrm{P,p}}}{x_{\mathrm{P,p}}^2 + y_{\mathrm{P,p}}^2} - \frac{y_{\mathrm{P,p}}}{(x_{\mathrm{P,p}} - l_\mathrm{p})^2 + y_{\mathrm{P,p}}^2}\right] \tag{2.30}$$

$$v_{\mathrm{P,p}} = \frac{\mu}{2\pi}\left[\frac{x_{\mathrm{P,p}}}{x_{\mathrm{P,p}}^2 + y_{\mathrm{P,p}}^2} - \frac{x_{\mathrm{P,p}} - l_\mathrm{p}}{(x_{\mathrm{P,p}} - l_\mathrm{p})^2 + y_\mathrm{p}^2}\right] \tag{2.31}$$

By comparing equations 1.80 and 1.81 with 2.29 and 2.30 and 2.31 respectively, it can be noted that a constant-strength doublet panel is mathematically equivalent to a pair of counter-rotating vortices (of strength $\pm\mu$) placed at the panel endpoints (see figure 2.9):

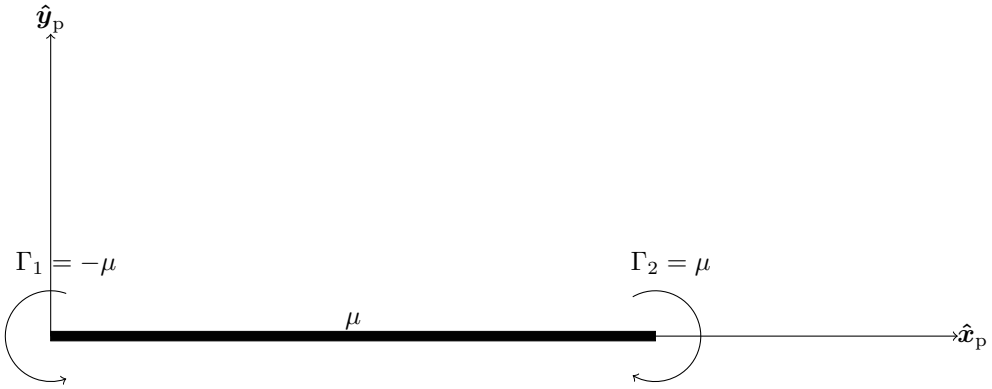

Figure 2.9: Equivalence of a constant-strength doublet panel of 'strength' μ, and a pair of counter-rotating vortex blobs (both with a circulation of magnitude $|\Gamma|$) placed at the panel corner points.

Conversion from a constant-strength doublet panel to a pair of counter-rotating vortices is sometimes preferable. Furthermore, it makes it possible to introduce vortex cores, thus adding some viscous effects to the simulation.

The equivalence of the constant-strength doublet panel and a counter-rotating vortex pair (placed at the panel end points) also makes it abundantly clear how lift can be predicted by methods such as the source-doublet panel method. Specifically, while individual panels may have zero net circulation in isolation, through superposition of vortex blobs from neighbouring panels (including body & most recently shed wake panels (see figure 2.10)) and the application of the Kutta condition, the net circulation on the aerofoil can be non-zero.

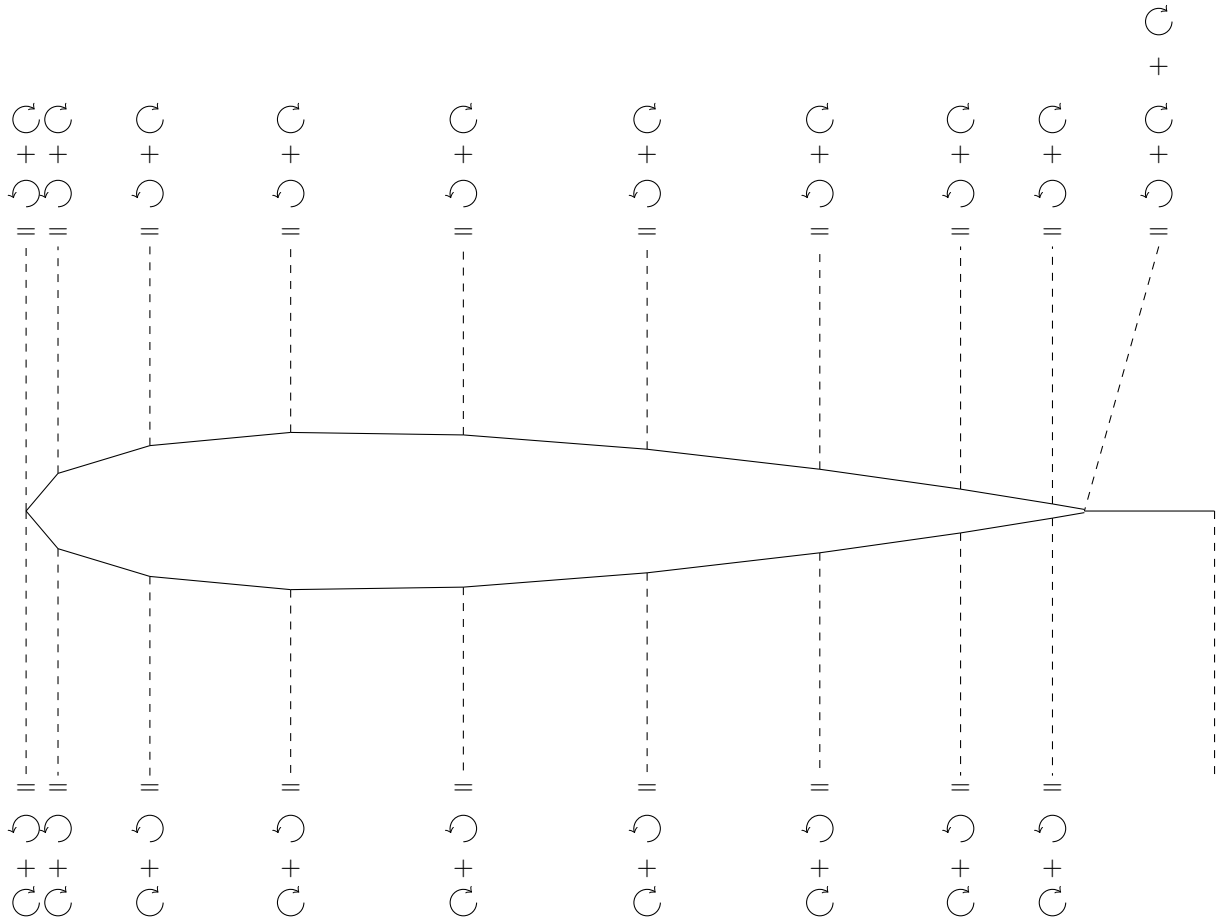

Figure 2.10: Doublet panels converted to counter-rotating vortex blob pairs at the panel corner points.

An additional feature of doublet-based panel methods is that the net circulation in the system is guaranteed to be zero; this means that Kelvin's circulation theorem is automatically satisfied.

2.5 From the panel reference frame to the body reference frame

If a system features a set of panels, the net velocity induced at some point of interest must be found by expressing all the velocities induced by each panel in a common reference frame. That is, once the velocity components have been calculated in a panel reference frame, they must be converted to the body reference frame. This can be achieved by simple manipulation of equation 2.4:

$$\begin{bmatrix} x_{\mathrm{P}} \\ y_{\mathrm{P}} \end{bmatrix} = \begin{bmatrix} \cos\theta & -\sin\theta \\ \sin\theta & \cos\theta \end{bmatrix} \begin{bmatrix} x_{\mathrm{P,p}} \\ y_{\mathrm{P,p}} \end{bmatrix} + \begin{bmatrix} x_{0_{\mathrm{i}}} \\ y_{0_{\mathrm{i}}} \end{bmatrix} \tag{2.32}$$

Thus, for velocity,

$$\begin{bmatrix} u_{\mathrm{P}} \\ v_{\mathrm{P}} \end{bmatrix} = \begin{bmatrix} \cos\theta & -\sin\theta \\ \sin\theta & \cos\theta \end{bmatrix} \begin{bmatrix} u_{\mathrm{i,p}} \\ v_{\mathrm{i,p}} \end{bmatrix} \tag{2.33}$$

Since potential is frame invariant, no reverse frame transformation is required for potential calculations. However, it is stressed that the frame transformations of coordinates into panel reference frames are still required for potential calculations since potential calculations, like velocity calculations, are based on derivations made using a panel reference frame.

2.6 Modelling 'static' stall

Stall is inherently an unsteady process with an element of chaos (mathematically speaking) in the wake. In this context, 'static' stall is used to allow distinction between systems where flow separation has occurred and the geometric angle of attack is constant, and systems where flow separation has/is/will occur and the geometric angle of attack is time dependent. The former scenario will be referred to as 'static' stall, while the latter will be referred to as 'dynamic' stall.

Chapter 3

Influence coefficients for three dimensional simulations

In this chapter, the influence coefficients for panels of different types of singularity element are derived. It is noted that the influence coefficient calculations are done in a panel reference frame; that is, one in which the panel is normal to $\hat{\boldsymbol{z}}_{\mathrm{p}}$ and start at the origin. Accordingly, in the panel reference frame, at all points on the panel, the value of the z_{p} coordinate is zero. The notation for the panel reference frame in this text is subscript p.

3.1 From the body reference frame to the panel reference frame

As with two-dimensional simulations, panel coordinates and final calculations relating to an object are given/performed in a (common) body reference frame. Thus, it is necessary to establish a connection between the body reference frame and a generic panel reference frame.

Let us consider the quadrilateral panel shown in figure 3.1:

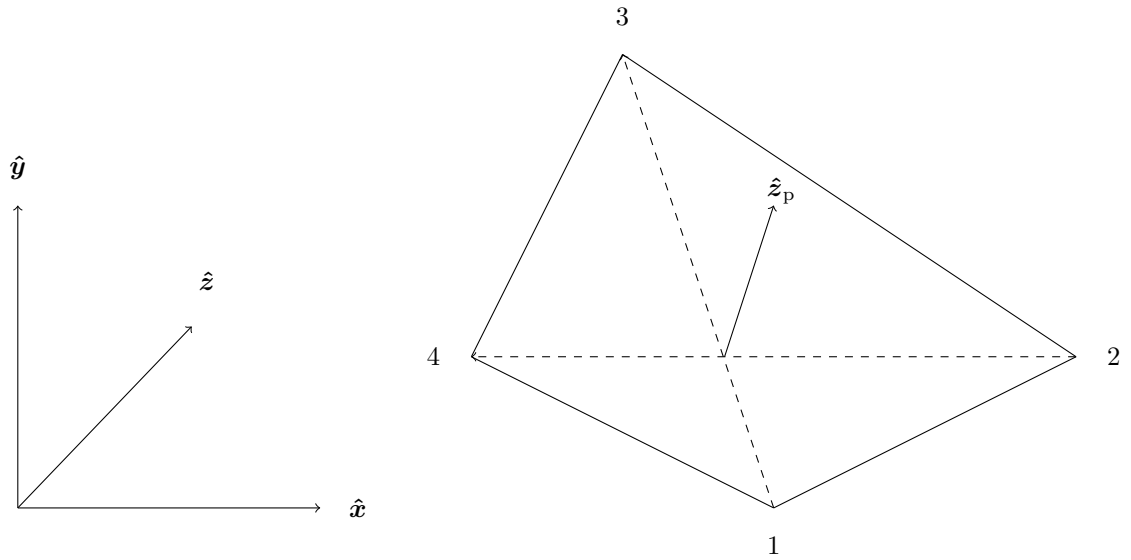

Figure 3.1: Illustration of a quadrilateral panel. The dashed lines denote $\boldsymbol{v}_1$ and $\boldsymbol{v}_2$

Two vectors, $\boldsymbol{v}_1$ and $\boldsymbol{v}_2$, can be defined as follows:

$$\boldsymbol{v}_1 = \begin{bmatrix} x_3 \\ y_3 \\ z_3 \end{bmatrix} - \begin{bmatrix} x_1 \\ y_1 \\ z_1 \end{bmatrix} \quad \boldsymbol{v}_2 = \begin{bmatrix} x_4 \\ y_4 \\ z_4 \end{bmatrix} - \begin{bmatrix} x_2 \\ y_2 \\ z_2 \end{bmatrix} \tag{3.1}$$

where $\begin{bmatrix} x_\mathrm{k} & y_\mathrm{k} & z_\mathrm{k} \end{bmatrix}$ are the coordinates for corner point 'k' as expressed in the body reference frame. The two vectors, by definition, lie in the plane of the panel. Thus, it follows that the cross-product of the two vectors will yield a vector normal to the panel surface. That is, $\hat{\boldsymbol{z}}_\mathrm{p}$ may be defined as

$$\hat{\boldsymbol{z}}_\mathrm{p} = \frac{\boldsymbol{v}_1 \times \boldsymbol{v}_2}{|\boldsymbol{v}_1 \times \boldsymbol{v}_2|} \tag{3.2}$$

A second unit vector can be defined as follows:

$$\hat{\boldsymbol{x}}_\mathrm{p} = \frac{\left[\left((x_2 + x_3) - (x_1 + x_4)\right)\hat{\boldsymbol{x}} + \left((y_2 + y_3) - (y_1 + y_4)\right)\hat{\boldsymbol{y}} + \left((z_2 + z_3) - (z_1 + z_4)\right)\hat{\boldsymbol{z}}\right]}{\sqrt{\left((x_2 + x_3) - (x_1 + x_4)\right)^2 + \left((y_2 + y_3) - (y_1 + y_4)\right)^2 + \left((z_2 + z_3) - (z_1 + z_4)\right)^2}} \tag{3.3}$$

The second vector will be in the plane of the panel.

A third unit vector, $\hat{\boldsymbol{y}}_\mathrm{p}$, will be normal to both $\hat{\boldsymbol{z}}_\mathrm{p}$ and $\hat{\boldsymbol{x}}_\mathrm{p}$ if it satisfies the following equation:

$$\hat{\boldsymbol{y}}_\mathrm{p} = \hat{\boldsymbol{x}}_\mathrm{p} \times \hat{\boldsymbol{z}}_\mathrm{p} \tag{3.4}$$

Now let us consider a point of interest whose coordinates are expressed in the body reference frame,

$$\boldsymbol{x}_\mathrm{P} = \begin{bmatrix} x_\mathrm{P} \\ y_\mathrm{P} \\ z_\mathrm{P} \end{bmatrix} \tag{3.5}$$

The point of interest as expressed in the panel reference frame belonging to panel 'i' is given by equation 3.6:

$$\begin{bmatrix} x_{\mathrm{P,p}} \\ y_{\mathrm{P,p}} \\ z_{\mathrm{P,p}} \end{bmatrix} = \begin{bmatrix} \hat{\boldsymbol{x}}_{\mathrm{p_i}}^\mathrm{T} \\ \hat{\boldsymbol{y}}_{\mathrm{p_i}}^\mathrm{T} \\ \hat{\boldsymbol{z}}_{\mathrm{p_i}}^\mathrm{T} \end{bmatrix} \begin{bmatrix} x_{\mathrm{P,p}} - x_{0_\mathrm{i}} \\ y_{\mathrm{P,p}} - y_{0_\mathrm{i}} \\ z_{\mathrm{P,p}} - z_{0_\mathrm{i}} \end{bmatrix} \tag{3.6}$$

where x_{0_i}, y_{0_i} and z_{0_i} are the coordinates of the panel reference frame origin (for panel 'i') as expressed in the body reference frame. In this text, the origin of the panel is chosen to coincide with corner point 1.

3.2 The vortex line segment

3.2.1 Velocity induced by a vortex line segment

Though not a panel, the vortex line segment is an important singularity element which is used extensively in wake modelling of 3D systems.

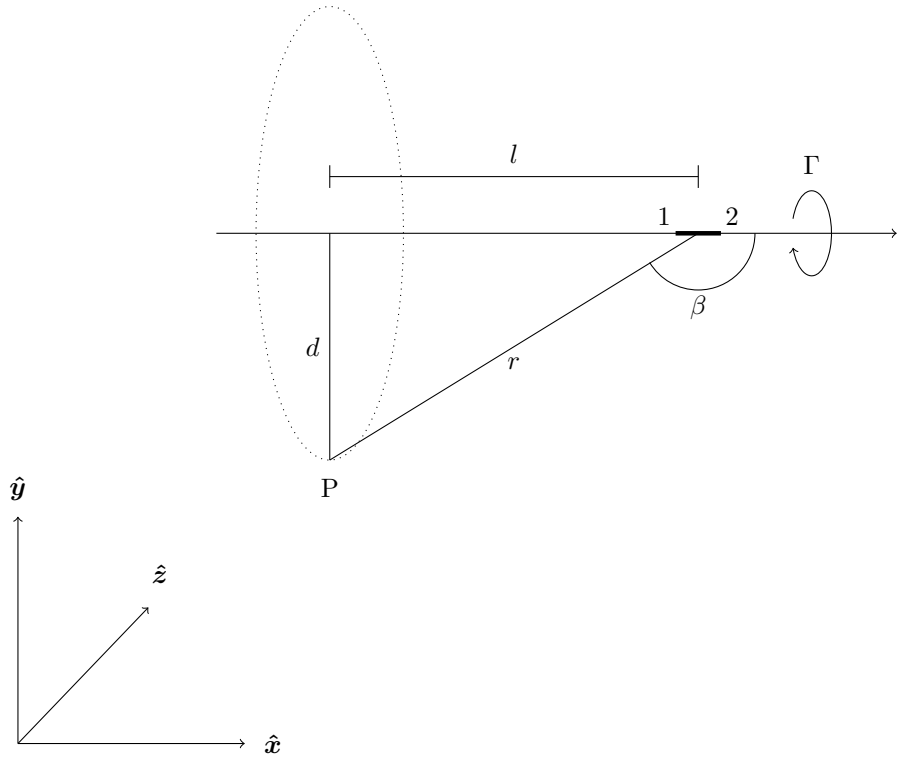

Figure 3.2: Definitions used for vortex line segment calculations. The vectors $\boldsymbol{x}_1$ and $\boldsymbol{x}_2$ denote the coordinates of the endpoints of the vortex line segment. These can be in any reference frame. Whatever reference frame is chosen, it must also be used to express the coordinates of the point of interest, $\boldsymbol{x}_\mathrm{P}$.

According to the Biot-Savart law, the velocity induced by a segment $\mathrm{d}\boldsymbol{l}$ on this line at point P is as follows:

$$\Delta \boldsymbol{u} = \frac{\Gamma}{4\pi}\frac{\mathrm{d}\boldsymbol{l} \times \boldsymbol{r}}{r^3} \tag{3.7}$$

Adopting a cylindrical polar coordinate system whose z-axis runs along the vortex segment, equation 3.7 may be expressed as follows:

$$\Delta u_\theta = \frac{\Gamma}{4\pi}\frac{\sin\beta}{r^2}\mathrm{d}l \tag{3.8}$$

From inspection of figure 3.2, it can be observed that

$$d = r\sin\beta$$

$$\tan(\pi - \beta) = \frac{d}{l} \tag{3.9}$$

Hence, by simple substitution,

$$l = -\frac{d}{\tan\beta} \tag{3.10}$$

since $\tan(\pi - \beta) = -\tan\beta$. Differentiating both sides yields the following result:

$$\mathrm{d}l = \frac{d}{\sin^2\beta}\mathrm{d}\beta \tag{3.11}$$

Hence, equation 3.8 may be reformulated as follows:

$$\Delta u_\theta = \frac{\Gamma}{4\pi d}\sin\beta\mathrm{d}\beta \tag{3.12}$$

The equation can then be integrated over the region $1 \rightarrow 2$ to give the velocity induced by the segment. Note, d is a constant (consider figure 3.2) and so can be taken outside of the integral.

$$\begin{aligned} u_\theta &= \frac{\Gamma}{4\pi d}\int_{\beta_1}^{\beta_2} \sin\beta \mathrm{d}\beta \\ &= \frac{\Gamma}{4\pi d}(\cos\beta_1 - \cos\beta_2) \end{aligned} \tag{3.13}$$

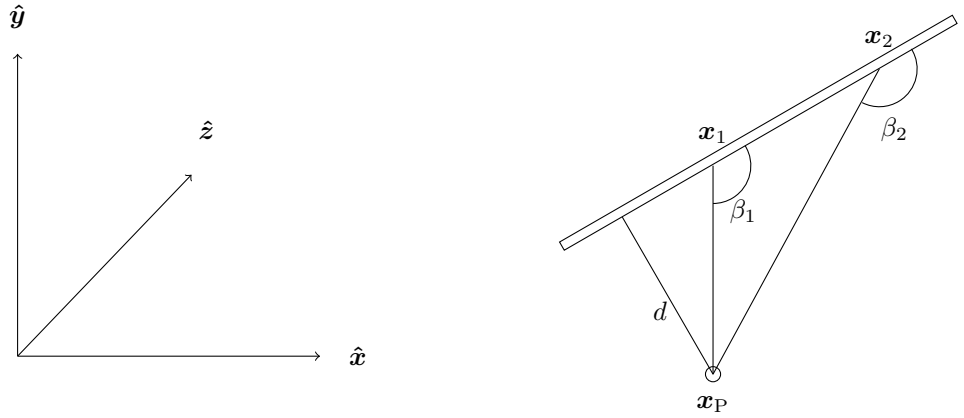

Figure 3.3: Definitions used for vortex line segment calculations. The vectors $\boldsymbol{x}_1$ and $\boldsymbol{x}_2$ denote the coordinates of the endpoints of the vortex line segment. These can be in any reference frame. Whatever reference frame is chosen, it must also be used to express the coordinates of the point of interest, $\boldsymbol{x}_\mathrm{P}$.

It is often more convenient to express the velocity in a Cartesian coordinate system. To convert from the cylindrical polar coordinates to the Cartesian coordinate system, first let us define a vector, $\boldsymbol{r}_0$ to be the vector extending from point 1 to point 2 of the line segment. If $\boldsymbol{r}_1$ is a vector extending from point 1 to the point of interest, P, and $\boldsymbol{r}_2$ is a vector extending from point 2 to the point of interest, P, then it immediately follows that

$$\boldsymbol{r}_0 = \boldsymbol{r}_1 - \boldsymbol{r}_2 \tag{3.14}$$

By considering the dot and cross products, it can then easily be shown that

$$\begin{aligned} d &= \frac{|\boldsymbol{r}_1 \times \boldsymbol{r}_2|}{|\boldsymbol{r}_0|} \\ \cos\beta_1 &= \frac{\boldsymbol{r}_0.\boldsymbol{r}_1}{|\boldsymbol{r}_0||\boldsymbol{r}_1|} \\ \cos\beta_2 &= \frac{\boldsymbol{r}_0.\boldsymbol{r}_2}{|\boldsymbol{r}_0||\boldsymbol{r}_2|} \end{aligned} \tag{3.15}$$

Substituting the above expressions into 3.13 yields the following result:

$$\boldsymbol{u} = \frac{\Gamma}{4\pi}\frac{\boldsymbol{r}_1 \times \boldsymbol{r}_2}{|\boldsymbol{r}_1 \times \boldsymbol{r}_2|^2}\boldsymbol{r}_0.\left(\frac{\boldsymbol{r}_1}{r_1} - \frac{\boldsymbol{r}_2}{r_2}\right) \tag{3.16}$$

Katz & Plotkin outline a simple process for implementing equation 3.16, which is provided below:

1. Calculate $\boldsymbol{r}_1 \times \boldsymbol{r}_2$:

$$\begin{aligned} (\boldsymbol{r}_1 \times \boldsymbol{r}_2)_x &= (y_\mathrm{p} - y_1)(z_\mathrm{p} - z_2) - (z_\mathrm{p} - z_1)(y_\mathrm{p} - y_2) \\ (\boldsymbol{r}_1 \times \boldsymbol{r}_2)_y &= (z_\mathrm{p} - z_1)(x_\mathrm{p} - x_2) - (x_\mathrm{p} - x_1)(z_\mathrm{p} - z_2) \\ (\boldsymbol{r}_1 \times \boldsymbol{r}_2)_z &= (x_\mathrm{p} - x_1)(y_\mathrm{p} - y_2) - (y_\mathrm{p} - y_1)(x_\mathrm{p} - x_2) \end{aligned} \tag{3.17}$$

2. Calculate $|\boldsymbol{r}_1 \times \boldsymbol{r}_2|^2$:

$$|\boldsymbol{r}_1 \times \boldsymbol{r}_2|^2 = (\boldsymbol{r}_1 \times \boldsymbol{r}_2)_x^2 + (\boldsymbol{r}_1 \times \boldsymbol{r}_2)_y^2 + (\boldsymbol{r}_1 \times \boldsymbol{r}_2)_z^2 \tag{3.18}$$

3. Calculate the distances r_1 and r_2:

$$r_1 = \sqrt{(x_\mathrm{p} - x_1)^2 + (y_\mathrm{p} - y_1)^2 + (z_\mathrm{p} - z_1)^2}$$
$$r_2 = \sqrt{(x_\mathrm{p} - x_2)^2 + (y_\mathrm{p} - y_2)^2 + (z_\mathrm{p} - z_2)^2} \tag{3.19}$$

4. Check for singular conditions - since the vortex solution is singular when the point P lies on the vortex, a special treatment is needed in the vicinity of the vortex segment which, for numerical purposes, is assumed to have a very small radius, ϵ:

   where ϵ (ep in the pseudo-code) is the vortex core size (which can be as small as the truncation error) or else u, v and w can be estimated by assuming solid body rotation or any other (more elaborate) vortex core model

5. Calculate the dot product:

$$\boldsymbol{r}_0.\boldsymbol{r}_1 = (x_2 - x_1)(x_\mathrm{p} - x_1) + (y_2 - y_1)(y_\mathrm{p} - y_1) + (z_2 - z_1)(z_\mathrm{p} - z_1)$$
$$\boldsymbol{r}_0.\boldsymbol{r}_2 = (x_2 - x_1)(x_\mathrm{p} - x_2) + (y_2 - y_1)(y_\mathrm{p} - y_2) + (z_2 - z_1)(z_\mathrm{p} - z_2) \tag{3.20}$$

6. Calculate the velocity components:

$$u = K.(\boldsymbol{r}_1 \times \boldsymbol{r}_2)_x$$
$$v = K.(\boldsymbol{r}_1 \times \boldsymbol{r}_2)_y$$
$$w = K.(\boldsymbol{r}_1 \times \boldsymbol{r}_2)_z \tag{3.21}$$

   where

$$K = \frac{\Gamma}{4\pi|\boldsymbol{r}_1 \times \boldsymbol{r}_2|^2}\left(\frac{\boldsymbol{r}_0.\boldsymbol{r}_1}{r_1} - \frac{\boldsymbol{r}_0.\boldsymbol{r}_2}{r_2}\right) \tag{3.22}$$

In Wind Panel, step 4 is updated so that a more realistic vortex core model is included.

While the above steps may suggest using the body reference frame, the calculation could just as easily be carried out in the global reference frame. Indeed, in many situations, it is preferable to do so to reduce the computational cost (arising from frame transformations).

3.3 The constant-strength source panel

A constant-strength source panel is depicted in figure 3.4:

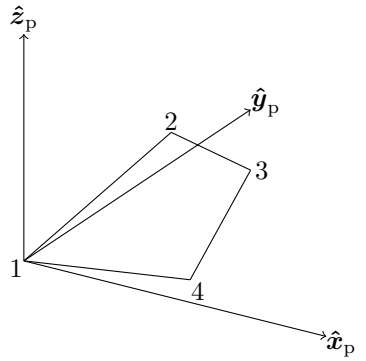

Figure 3.4: Illustration of a constant-strength source panel. The origin of the panel reference frame coincides with the corner point 1 and $\hat{\boldsymbol{z}}_\mathrm{p}$ is normal to the panel. There are no strict requirements on the relationship between corner points and $\hat{\boldsymbol{x}}$ and/or $\hat{\boldsymbol{y}}$.

The corresponding panel coordinate system is defined that has its origin located at corner point 1 and is orientated such that the $\hat{\boldsymbol{z}}_\mathrm{p}$ axis is normal to the panel. That is to say, the z-components of the panel corner points expressed in its own panel

coordinate system are 0 ($z_{1,\mathrm{p}} = 0$, $z_{2,\mathrm{p}} = 0$, $z_{3,\mathrm{p}} = 0$, $z_{4,\mathrm{p}} = 0$). The velocity potential produced by the panel at some point of interest with coordinates (as expressed in the panel coordinate system) $x_{\mathrm{P,p}}, y_{\mathrm{P,p}}, z_{\mathrm{P,p}}$ may be found using equation 3.23:

$$\Phi(x_{\mathrm{P,p}}, y_{\mathrm{P,p}}, z_{\mathrm{P,p}}) = -\frac{\sigma}{4\pi}\int_S \frac{\mathrm{d}S}{\sqrt{(x_{\mathrm{P,p}} - x_{0,\mathrm{p}})^2 + (y_{\mathrm{P,p}} - y_{0,\mathrm{p}})^2 + z_{\mathrm{P,p}}^2}} \tag{3.23}$$

where $x_{0,\mathrm{p}}$ and $y_{0,\mathrm{p}}$ denote the coordinates of the infinitesimally small element $\mathrm{d}S$.

The corresponding induced velocity being found through equation 3.24:

$$\begin{aligned}\boldsymbol{u}_{\mathrm{P,p}}^{\mathrm{T}} &= \begin{bmatrix} u_{\mathrm{P,p}} & v_{\mathrm{P,p}} & w_{\mathrm{P,p}} \end{bmatrix} \\ &= \begin{bmatrix} \dfrac{\partial\Phi}{\partial x_{\mathrm{p}}} & \dfrac{\partial\Phi}{\partial y_{\mathrm{p}}} & \dfrac{\partial\Phi}{\partial z_{\mathrm{p}}} \end{bmatrix}\end{aligned} \tag{3.24}$$

According to Hess & Smith, performing the integration in equation 3.23 over the area bound by the four straight lines (see figure 3.4) produces the following result:

$$\begin{aligned}\Phi = -\frac{\sigma}{4\pi}\Bigg\{\Bigg[&\left(\frac{x_{\mathrm{P,p}}y_{2,\mathrm{p}} - y_{\mathrm{P,p}}x_{2,\mathrm{p}}}{d_{12}}\right)\log\left(\frac{r_1 + r_2 + d_{12}}{r_1 + r_2 - d_{12}}\right) + \dots \\ &\left(\frac{(x_{\mathrm{P,p}} - x_{2,\mathrm{p}})(y_{3,\mathrm{p}} - y_{2,\mathrm{p}}) - (y_{\mathrm{P,p}} - y_{2,\mathrm{p}})(x_{3,\mathrm{p}} - x_{2,\mathrm{p}})}{d_{23}}\right)\log\left(\frac{r_2 + r_3 + d_{23}}{r_2 + r_3 - d_{23}}\right) + \dots \\ &\left(\frac{(x_{\mathrm{P,p}} - x_{3,\mathrm{p}})(y_{4,\mathrm{p}} - y_{3,\mathrm{p}}) - (y_{\mathrm{P,p}} - y_{3,\mathrm{p}})(x_{4,\mathrm{p}} - x_{3,\mathrm{p}})}{d_{34}}\right)\log\left(\frac{r_3 + r_4 + d_{34}}{r_3 + r_4 - d_{34}}\right) + \dots \\ &\left(\frac{x_{4,\mathrm{p}}(y_{\mathrm{P,p}} - y_{4,\mathrm{p}}) - y_{4,\mathrm{p}}(x_{\mathrm{P,p}} - x_{4,\mathrm{p}})}{d_{41}}\right)\log\left(\frac{r_4 + r_1 + d_{41}}{r_4 + r_1 - d_{41}}\right)\Bigg] - \dots \\ &|z_{\mathrm{P,p}}|\Bigg[\tan^{-1}\left(\frac{m_{12}e_1 - h_1}{z_{\mathrm{P,p}}r_1}\right) - \tan^{-1}\left(\frac{m_{12}e_2 - h_2}{z_{\mathrm{P,p}}r_2}\right) + \tan^{-1}\left(\frac{m_{23}e_2 - h_2}{z_{\mathrm{P,p}}r_2}\right) - \tan^{-1}\left(\frac{m_{23}e_3 - h_3}{z_{\mathrm{P,p}}r_3}\right) + \dots \\ &\tan^{-1}\left(\frac{m_{34}e_3 - h_3}{z_{\mathrm{P,p}}r_3}\right) - \tan^{-1}\left(\frac{m_{34}e_4 - h_4}{z_{\mathrm{P,p}}r_4}\right) + \tan^{-1}\left(\frac{m_{41}e_4 - h_4}{z_{\mathrm{P,p}}r_4}\right) - \tan^{-1}\left(\frac{m_{41}e_1 - h_1}{z_{\mathrm{P,p}}r_1}\right)\Bigg]\Bigg\}\end{aligned} \tag{3.25}$$

where

$$\begin{aligned} d_{12} &= \sqrt{(x_2 - x_1)^2 + (y_2 - y_1)^2} \\ d_{23} &= \sqrt{(x_3 - x_2)^2 + (y_3 - y_2)^2} \\ d_{34} &= \sqrt{(x_4 - x_3)^2 + (y_4 - y_3)^2} \\ d_{41} &= \sqrt{(x_1 - x_4)^2 + (y_1 - y_4)^2} \end{aligned} \tag{3.26}$$

and

$$\begin{aligned} m_{12} &= \frac{y_{2,\mathrm{p}}}{x_{2,\mathrm{p}}} \\ m_{23} &= \frac{y_{3,\mathrm{p}} - y_{2,\mathrm{p}}}{x_{3,\mathrm{p}} - x_{2,\mathrm{p}}} \\ m_{34} &= \frac{y_{4,\mathrm{p}} - y_{3,\mathrm{p}}}{x_{4,\mathrm{p}} - x_{3,\mathrm{p}}} \\ m_{41} &= \frac{y_{4,\mathrm{p}}}{x_{4,\mathrm{p}}} \end{aligned} \tag{3.27}$$

and

$$\begin{aligned} r_{\mathrm{k}} &= \sqrt{(x_{\mathrm{P}} - x_{\mathrm{k}})^2 + (y_{\mathrm{P}} - y_{\mathrm{k}})^2 + z_{\mathrm{P}}^2} \\ e_{\mathrm{k}} &= (x_{\mathrm{P,p}} - x_{\mathrm{k}})^2 + z_{\mathrm{P,p}}^2 \\ h_{\mathrm{k}} &= (x_{\mathrm{P,p}} - x_{\mathrm{k}})(y_{\mathrm{P,p}} - y_{\mathrm{k}}) \qquad\qquad k = 1, 2, 3, 4 \end{aligned} \tag{3.28}$$

Note, d_{ij} and r_{k} values are frame independent; hence, the body or global reference frame may be used for the calculation of these terms. The choice is ultimately determined by which one results in the lowest computational cost.

The velocity components are as follows:

$$u_{\mathrm{P,p}} = \frac{\sigma}{4\pi}\left[\frac{y_{2,\mathrm{p}}}{d_{12}}\log\left(\frac{r_1+r_2-d_{12}}{r_1+r_2+d_{12}}\right)+\frac{y_{3,\mathrm{p}}-y_{2,\mathrm{p}}}{d_{23}}\log\left(\frac{r_2+r_3-d_{23}}{r_2+r_3+d_{23}}\right)+\ldots\right.$$
$$\left.\frac{y_{4,\mathrm{p}}-y_{3,\mathrm{p}}}{d_{34}}\log\left(\frac{r_3+r_4-d_{34}}{r_3+r_4+d_{34}}\right)-\frac{y_{4,\mathrm{p}}}{d_{41}}\log\left(\frac{r_4+r_1-d_{41}}{r_4+r_1+d_{41}}\right)\right] \tag{3.29}$$

$$v_{\mathrm{P,p}} = \frac{\sigma}{4\pi}\left[-\frac{x_{2,\mathrm{p}}}{d_{12}}\log\left(\frac{r_1+r_2-d_{12}}{r_1+r_2+d_{12}}\right)+\frac{x_{2,\mathrm{p}}-x_{3,\mathrm{p}}}{d_{23}}\log\left(\frac{r_2+r_3-d_{23}}{r_2+r_3+d_{23}}\right)+\ldots\right.$$
$$\left.\frac{x_{3,\mathrm{p}}-x_{4,\mathrm{p}}}{d_{34}}\log\left(\frac{r_3+r_4-d_{34}}{r_3+r_4+d_{34}}\right)+\frac{x_{4,\mathrm{p}}}{d_{41}}\log\left(\frac{r_4+r_1-d_{41}}{r_4+r_1+d_{41}}\right)\right] \tag{3.30}$$

$$w_{\mathrm{P,p}} = \frac{\sigma}{4\pi}\left[\tan^{-1}\left(\frac{m_{12}e_1-h1}{z_{\mathrm{P,p}}r_1}\right)-\tan^{-1}\left(\frac{m_{12}e_2-h_2}{z_{\mathrm{P,p}}r_2}\right)+\tan^{-1}\left(\frac{m_{23}e_2-h_2}{zr_2}\right)-\tan^{-1}\left(\frac{m_{23}e_3-h_3}{z_{\mathrm{P,p}}r_3}\right)+\ldots\right.$$
$$\left.\tan^{-1}\left(\frac{m_{34}e_3-h_3}{z_{\mathrm{P,p}}r_3}\right)-\tan^{-1}\left(\frac{m_{34}e_4-h_4}{z_{\mathrm{P,p}}r_4}\right)+\tan^{-1}\left(\frac{m_{41}e_4-h_4}{z_{\mathrm{P,p}}r_4}\right)-\tan^{-1}\left(\frac{m_{41}e_1-h_1}{z_{\mathrm{P,p}}r_1}\right)\right] \tag{3.31}$$

$$\tag{3.32}$$

3.3.1 Far-field

As the separation between the panel and the point of interest tends to infinity, the $x_{\mathrm{P,p}}$, $y_{\mathrm{P,p}}$ and $z_{\mathrm{P,p}}$ terms dominate the $x_{0,\mathrm{p}}$ and $y_{0,\mathrm{p}}$ terms. Thus, the denominator in the integral is effectively constant over the panel surface. In this event, the potential may be evaluated as

$$\Phi(x_{\mathrm{P,p}}, y_{\mathrm{P,p}}, z_{\mathrm{P,p}}) = -\frac{\sigma A}{4\pi\sqrt{(x_{\mathrm{P,p}}-x_{\mathrm{c,p}})^2+(y_{\mathrm{P,p}}-y_{\mathrm{c,p}})^2+z_{\mathrm{P,p}}^2}} \tag{3.33}$$

where $x_{\mathrm{c,p}}$ and $y_{\mathrm{c,p}}$ are the coordinates of the panel centre (expressed in the panel reference frame). A is the area of the panel.

The corresponding velocity components are as follows:

$$u_{\mathrm{P,p}} = \frac{\sigma A(x-x_{\mathrm{c}})}{4\pi\left[(x_{\mathrm{P,p}}-x_{\mathrm{c,p}})^2+(y_{\mathrm{P,p}}-y_{\mathrm{c,p}})^2+z_{\mathrm{P,p}}^2\right]^{3/2}} \tag{3.34}$$

$$v_{\mathrm{P,p}} = \frac{\sigma A(x-x_{\mathrm{c}})}{4\pi\left[(x_{\mathrm{P,p}}-x_{\mathrm{c,p}})^2+(y_{\mathrm{P,p}}-y_{\mathrm{c,p}})^2+z_{\mathrm{P,p}}^2\right]^{3/2}} \tag{3.35}$$

$$w_{\mathrm{P,p}} = \frac{\sigma A(z-z_{\mathrm{c}})}{4\pi\left[(x_{\mathrm{P,p}}-x_{\mathrm{c,p}})^2+(y_{\mathrm{P,p}}-y_{\mathrm{c,p}})^2+z_{\mathrm{P,p}}^2\right]^{3/2}} \tag{3.36}$$

The far-field expressions represent a significant saving in computational cost and so should be used wherever possible. As a rule of thumb, the far-field and near field expressions become equivalent as the distance from the point of interest to the panel becomes 10 (or more) times as great as the average panel length (of the panel of interest).

3.4 The constant-strength doublet panel

Consider the constant-strength doublet panel as shown in figure 3.5. Analysis of the panel will be performed in the panel reference frame. The panel lies in the $x_{\mathrm{p}}y_{\mathrm{p}}$ plane. Furthermore, the origin of the panel reference frame is defined to coincide with corner point 1 of the panel.

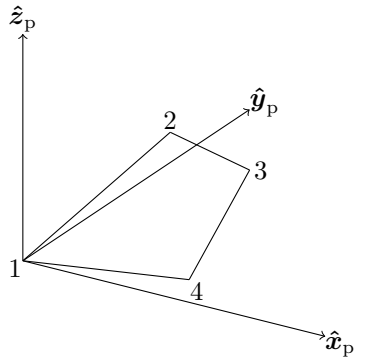

Figure 3.5: Illustration of a constant-strength doublet panel. The origin of the panel reference frame coincides with the corner point 1 and $\hat{\boldsymbol{z}}_\mathrm{p}$ is normal to the panel. There are no strict requirements on the relationship between corner points and $\hat{\boldsymbol{x}}$ and/or $\hat{\boldsymbol{y}}$.

$$\Phi(x_{\mathrm{P,p}}, y_{\mathrm{P,p}}, z_{\mathrm{P,p}}) = -\frac{\mu}{4\pi}\int_S \frac{z\mathrm{d}S}{\left[(x_{\mathrm{P,p}}-x)^2+(y_{\mathrm{P,p}}-y)^2+z_{\mathrm{P,p}}^2\right]^{3/2}} \tag{3.37}$$

According to Hess & Smith, equation 3.37 may be shown to be

$$\begin{aligned}\Phi = \frac{\mu}{4\pi}\Bigg[&\tan^{-1}\left(\frac{m_{12}e_1-h_1}{z_{\mathrm{P,p}}r_1}\right)-\tan^{-1}\left(\frac{m_{12}e_2-h_2}{z_{\mathrm{P,p}}r_2}\right)+\tan^{-1}\left(\frac{m_{23}e_2-h_2}{z_{\mathrm{P,p}}r_2}\right)-\tan^{-1}\left(\frac{m_{23}e_3-h_3}{z_{\mathrm{P,p}}r_3}\right)+\ldots\\ &\tan^{-1}\left(\frac{m_{34}e_3-h_3}{z_{\mathrm{P,p}}r_3}\right)-\tan^{-1}\left(\frac{m_{34}e_4-h_4}{z_{\mathrm{P,p}}r_4}\right)+\tan^{-1}\left(\frac{m_{41}e_4-h_4}{z_{\mathrm{P,p}}r_4}\right)-\tan^{-1}\left(\frac{m_{41}e_1-h_1}{z_{\mathrm{P,p}}r_1}\right)\Bigg]\end{aligned} \tag{3.38}$$

Correspondingly, the velocity components are as follows:

$$u_{\mathrm{P,p}} = \frac{\mu}{4\pi}\left[-\frac{z_{\mathrm{P,p}}y_{2,\mathrm{p}}(r_1+r_2)}{r_1r_2\left\{r_1r_2-\left[x_{\mathrm{P,p}}(x_{\mathrm{P,p}}-x_{2,\mathrm{p}})+y_{\mathrm{P,p}}(y_{\mathrm{P,p}}-y_{2,\mathrm{p}})+z_{\mathrm{P,p}}^2\right]\right\}}+\dots\right.$$
$$\frac{z_{\mathrm{P,p}}(y_{2,\mathrm{p}}-y_{3,\mathrm{p}})(r_2+r_3)}{r_2r_3\left\{r_2r_3-\left[(x_{\mathrm{P,p}}-x_{2,\mathrm{p}})(x_{\mathrm{P,p}}-x_{3,\mathrm{p}})+(y_{\mathrm{P,p}}-y_{2,\mathrm{p}})(y_{\mathrm{P,p}}-y_{3,\mathrm{p}})+z_{\mathrm{P,p}}^2\right]\right\}}+\dots$$
$$\frac{z_{\mathrm{P,p}}(y_{3,\mathrm{p}}-y_{4,\mathrm{p}})(r_3+r_4)}{r_3r_4\left\{r_3r_4-\left[(x_{\mathrm{P,p}}-x_{3,\mathrm{p}})(x_{\mathrm{P,p}}-x_{4,\mathrm{p}})+(y_{\mathrm{P,p}}-y_{3,\mathrm{p}})(y_{\mathrm{P,p}}-y_{4,\mathrm{p}})+z_{\mathrm{P,p}}^2\right]\right\}}+\dots$$
$$\left.\frac{z_{\mathrm{P,p}}y_{4,\mathrm{p}}(r_4+r_1)}{r_4r_1\left\{r_4r_1-\left[(x_{\mathrm{P,p}}-x_{4,\mathrm{p}})x_{\mathrm{P,p}}+(y_{\mathrm{P,p}}-y_{4,\mathrm{p}})y_{\mathrm{P,p}}+z_{\mathrm{P,p}}^2\right]\right\}}\right] \tag{3.39}$$

$$v_{\mathrm{P,p}} = \frac{\mu}{4\pi}\left[\frac{z_{\mathrm{P,p}}x_{2,\mathrm{p}}(r_1+r_2)}{r_1r_2\left\{r_1r_2-\left[x_{\mathrm{P,p}}(x_{\mathrm{P,p}}-x_{2,\mathrm{p}})+y_{\mathrm{P,p}}(y_{\mathrm{P,p}}-y_{2,\mathrm{p}})+z_{\mathrm{P,p}}^2\right]\right\}}+\dots\right.$$
$$\frac{z_{\mathrm{P,p}}(x_{3,\mathrm{p}}-x_{2,\mathrm{p}})(r_2+r_3)}{r_2r_3\left\{r_2r_3-\left[(x_{\mathrm{P,p}}-x_{2,\mathrm{p}})(x_{\mathrm{P,p}}-x_{3,\mathrm{p}})+(y_{\mathrm{P,p}}-y_{2,\mathrm{p}})(y_{\mathrm{P,p}}-y_{3,\mathrm{p}})+z_{\mathrm{P,p}}^2\right]\right\}}+\dots$$
$$\frac{z_{\mathrm{P,p}}(x_{4,\mathrm{p}}-x_{3,\mathrm{p}})(r_3+r_4)}{r_3r_4\left\{r_3r_4-\left[(x_{\mathrm{P,p}}-x_{3,\mathrm{p}})(x_{\mathrm{P,p}}-x_{4,\mathrm{p}})+(y_{\mathrm{P,p}}-y_{3,\mathrm{p}})(y_{\mathrm{P,p}}-y_{4,\mathrm{p}})+z_{\mathrm{P,p}}^2\right]\right\}}-\dots$$
$$\left.\frac{z_{\mathrm{P,p}}x_{4,\mathrm{p}}(r_4+r_1)}{r_4r_1\left\{r_4r_1-\left[(x_{\mathrm{P,p}}-x_{4,\mathrm{p}})x_{\mathrm{P,p}}+(y_{\mathrm{P,p}}-y_{4,\mathrm{p}})y_{\mathrm{P,p}}+z_{\mathrm{P,p}}^2\right]\right\}}\right] \tag{3.40}$$

$$w_{\mathrm{P,p}} = \frac{\mu}{4\pi}\left[-\frac{z_{\mathrm{P,p}}y_{2,\mathrm{p}}(r_1+r_2)}{r_1r_2\left\{r_1r_2-\left[x_{\mathrm{P,p}}(x_{\mathrm{P,p}}-x_{2,\mathrm{p}})+y_{\mathrm{P,p}}(y_{\mathrm{P,p}}-y_{2,\mathrm{p}})+z_{\mathrm{P,p}}^2\right]\right\}}+\dots\right.$$
$$\frac{z_{\mathrm{P,p}}(y_{2,\mathrm{p}}-y_{3,\mathrm{p}})(r_2+r_3)}{r_2r_3\left\{r_2r_3-\left[(x_{\mathrm{P,p}}-x_{2,\mathrm{p}})(x_{\mathrm{P,p}}-x_{3,\mathrm{p}})+(y_{\mathrm{P,p}}-y_{2,\mathrm{p}})(y_{\mathrm{P,p}}-y_{3,\mathrm{p}})+z_{\mathrm{P,p}}^2\right]\right\}}+\dots$$
$$\frac{z_{\mathrm{P,p}}(y_{3,\mathrm{p}}-y_{4,\mathrm{p}})(r_3+r_4)}{r_3r_4\left\{r_3r_4-\left[(x_{\mathrm{P,p}}-x_{3,\mathrm{p}})(x_{\mathrm{P,p}}-x_{4,\mathrm{p}})+(y_{\mathrm{P,p}}-y_{3,\mathrm{p}})(y_{\mathrm{P,p}}-y_{4,\mathrm{p}})+z_{\mathrm{P,p}}^2\right]\right\}}+\dots$$
$$\left.\frac{z_{\mathrm{P,p}}y_{4,\mathrm{p}}(r_4+r_1)}{r_4r_1\left\{r_4r_1-\left[(x_{\mathrm{P,p}}-x_{4,\mathrm{p}})x_{\mathrm{P,p}}+(y_{\mathrm{P,p}}-y_{4,\mathrm{p}})y_{\mathrm{P,p}}+z_{\mathrm{P,p}}^2\right]\right\}}\right] \tag{3.41}$$

3.4.1 Far field

As the separation between the panel and the point of interest tends to infinity, the $x_{\mathrm{P,p}}$, $y_{\mathrm{P,p}}$ and $z_{\mathrm{P,p}}$ terms dominate the $x_{0,\mathrm{p}}$ and $y_{0,\mathrm{p}}$ terms. Thus, the denominator in the integral is effectively constant over the panel surface. In this event, the potential may be evaluated as

$$\phi = -\frac{\mu A z_{\mathrm{P,p}}}{4\pi\left[(x_{\mathrm{P,p}}-x_{\mathrm{c,p}})^2+(y_{\mathrm{P,p}}-y_{\mathrm{c,p}})^2+z_{\mathrm{P,p}}^2\right]^{3/2}} \tag{3.42}$$

where $\begin{bmatrix} x_{\mathrm{c,p}} & y_{\mathrm{c,p}} & z_{\mathrm{c,p}} \end{bmatrix}$ are the coordinates of the panel centre as expressed in the panel reference frame.

$$u_{\mathrm{P,p}} = \frac{3\mu A(x_{\mathrm{P,p}} - x_{\mathrm{c,p}})z_{\mathrm{P,p}}}{4\pi\left[(x_{\mathrm{P,p}} - x_{\mathrm{c,p}})^2 + (y_{\mathrm{P,p}} - y_{\mathrm{c,p}})^2 + z_{\mathrm{P,p}}^2\right]^{5/2}} \tag{3.43}$$

$$v_{\mathrm{P,p}} = \frac{3\mu A(y_{\mathrm{P,p}} - y_{\mathrm{c,p}})z_{\mathrm{P,p}}}{4\pi\left[(x_{\mathrm{P,p}} - x_{\mathrm{c,p}})^2 + (y_{\mathrm{P,p}} - y_{\mathrm{c,p}})^2 + z_{\mathrm{P,p}}^2\right]^{5/2}} \tag{3.44}$$

$$w_{\mathrm{P,p}} = \frac{3\mu A\left((x_{\mathrm{P,p}} - x_{\mathrm{c,p}})^2 + (y_{\mathrm{P,p}} - y_{\mathrm{c,p}})^2 - 2z_{\mathrm{P,p}}^2\right)}{4\pi\left[(x_{\mathrm{P,p}} - x_{\mathrm{c,p}})^2 + (y_{\mathrm{P,p}} - y_{\mathrm{c,p}})^2 + z_{\mathrm{P,p}}^2\right]^{5/2}} \tag{3.45}$$

The far-field expressions represent a significant saving in computational cost and so should be used wherever possible. As a rule of thumb, the far-field and near field expressions become equivalent as the distance from the point of interest to the panel becomes 10 (or more) times as great as the average panel length (of the panel of interest).

3.4.2 Equivalence of the constant-strength doublet panel and a vortex ring

$$\Phi = -\frac{\mu}{4\pi}\int_S \frac{z\mathrm{d}S}{r^3} \tag{3.46}$$

$$\begin{aligned} \boldsymbol{u} &= \nabla\phi \\ &= -\frac{\mu}{4\pi}\int_{\mathrm{S}} \nabla\left(\frac{z_{\mathrm{P,p}}}{r^3}\right)\mathrm{d}S \\ &= \frac{\mu}{4\pi}\int_{\mathrm{S}}\left[\frac{\partial}{\partial x_0}\frac{z}{r^3}\hat{\boldsymbol{x}} + \frac{\partial}{\partial y_0}\frac{z}{r^3}\hat{\boldsymbol{y}} - \left(\frac{1}{r^3} - \frac{3z^2}{r^5}\right)\hat{\boldsymbol{z}}\right]\mathrm{d}S \end{aligned} \tag{3.47}$$

$$\boldsymbol{u} = \frac{\Gamma}{4\pi}\int_{\mathrm{C}} \frac{\mathrm{d}\boldsymbol{l}\times\boldsymbol{r}}{r^3} \tag{3.48}$$

$$\boldsymbol{u} = \frac{\Gamma}{4\pi}\int_{\mathrm{C}}\left\{\frac{z}{r^3}\mathrm{d}y_0\hat{\boldsymbol{x}} - \frac{z}{r^3}\mathrm{d}x_0\hat{\boldsymbol{y}} + \left[\frac{(y-y_0)\mathrm{d}x_0}{r^3} - \frac{(x-x_0)\mathrm{d}y_0}{r^3}\right]\hat{\boldsymbol{z}}\right\} \tag{3.49}$$

$$\oint_{\mathrm{C}} \boldsymbol{A}.\mathrm{d}\boldsymbol{l} = \int_{\mathrm{S}} \hat{\boldsymbol{n}}.\nabla\times\boldsymbol{A}\mathrm{d}S \tag{3.50}$$

Let us set $\hat{\boldsymbol{n}} = \hat{\boldsymbol{z}}$. Hence,

$$\oint_{\mathrm{C}} \boldsymbol{A}.\mathrm{d}\boldsymbol{l} = \int_{\mathrm{S}}\left(\frac{\partial A_y}{\partial x_0} - \frac{\partial A_x}{\partial y_0}\right)\mathrm{d}S \tag{3.51}$$

Thus,

$$\boldsymbol{u} = \frac{\Gamma}{4\pi}\int_{\mathrm{S}}\left[\frac{\partial}{\partial x_0}\left(\frac{z}{r^3}\right)\hat{\boldsymbol{x}} + \frac{\partial}{\partial y_0}\left(\frac{z}{r^3}\right)\hat{\boldsymbol{y}} - \left(\frac{\partial}{\partial x_0}\left(\frac{x-x_0}{r^3}\right) + \frac{\partial}{\partial y_0}\left(\frac{y-y_0}{r^3}\right)\right)\hat{\boldsymbol{z}}\right]\mathrm{d}S \tag{3.52}$$

3.5 From the panel reference frame to the body reference frame

As with the 2D case, it is necessary to have expressions which allow conversion from the panel reference frame to the body reference frame. For coordinates, it can be noted that this is achieved by adopting a manipulated form of equation 3.6:

$$\begin{bmatrix} x_{\mathrm{P}} \\ y_{\mathrm{P}} \\ z_{\mathrm{P}} \end{bmatrix} = \begin{bmatrix} \hat{\boldsymbol{x}}_{\mathrm{p_i}}^{\mathrm{T}} \\ \hat{\boldsymbol{y}}_{\mathrm{p_i}}^{\mathrm{T}} \\ \hat{\boldsymbol{z}}_{\mathrm{p_i}}^{\mathrm{T}} \end{bmatrix}^{-1} \begin{bmatrix} x_{\mathrm{P,p}} \\ y_{\mathrm{P,p}} \\ z_{\mathrm{P,p}} \end{bmatrix} + \begin{bmatrix} x_{0_{\mathrm{i}}} \\ y_{0_{\mathrm{i}}} \\ z_{0_{\mathrm{i}}} \end{bmatrix} \tag{3.53}$$

Hence, the transformation for velocity is simply

$$\begin{bmatrix} u_{\mathrm{P}} \\ v_{\mathrm{P}} \\ w_{\mathrm{P}} \end{bmatrix} = \begin{bmatrix} \hat{\boldsymbol{x}}_{\mathrm{p_i}}^{\mathrm{T}} \\ \hat{\boldsymbol{y}}_{\mathrm{p_i}}^{\mathrm{T}} \\ \hat{\boldsymbol{z}}_{\mathrm{p_i}}^{\mathrm{T}} \end{bmatrix}^{-1} \begin{bmatrix} u_{\mathrm{P,p}} \\ v_{\mathrm{P,p}} \\ w_{\mathrm{P,p}} \end{bmatrix} \tag{3.54}$$

Chapter 4

The first order panel method

Let us consider an aerofoil whose shape has been represented by a set of lines as shown in figure 4.1:

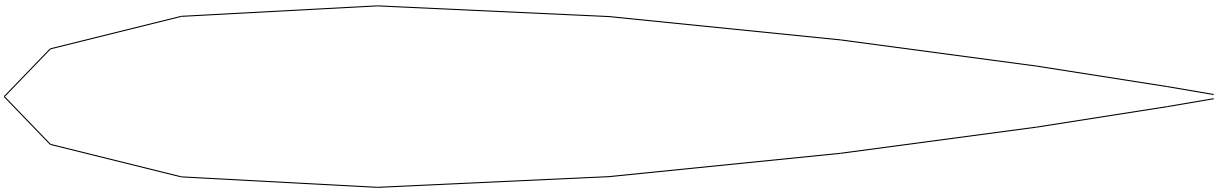

Figure 4.1: Panel representation of an aerofoil.

The aim is to determine the forces acting on an object. If the fluid is assumed to be inviscid, irrotational and incompressible, we know that it must be possible to describe the flow field by Laplace's equation. Let us also recall that the velocity potential is related to velocity by

$$\boldsymbol{u} = \nabla\Phi \tag{4.1}$$

Far from the aerofoil (and its associated wake), the disturbances to the velocity potential (arising from the aerofoil and its wake) must tend to zero. That is,

$$\lim_{r\to\infty} (\nabla\Phi - \boldsymbol{u}_{\mathrm{bgd}}) \to 0 \tag{4.2}$$

4.1 Panel methods using the Neumann boundary condition

4.1.1 Steady flow past a single aerofoil in two dimensions

Let us imagine that each line in figure 4.1 is a constant-strength panel. Each panel may be composed of one or more of the fundamental solutions. In the following examples, each panel shall be a constant-strength doublet panel.

Given the linearity of the velocity potential, it also follows that the velocity field is itself linear. That is to say, the velocity at some point in space is the linear sum of the velocities induced by all elements in the flow on the point of interest.

Let us define a set of 'collocation points', one for each panel. Collocation points are points of interest where boundary conditions will be enforced. The Neumann boundary condition stipulates that the fluid velocity normal to a solid surface must be zero as expressed in the body reference frame. That is, for some collocation point 'i',

$$\left(\boldsymbol{u}_{\infty,\mathrm{i}} + \sum_{j=1}^{N_{\mathrm{p}}} \mu_{\mathrm{j}} \boldsymbol{a}'_{\mathrm{j}\to\mathrm{i}}\right) . \hat{\boldsymbol{n}}_{\mathrm{i}} = 0 \tag{4.3}$$

where

$$\boldsymbol{a}'_{\mathrm{j}\to\mathrm{i}} = \begin{bmatrix} u_{\mathrm{j}\to\mathrm{i}} & v_{\mathrm{j}\to\mathrm{i}} \end{bmatrix} \tag{4.4}$$

where $u_{j\to i}$ is the x-component velocity induced by panel 'j' on collocation point 'i' when the strength of the panel is set to $\mu_j = 1$ (found using equation 2.30 and the necessary frame transformations); $v_{j\to i}$ is the corresponding y-component (found using equation 2.31 and the necessary frame transformations). $\hat{\boldsymbol{n}}_i$ is a unit vector which is normal to the panel associated with collocation point 'i' (see figure 4.2).

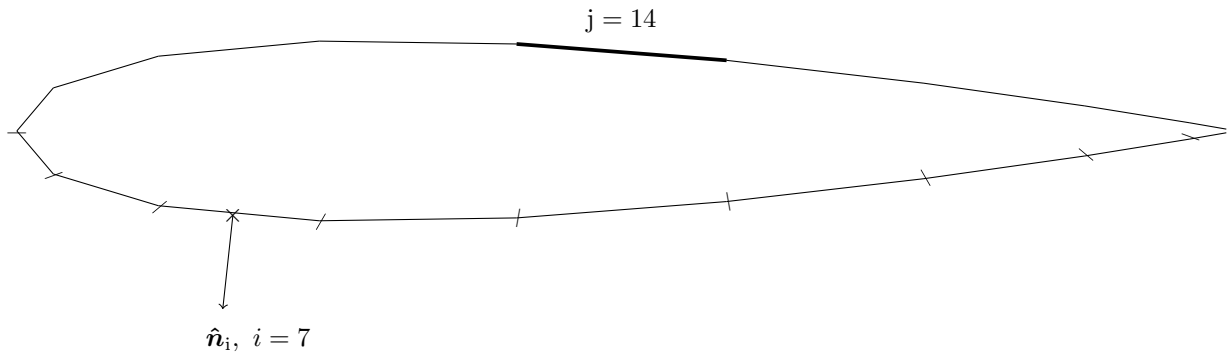

Figure 4.2: Illustration of a collocation point located at the midpoint between a panel's end points.

Referring to equation 4.3, it can be noted that the entire system may be represented in the following way:

$$0 = \underbrace{\begin{bmatrix} \boldsymbol{u}_{\infty,1}.\hat{\boldsymbol{n}}_1 \\ \boldsymbol{u}_{\infty,2}.\hat{\boldsymbol{n}}_2 \\ \boldsymbol{u}_{\infty,3}.\hat{\boldsymbol{n}}_3 \\ \vdots \\ \boldsymbol{u}_{\infty,N_p-1}.\hat{\boldsymbol{n}}_{N_p-1} \\ \boldsymbol{u}_{\infty,N_p}.\hat{\boldsymbol{n}}_{N_p} \end{bmatrix}}_{\mathbf{RHS}} + \underbrace{\begin{bmatrix} a'_{1,1} & a'_{1,2} & a'_{1,3} & \cdots & a'_{1,N_p-1} & a'_{1,N_p} \\ a'_{2,1} & a'_{2,2} & a'_{2,3} & \cdots & a'_{2,N_p-1} & a'_{2,N_p} \\ a'_{3,1} & a'_{3,2} & a'_{3,3} & \cdots & a'_{3,N_p-1} & a'_{3,N_p} \\ \vdots & \vdots & \vdots & \ddots & \vdots & \vdots \\ a'_{N_p-1,1} & a'_{N_p-1,2} & a'_{N_p-1,3} & \cdots & a'_{N_p-1,N_p-1} & a'_{N_p-1,N_p} \\ a'_{N_p,1} & a'_{N_p,2} & a'_{N_p,3} & \cdots & a'_{N_p,N_p-1} & a'_{N_p,N_p} \end{bmatrix}}_{\boldsymbol{A}'} \underbrace{\begin{bmatrix} \mu_1 \\ \mu_2 \\ \mu_3 \\ \vdots \\ \mu_{N_p-1} \\ \mu_{N_p} \end{bmatrix}}_{\boldsymbol{\mu}} \tag{4.5}$$

where $a'_{i,j} = \boldsymbol{a}'_{j\to i}.\hat{\boldsymbol{n}}_i$.

To complete the problem formulation, the Kutta condition must be enforced (if it is not, uniqueness cannot be guaranteed). In Wind Panel, the Kutta condition is introduced according to the following statement: *the circulation around any trailing edge must be zero.*

That is, $\Gamma_{TE} = 0$. Given that a constant-strength doublet panel is equivalent to two counter-rotating vortices placed at the panel corners, it follows that the circulation due to the two body panels that meet at the trailing edge evaluated at the trailing edge is $\mu_l - \mu_u$. For steady flow, the Kutta condition is fulfilled by introducing a wake doublet panel (which again may be thought of as a pair of counter-rotating vortices placed at the panel corners) whose strength, μ_w, satisfies the following condition:

$$\mu_w + (\mu_l - \mu_u) = 0 \tag{4.6}$$

In steady flow conditions, the length of the wake panel is set such that the equivalent vortex (from the wake doublet panel) which is not at the trailing edge is sufficiently far from the aerofoil. This vortex becomes equivalent to a starting vortex.

Additionally, the orientation of the wake panel is chosen such that it is parallel to the bisector at the trailing edge as shown in figure 4.3:

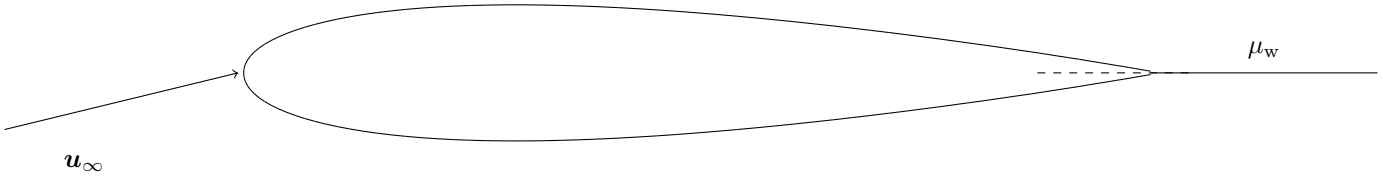

Figure 4.3: Illustration of the orientation of the wake panel and the bisector at the trailing edge.

At this point, the influence of the wake doublet panel on all collocation points needs to be factored in. Equation 4.5 could

be expressed as

$$0 = \underbrace{\begin{bmatrix} \boldsymbol{u}_{\infty,1}.\hat{\boldsymbol{n}}_1 \\ \boldsymbol{u}_{\infty,2}.\hat{\boldsymbol{n}}_2 \\ \boldsymbol{u}_{\infty,3}.\hat{\boldsymbol{n}}_3 \\ \vdots \\ \boldsymbol{u}_{\infty,\mathrm{N_p}-1}.\hat{\boldsymbol{n}}_{\mathrm{N_p}-1} \\ \boldsymbol{u}_{\infty,\mathrm{N_p}}.\hat{\boldsymbol{n}}_{\mathrm{N_p}} \end{bmatrix}}_{\mathbf{RHS}} + \underbrace{\begin{bmatrix} a'_{1,1} & a'_{1,2} & a'_{1,3} & \cdots & a'_{1,\mathrm{N_p}-1} & a'_{1,\mathrm{N_p}} \\ a'_{2,1} & a'_{2,2} & a'_{2,3} & \cdots & a'_{2,\mathrm{N_p}-1} & a'_{2,\mathrm{N_p}} \\ a'_{3,1} & a'_{3,2} & a'_{3,3} & \cdots & a'_{3,\mathrm{N_p}-1} & a'_{3,\mathrm{N_p}} \\ \vdots & \vdots & \vdots & \ddots & \vdots & \vdots \\ a'_{\mathrm{N_p}-1,1} & a'_{\mathrm{N_p}-1,2} & a'_{\mathrm{N_p}-1,3} & \cdots & a'_{\mathrm{N_p}-1,\mathrm{N_p}-1} & a'_{\mathrm{N_p}-1,\mathrm{N_p}} \\ a'_{\mathrm{N_p},1} & a'_{\mathrm{N_p},2} & a'_{\mathrm{N_p},3} & \cdots & a'_{\mathrm{N_p},\mathrm{N_p}-1} & a'_{\mathrm{N_p},\mathrm{N_p}} \end{bmatrix}}_{\boldsymbol{A'}} \underbrace{\begin{bmatrix} \mu_1 \\ \mu_2 \\ \mu_3 \\ \vdots \\ \mu_{\mathrm{N_p}-1} \\ \mu_{\mathrm{N_p}} \end{bmatrix}}_{\boldsymbol{\mu}} + \underbrace{\begin{bmatrix} c_1 \\ c_2 \\ c_3 \\ \vdots \\ c_{\mathrm{N_p}-1} \\ c_{\mathrm{N_p}} \end{bmatrix}}_{\boldsymbol{C}_\mathrm{W}} \mu_\mathrm{w} \tag{4.7}$$

where $c'_\mathrm{i} = \boldsymbol{c}'_{\mathrm{w}\to\mathrm{i}}.\hat{\boldsymbol{n}}_\mathrm{i}$

$$\boldsymbol{c}'_{\mathrm{w}\to\mathrm{i}} = \begin{bmatrix} u_{\mathrm{w}\to\mathrm{i}} & v_{\mathrm{w}\to\mathrm{i}} \end{bmatrix} \tag{4.8}$$

By exploiting the Kutta condition, equation 4.7 may be reduced to the following expression:

$$0 = \underbrace{\begin{bmatrix} \boldsymbol{u}_{\infty,1}.\hat{\boldsymbol{n}}_1 \\ \boldsymbol{u}_{\infty,2}.\hat{\boldsymbol{n}}_2 \\ \boldsymbol{u}_{\infty,3}.\hat{\boldsymbol{n}}_3 \\ \vdots \\ \boldsymbol{u}_{\infty,\mathrm{N_p}-1}.\hat{\boldsymbol{n}}_{\mathrm{N_p}-1} \\ \boldsymbol{u}_{\infty,\mathrm{N_p}}.\hat{\boldsymbol{n}}_{\mathrm{N_p}} \end{bmatrix}}_{\mathbf{RHS}} + \underbrace{\begin{bmatrix} a_{1,1} & a_{1,2} & a_{1,3} & \cdots & a_{1,\mathrm{N_p}-1} & a_{1,\mathrm{N_p}} \\ a_{2,1} & a_{2,2} & a_{2,3} & \cdots & a_{2,\mathrm{N_p}-1} & a_{2,\mathrm{N_p}} \\ a_{3,1} & a_{3,2} & a_{3,3} & \cdots & a_{3,\mathrm{N_p}-1} & a_{3,\mathrm{N_p}} \\ \vdots & \vdots & \vdots & \ddots & \vdots & \vdots \\ a_{\mathrm{N_p}-1,1} & a_{\mathrm{N_p}-1,2} & a_{\mathrm{N_p}-1,3} & \cdots & a_{\mathrm{N_p}-1,\mathrm{N_p}-1} & a_{\mathrm{N_p}-1,\mathrm{N_p}} \\ a_{\mathrm{N_p},1} & a_{\mathrm{N_p},2} & a_{\mathrm{N_p},3} & \cdots & a_{\mathrm{N_p},\mathrm{N_p}-1} & a_{\mathrm{N_p},\mathrm{N_p}} \end{bmatrix}}_{\boldsymbol{A}} \underbrace{\begin{bmatrix} \mu_1 \\ \mu_2 \\ \mu_3 \\ \vdots \\ \mu_{\mathrm{N_p}-1} \\ \mu_{\mathrm{N_p}} \end{bmatrix}}_{\boldsymbol{\mu}} \tag{4.9}$$

where

$$a_{\mathrm{i,j}} = \begin{cases} a'_{\mathrm{i,j}} - c_\mathrm{j} & \text{if } j = 1 \\ a'_{\mathrm{i,j}} + c_\mathrm{j} & \text{if } j = N_\mathrm{p} \\ a'_{\mathrm{i,j}} & \text{if } j \neq 1 \ \& \ j \neq N_\mathrm{p} \end{cases}$$

That is, the system has become a classic $\boldsymbol{Ax} = \boldsymbol{b}$ style equation, which can be solved using standard matrix algorithms. Once the 'strengths' of the panels (in this case $\boldsymbol{\mu}$) are determined, the system is sufficiently described for a calculation of the pressure distribution over the aerofoil to be carried out.

An example of the doublet panel method with the Neumann boundary condition is shown in figure 4.4. In this figure, the pressure distribution as predicted by the panel method is provided. The number of panels used to represent the aerofoil was 200.

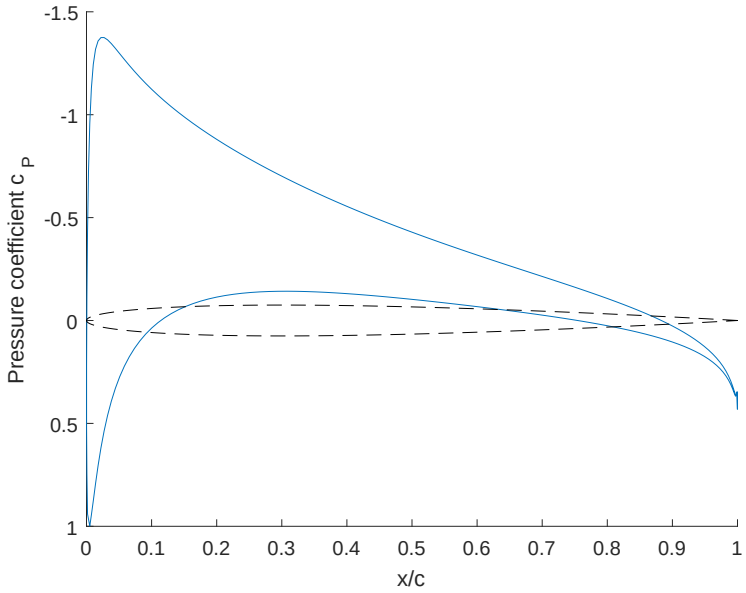

Figure 4.4: Pressure distribution as predicted using the 2D doublet panel method with the Neumann boundary conditin. The angle of attack was 4^o.

4.1.2 Steady flow past a wing in three dimensions

Consider the wing as shown in figure 4.5:

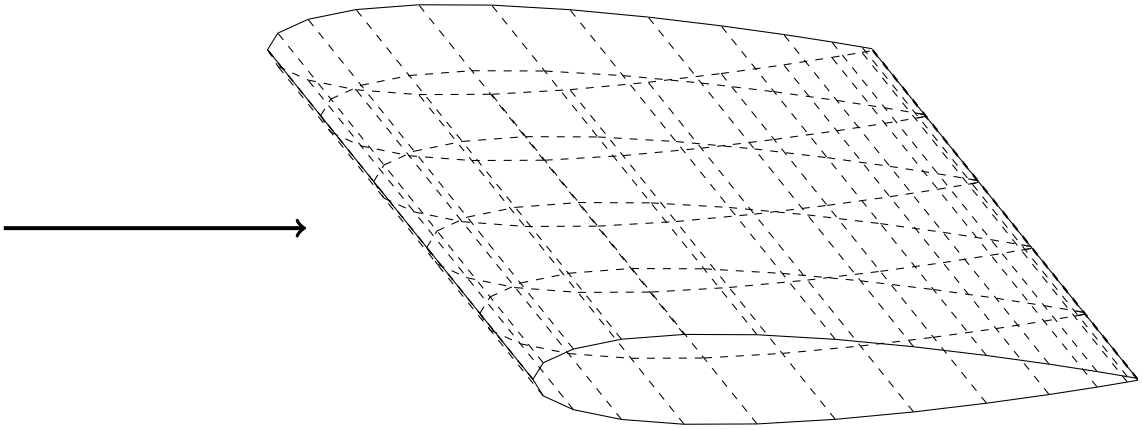

Figure 4.5: The number of segments into which the trailing edge line has been divided, N_{TE}, in this case is five.

It has been represented by a set of quadrilateral (constant-strength doublet) panels. The problem formulation is similar. Referring to figure 4.5, it can be noted that there are now $2\mathrm{N_{TE}}$ body panels that are connected to the trailing edge (two for each height (upper and lower surfaces)).

Recall that in three dimensions, a constant-strength doublet panel is equivalent to a vortex ring. That is, at a given segment of the trailing edge, 'k', the contribution to circulation from the body panels is $\mu_{\mathrm{l_k}} - \mu_{\mathrm{u_k}}$. This is balanced by the contribution to circulation from the wake panel which connects to the body at the trailing edge segment of interest. That is,

$$\mu_{\mathrm{w_k}} + (\mu_{\mathrm{l_k}} - \mu_{\mathrm{u_k}}) = 0 \tag{4.10}$$

That is, to enforce the Kutta condition along the whole of the trailing edge, N_{TE} wake panels are introduced as shown in figure 4.6 whose strengths are determined using equation 4.10.

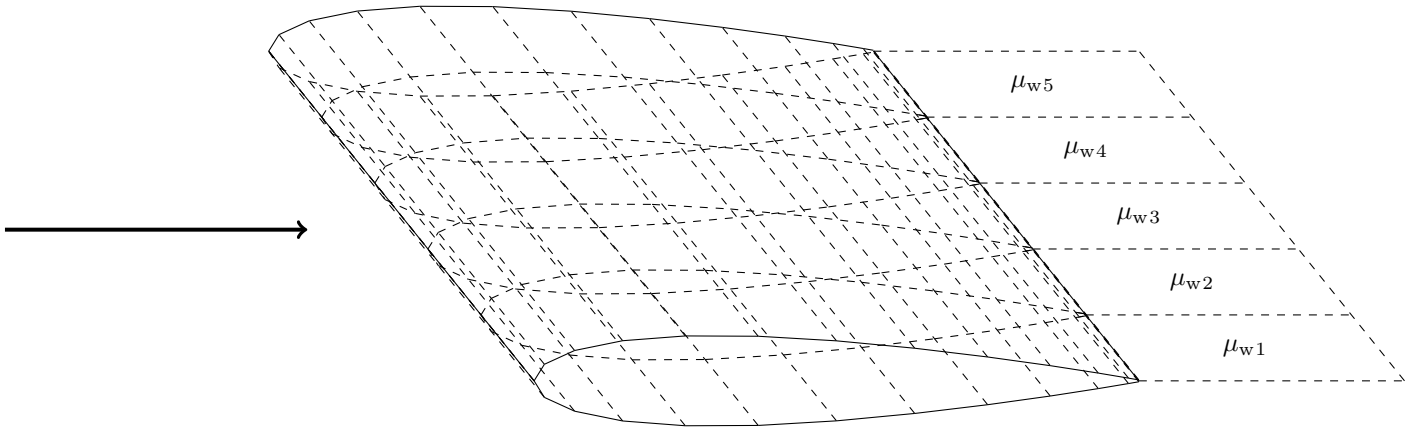

Figure 4.6: Illustration of the orientation of the wake panel and the bisector at the trailing edge.

The system is thus described by equation 4.11:

$$0 = \underbrace{\begin{bmatrix} \boldsymbol{u}_{\infty,1}.\hat{\boldsymbol{n}}_1 \\ \boldsymbol{u}_{\infty,2}.\hat{\boldsymbol{n}}_2 \\ \boldsymbol{u}_{\infty,3}.\hat{\boldsymbol{n}}_3 \\ \vdots \\ \boldsymbol{u}_{\infty,\mathrm{N_t}-1}.\hat{\boldsymbol{n}}_{\mathrm{N_t}-1} \\ \boldsymbol{u}_{\infty,\mathrm{N_t}}.\hat{\boldsymbol{n}}_{\mathrm{N_t}} \end{bmatrix}}_{\mathbf{RHS}} + \underbrace{\begin{bmatrix} a'_{1,1} & a'_{1,2} & a'_{1,3} & \cdots & a'_{1,\mathrm{N_t}-1} & a'_{1,\mathrm{N_t}} \\ a'_{2,1} & a'_{2,2} & a'_{2,3} & \cdots & a'_{2,\mathrm{N_t}-1} & a'_{2,\mathrm{N_t}} \\ a'_{3,1} & a'_{3,2} & a'_{3,3} & \cdots & a'_{3,\mathrm{N_t}-1} & a'_{3,\mathrm{N_t}} \\ \vdots & \vdots & \vdots & \ddots & \vdots & \vdots \\ a'_{\mathrm{N_t}-1,1} & a'_{\mathrm{N_t}-1,2} & a'_{\mathrm{N_t}-1,3} & \cdots & a'_{\mathrm{N_t}-1,\mathrm{N_t}-1} & a'_{\mathrm{N_t}-1,\mathrm{N_t}} \\ a'_{\mathrm{N_t},1} & a'_{\mathrm{N_t},2} & a'_{\mathrm{N_t},3} & \cdots & a'_{\mathrm{N_t},\mathrm{N_t}-1} & a'_{\mathrm{N_t},\mathrm{N_t}} \end{bmatrix}}_{\boldsymbol{A'}} \underbrace{\begin{bmatrix} \mu_1 \\ \mu_2 \\ \mu_3 \\ \vdots \\ \mu_{\mathrm{N_p}-1} \\ \mu_{\mathrm{N_p}} \end{bmatrix}}_{\boldsymbol{\mu}_\mathrm{b}} + \cdots$$

$$\underbrace{\begin{bmatrix} c_{1,1} & c_{1,2} & c_{1,3} & \cdots & c_{1,\mathrm{N_{TE}}-1} & c_{1,\mathrm{N_{TE}}} \\ c_{2,1} & c_{2,2} & c_{2,3} & \cdots & c_{2,\mathrm{N_{TE}}-1} & c_{2,\mathrm{N_{TE}}} \\ c_3 & c_{3,2} & c_{3,3} & \cdots & c_{3,\mathrm{N_{TE}}-1} & c_{3,\mathrm{N_{TE}}} \\ \vdots & \vdots & \vdots & \ddots & \vdots & \vdots \\ c_{\mathrm{N_t}-1,1} & c_{\mathrm{N_t}-1,2} & c_{\mathrm{N_t}-1,3} & \cdots & c_{\mathrm{N_t}-1,\mathrm{N_{TE}}-1} & c_{\mathrm{N_t}-1,\mathrm{N_{TE}}} \\ c_{\mathrm{N_t},\mathrm{w}_1} & c_{\mathrm{N_t},\mathrm{w}_2} & c_{\mathrm{N_t},\mathrm{w}_3} & \cdots & c_{\mathrm{N_t},\mathrm{w}_{\mathrm{N_{TE}}}} & c_{\mathrm{N_t},\mathrm{w}_{\mathrm{N_{TE}}}} \end{bmatrix}}_{\boldsymbol{C}_\mathrm{w}} \underbrace{\begin{bmatrix} \mu_{\mathrm{w}_1} \\ \mu_{\mathrm{w}_2} \\ \mu_{\mathrm{w}_3} \\ \vdots \\ \mu_{\mathrm{N_{TE}}-1} \\ \mu_{\mathrm{N_{TE}}} \end{bmatrix}}_{\boldsymbol{\mu}_\mathrm{w}} \tag{4.11}$$

As before, $a'_{\mathrm{i,j}} = \boldsymbol{a}'_{\mathrm{j}\to\mathrm{i}}.\hat{\boldsymbol{n}}_\mathrm{i}$; however, in this case, $\boldsymbol{a}'_{\mathrm{j}\to\mathrm{i}} = \begin{bmatrix} u_{\mathrm{j}\to\mathrm{i}} & v_{\mathrm{j}\to\mathrm{i}} & w_{\mathrm{j}\to\mathrm{i}} \end{bmatrix}$ where $u_{\mathrm{j}\to\mathrm{i}}$, $v_{\mathrm{j}\to\mathrm{i}}$ and $w_{\mathrm{j}\to\mathrm{i}}$ are the velocity components induced by panel 'j' on collocation point 'i' according to equations 3.39, 3.40 and 3.41 respectively when the strength of panel 'j' is set to unity. Accordingly, $\hat{\boldsymbol{n}}_\mathrm{i}$ is the normal unit vector associated with panel 'i'. The wake influence coefficients, $c_{\mathrm{i,k}}$, are given by $c_{\mathrm{i,k}} = \boldsymbol{c}'_{\mathrm{k}\to\mathrm{i}}.\hat{\boldsymbol{n}}_\mathrm{i}$ where $\boldsymbol{c}'_{\mathrm{k}\to\mathrm{i}} = \begin{bmatrix} u_{\mathrm{k}\to\mathrm{i}} & v_{\mathrm{k}\to\mathrm{i}} & w_{\mathrm{k}\to\mathrm{i}} \end{bmatrix}$ where $u_{\mathrm{k}\to\mathrm{i}}$, $v_{\mathrm{k}\to\mathrm{i}}$ and $w_{\mathrm{k}\to\mathrm{i}}$ are the velocity components induced by wake panel 'k' on collocation point 'i' according to equations 3.39, 3.40 and 3.41 respectively when the strength of the wake panel 'k' is set to unity.

The wake influence coefficient matrix may be factored into the body influence coefficient matrix as before. In this case, the following logic is implemented:

for $k = 1, 2, ..., \mathrm{N_{TE}}$

$$a_{\mathrm{i,j}} = \begin{cases} a'_{\mathrm{i,j}} - c_{\mathrm{j,k}} & \text{if } j = 1 + (k-1)\mathrm{N_p} \\ a'_{\mathrm{i,j}} + c_{\mathrm{j,k}} & \text{if } j = k\mathrm{N_p} \\ a'_{\mathrm{i,j}} & \text{if } j \neq 1 + (k-1)\mathrm{N_p} \;\&\; j \neq k\mathrm{N_p} \end{cases} \tag{4.12}$$

After applying the above logic, the system is now described by an equation of the form $\boldsymbol{Ax} = \boldsymbol{b}$, meaning that the 'strengths' of the body doublet panels can be determined.

4.1.3 Unsteady flow past an aerofoil

For the majority of simulations, the object will experience time-varying operating conditions. For example, with a vertical axis machine the geometric angle of attack[1] and the vector sum of the free-stream wind speed and the rotor speed are both time dependent. As a result, the lift forces acting on the vertical axis machine's blades are time dependent. Through the Kutta-Joukowski theorem, this implies that the bound circulation on the blades is time dependent. By Kelvin's circulation theorem, this implies that time-varying circulation is being shed into the wake. Thus, the entire system is dynamic.

To model such systems, a more elaborate model of the wake is required. Furthermore, additional reference frames are introduced.

Let us define a global reference frame to be one which is stationary. The free-stream velocity vector, $\boldsymbol{u}_\mathrm{g}$, in this frame of reference adopts the following notation:

$$\boldsymbol{u}_\mathrm{g} = \begin{bmatrix} U & V & W \end{bmatrix} \tag{4.13}$$

Now let us define the body reference frame to be one which co-rotates and co-translates with the hub/low-speed shaft. If the rotor is not rotating but there is a free-stream wind speed of $\boldsymbol{u}_\mathrm{g} = \begin{bmatrix} u & 0 & 0 \end{bmatrix}$, it as though there were no free-stream wind speed but instead that the body reference frame were being translated through the fluid (in the opposite direction).

[1] text

Accordingly, the origin of the body reference frame given in a global (stationary) reference frame at time t is

$$\begin{aligned}\boldsymbol{O} &= \begin{bmatrix} X_0 & Y_0 & Z_0 \end{bmatrix} \\ &= \begin{bmatrix} -ut & 0 & 0 \end{bmatrix}\end{aligned} \tag{4.14}$$

By extension, for a generic free-stream wind speed of $\boldsymbol{u} = \begin{bmatrix} u & v & w \end{bmatrix}$, the origin of the body reference frame is

$$\boldsymbol{O} = \begin{bmatrix} -ut & -vt & -wt \end{bmatrix} \tag{4.15}$$

Now let us suppose that the rotor is rotating with some angular velocity $\boldsymbol{\Omega}$. At time t, the rotation of the body reference frame relative to the global reference frame is given by $\boldsymbol{\Omega} t$.

In general, rotation is quantified by a vector since there are three rotational degrees of freedom (roll-pitch-yaw). However, for wind turbine machines, there will only be one degree of freedom. For a vertical axis machine, rotation is defined to be about $\hat{\boldsymbol{z}}$; for a horizontal axis machine, rotation is defined to be about $\hat{\boldsymbol{x}}$.

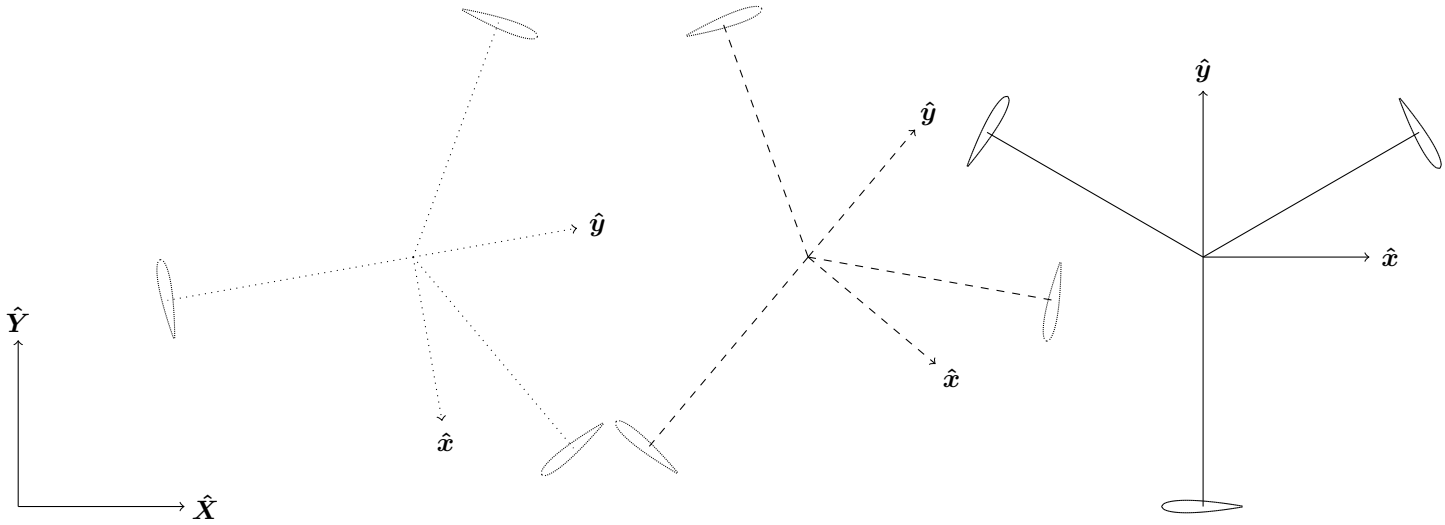

Figure 4.7: Illustration of the body reference frame for 2D simulations at three different time steps (solid, dashed and dotted). The simulation involves a steady free-stream wind speed which is aligned with $\hat{\boldsymbol{X}}$; hence, only the X component of the origin of the body reference frame changes with time.

For simulations involving a vertical axis machine with a rotor speed $\boldsymbol{\Omega} = -\omega(t)\hat{\boldsymbol{z}}$ (corresponding to clockwise rotation in the xy plane as shown in figure 4.7), the transformation from the global reference frame to the global reference frame at time t is given by equation 4.16:

$$\begin{bmatrix} x \\ y \\ z \end{bmatrix} \begin{bmatrix} \cos\theta & \sin\theta & 0 \\ -\sin\theta & \cos\theta & 0 \\ 0 & 0 & 1 \end{bmatrix} \begin{bmatrix} X - X_0 \\ Y - Y_0 \\ Z - Z_0 \end{bmatrix} \tag{4.16}$$

Correspondingly, the transformation from the body reference frame to the global reference frame is achieved using equation 4.17:

$$\begin{bmatrix} X \\ Y \\ Z \end{bmatrix} = \begin{bmatrix} \cos\theta & -\sin\theta & 0 \\ \sin\theta & \cos\theta & 0 \\ 0 & 0 & 1 \end{bmatrix} \begin{bmatrix} x \\ y \\ z \end{bmatrix} + \begin{bmatrix} X_0 \\ Y_0 \\ Z_0 \end{bmatrix} \tag{4.17}$$

where θ is the orientation of the body reference frame relative to the global reference frame measured anti-clockwise positive from $\hat{\boldsymbol{X}}$ to $\hat{\boldsymbol{x}}$. Mathematically,

$$\theta = -\int_0^t \omega(t)\mathrm{d}t \tag{4.18}$$

The velocity experienced at a collocation point due to the free-stream wind speed is thus

$$\begin{aligned}\begin{bmatrix} u \\ v \\ w \end{bmatrix} &= \begin{bmatrix} \cos\theta & \sin\theta & 0 \\ -\sin\theta & \cos\theta & 0 \\ 0 & 0 & 1 \end{bmatrix} \begin{bmatrix} -\dot{X}_0 \\ -\dot{Y}_0 \\ -\dot{Z}_0 \end{bmatrix} \\ &= \begin{bmatrix} \cos\theta & \sin\theta & 0 \\ -\sin\theta & \cos\theta & 0 \\ 0 & 0 & 1 \end{bmatrix} \begin{bmatrix} U \\ V \\ W \end{bmatrix} \end{aligned} \tag{4.19}$$

For simulations involving a horizontal axis machine with a rotor speed $\boldsymbol{\Omega} = -\omega(t)\hat{\boldsymbol{x}}$, the connection between the body reference frame and the global reference frame is given by equation 4.20:

$$\begin{bmatrix} x \\ y \\ z \end{bmatrix} = \begin{bmatrix} 1 & 0 & 0 \\ 0 & \cos\theta & \sin\theta \\ 0 & -\sin\theta & \cos\theta \end{bmatrix} \begin{bmatrix} X - X_0 \\ Y - Y_0 \\ Z - Z_0 \end{bmatrix} \tag{4.20}$$

Correspondingly, the transformation from the body reference frame to the global reference frame is achieved using equation 4.21:

$$\begin{bmatrix} X \\ Y \\ Z \end{bmatrix} = \begin{bmatrix} 1 & 0 & 0 \\ 0 & \cos\theta & -\sin\theta \\ 0 & \sin\theta & \cos\theta \end{bmatrix} \begin{bmatrix} x \\ y \\ z \end{bmatrix} + \begin{bmatrix} X_0 \\ Y_0 \\ Z_0 \end{bmatrix} \tag{4.21}$$

where

$$\theta = \int_0^t \omega(t)\mathrm{d}t \tag{4.22}$$

The velocity experienced at a collocation point due to the free-stream wind speed is thus,

$$\begin{aligned}\begin{bmatrix} u \\ v \\ w \end{bmatrix} &= \begin{bmatrix} 1 & 0 & 0 \\ 0 & \cos\theta & \sin\theta \\ 0 & -\sin\theta & \cos\theta \end{bmatrix} \begin{bmatrix} -\dot{X}_0 \\ -\dot{Y}_0 \\ -\dot{Z}_0 \end{bmatrix} \\ &= \begin{bmatrix} 1 & 0 & 0 \\ 0 & \cos\theta & \sin\theta \\ 0 & -\sin\theta & \cos\theta \end{bmatrix} \begin{bmatrix} U \\ V \\ W \end{bmatrix} \end{aligned} \tag{4.23}$$

The velocity experienced at a collocation point due to the rotation of the machine is determined through equation 4.24:

$$\boldsymbol{u}_{\mathrm{rot_i}} = -\boldsymbol{\Omega} \times \boldsymbol{r}_{\mathrm{i}} \tag{4.24}$$

where $\boldsymbol{r}_{\mathrm{i}} = \begin{bmatrix} x_{\mathrm{c_i}} & y_{\mathrm{c_i}} & z_{\mathrm{c_i}} \end{bmatrix}$ are the coordinates of the collocation point as expressed in the body reference frame. The minus sign is due to relativity of the reference frames.

For a vertical axis machine, it follows that

$$\boldsymbol{u}_{\mathrm{rot_i}} = -\omega(t) y_{\mathrm{c_i}} \hat{\boldsymbol{x}} + \omega(t) x_{\mathrm{c_i}} \hat{\boldsymbol{y}} \tag{4.25}$$

Similarly, for a horizontal axis machine,

$$\boldsymbol{u}_{\mathrm{rot_i}} = -\omega(t) z_{\mathrm{c_i}} \hat{\boldsymbol{y}} + \omega(t) y_{\mathrm{c_i}} \hat{\boldsymbol{z}} \tag{4.26}$$

The velocity experienced at each and every collocation points is the vector sum of the above, the velocities induced by the body panels, and the velocities induced by everything in the wake.

In the unsteady flow case, the wake evolves with every time step. For the first time step, assuming a constant-strength doublet representation, the number of wake panels is equal to the number of trailing edge segments. For a 2D simulation, this is just the number of blades; for a 3D simulation this is the number of blade elements per blade multiplied by the number of blades. The strengths of the newly shed panels are, at the start of the time step, unknown. However, the strengths may be determined by following a process similar to that for the steady flow cases. The length of the panel is set such that the Kutta condition is met. For unsteady flow, the Kutta condition encompasses the statement that the trailing edge is a stagnation point. For this to be upheld, the induced velocity at the trailing edge (as expressed in the global reference frame) due to all singularity elements in the system should add up to zero. This would correspond to the fluid moving off from the trailing at a velocity $(\boldsymbol{u}_{\mathrm{free}} + \boldsymbol{u}_{\mathrm{rot}})$ in the body reference frame.

Since constant-strength doublet panels are equivalent to vortex rings in 3D, it can easily be noted that the wake model is a discrete version of reality. In reality, circulation is continuously changing and vortices/vortex segments are continuously shed into the wake. Owing to this there is an underestimation of the

Taking this into account along with the objective of satisfying the Kutta condition, the panel side parallel to the trailing edge (but not at the trailing edge) is placed roughly 0.25 times the distance covered in the last time step. This is due to the fact that the system has been discretised and so the effect of singularity elements in the flow field is underestimated.

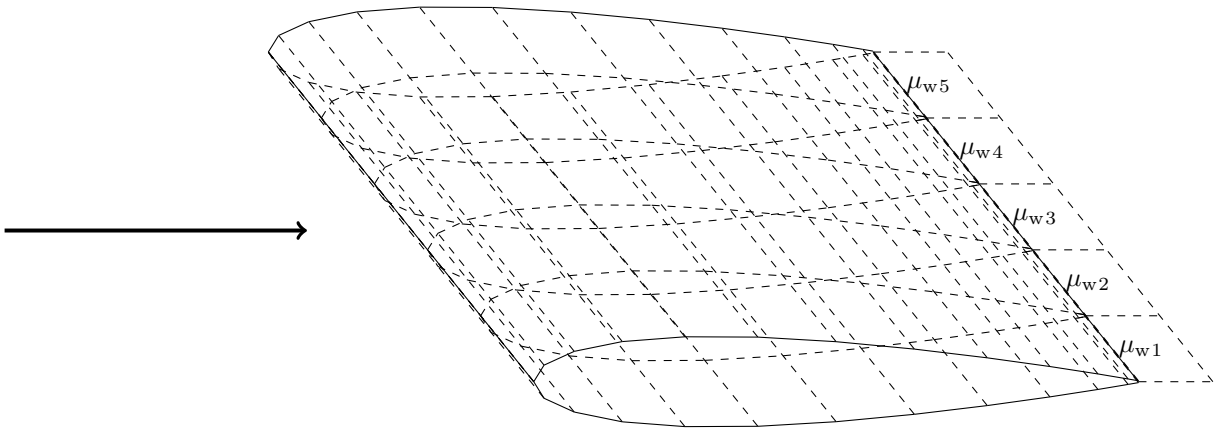

Figure 4.8: Illustration of the orientation of the wake panel and the bisector at the trailing edge. Wake rollup has not been illustrated for simplicity reasons.

Once the strengths of the body panels and most recently shed wake panels have been determined, the velocities induced by these elements can be calculated at any point. Of interest are the corner points of the wake panels since the wake is a free (to deform) system.

For the second time step, the wake now consists of known and unknowns. The knowns are the strengths and coordinates of the panels from the previous time step. The unknowns are the strengths of the newly shed wake panels. Again, the

$$
\underbrace{0 = \begin{bmatrix} \boldsymbol{u}_{\infty,1}.\hat{\boldsymbol{n}}_1 \\ \boldsymbol{u}_{\infty,2}.\hat{\boldsymbol{n}}_2 \\ \boldsymbol{u}_{\infty,3}.\hat{\boldsymbol{n}}_3 \\ \vdots \\ \boldsymbol{u}_{\infty,\mathrm{N_t}-1}.\hat{\boldsymbol{n}}_{\mathrm{N_t}-1} \\ \boldsymbol{u}_{\infty,\mathrm{N_t}}.\hat{\boldsymbol{n}}_{\mathrm{N_t}} \end{bmatrix} + \underbrace{\begin{bmatrix} d_{1,1} & d_{1,2} & d_{1,3} & \dots & d_{1,\mathrm{N_{TE}}-1} & d_{1,\mathrm{N_{TE}}} \\ d_{2,1} & d_{2,2} & d_{2,3} & \dots & d_{2,\mathrm{N_{TE}}-1} & d_{2,\mathrm{N_{TE}}} \\ d_3 & d_{3,2} & d_{3,3} & \dots & d_{3,\mathrm{N_{TE}}-1} & d_{3,\mathrm{N_{TE}}} \\ \vdots & \vdots & \vdots & \ddots & \vdots & \vdots \\ d_{\mathrm{N_{TE}}-1,1} & d_{\mathrm{N_{TE}}-1,2} & d_{\mathrm{N_{TE}}-1,3} & \dots & d_{\mathrm{N_{TE}}-1,\mathrm{N_{TE}}-1} & d_{\mathrm{N_{TE}}-1,\mathrm{N_{TE}}} \\ d_{\mathrm{N_{TE}},1} & d_{\mathrm{N_{TE}},2} & d_{\mathrm{N_{TE}},3} & \dots & d_{\mathrm{N_{TE}},\mathrm{N_{TE}}} & d_{\mathrm{N_{TE}},\mathrm{N_{TE}}} \end{bmatrix}}_{\boldsymbol{D}_\mathrm{W}} \begin{bmatrix} \mu_{w_1} \\ \mu_{w_2} \\ \mu_{w_3} \\ \vdots \\ \mu_{\mathrm{N_{TE}}-1} \\ \mu_{\mathrm{N_{TE}}} \end{bmatrix} + \dots}_{\textbf{RHS}} \\
\underbrace{\begin{bmatrix} a_{1,1} & a_{1,2} & a_{1,3} & \dots & a_{1,\mathrm{N_t}-1} & a_{1,\mathrm{N_t}} \\ a_{2,1} & a_{2,2} & a_{2,3} & \dots & a_{2,\mathrm{N_t}-1} & a_{2,\mathrm{N_t}} \\ a_{3,1} & a_{3,2} & a_{3,3} & \dots & a_{3,\mathrm{N_t}-1} & a_{3,\mathrm{N_t}} \\ \vdots & \vdots & \vdots & \ddots & \vdots & \vdots \\ a_{\mathrm{N_t}-1,1} & a_{\mathrm{N_t}-1,2} & a_{\mathrm{N_t}-1,3} & \dots & a_{\mathrm{N_t}-1,\mathrm{N_t}-1} & a_{\mathrm{N_t}-1,\mathrm{N_t}} \\ a_{\mathrm{N_t},1} & a_{\mathrm{N_t},2} & a_{\mathrm{N_t},3} & \dots & a_{\mathrm{N_t},\mathrm{N_t}-1} & a_{\mathrm{N_t},\mathrm{N_t}} \end{bmatrix}}_{\boldsymbol{A}} \underbrace{\begin{bmatrix} \mu_1 \\ \mu_2 \\ \mu_3 \\ \vdots \\ \mu_{\mathrm{N_p}-1} \\ \mu_{\mathrm{N_p}} \end{bmatrix}}_{\boldsymbol{\mu}}
\tag{4.27}
$$

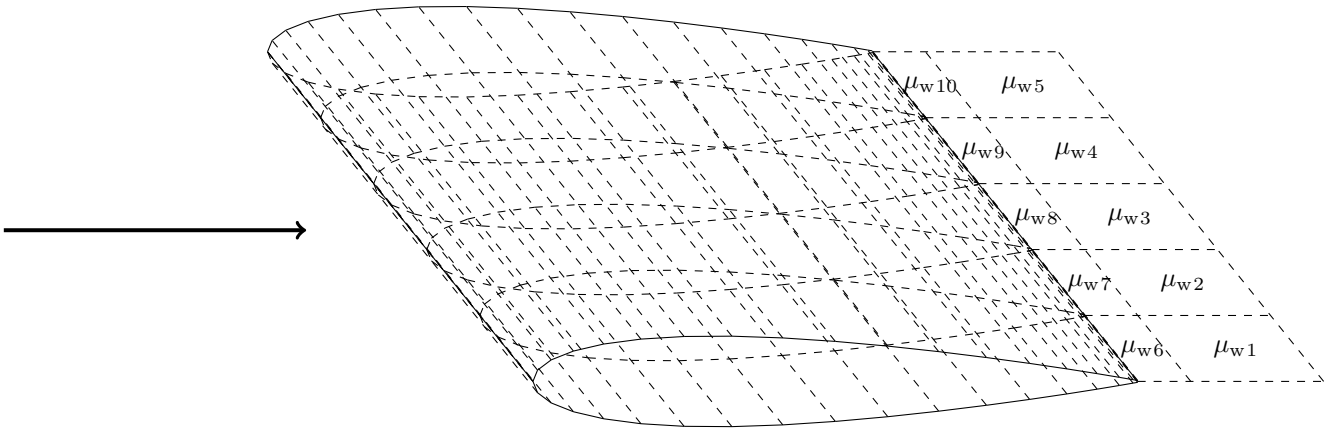

Figure 4.9: Illustration of the orientation of the wake panel and the bisector at the trailing edge. Wake rollup has not been illustrated for simplicity reasons.

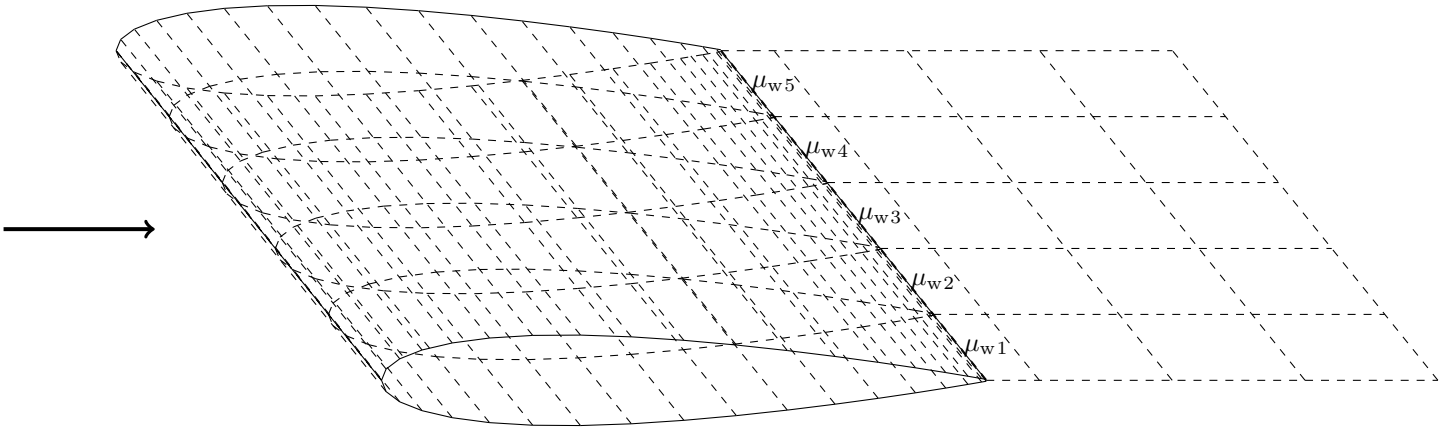

Figure 4.10: Illustration of the orientation of the wake panel and the bisector at the trailing edge. Wake rollup has not been illustrated for simplicity reasons.

The velocity calculations associated with constant-strength doublet panels are computationally intensive, especially for 3D systems. Owing to the equivalence of a constant-strength doublet panel and a pair of counter-rotating vortices (located at the panel corners), the wake may be converted into a vortex system.

$$
\begin{aligned}
0 = \underbrace{\begin{bmatrix} \boldsymbol{u}_{\infty,1}.\hat{\boldsymbol{n}}_1 \\ \boldsymbol{u}_{\infty,2}.\hat{\boldsymbol{n}}_2 \\ \boldsymbol{u}_{\infty,3}.\hat{\boldsymbol{n}}_3 \\ \vdots \\ \boldsymbol{u}_{\infty,\mathrm{N_t}-1}.\hat{\boldsymbol{n}}_{\mathrm{N_t}-1} \\ \boldsymbol{u}_{\infty,\mathrm{N_t}}.\hat{\boldsymbol{n}}_{\mathrm{N_t}} \end{bmatrix} + \underbrace{\begin{bmatrix} e_{1,1} & e_{1,2} & e_{1,3} & \cdots & e_{1,\mathrm{N_{TE}}-1} & e_{1,\mathrm{N_{TE}}} \\ e_{2,1} & e_{2,2} & e_{2,3} & \cdots & e_{2,\mathrm{N_{TE}}-1} & e_{2,\mathrm{N_{TE}}} \\ e_3 & e_{3,2} & e_{3,3} & \cdots & e_{3,\mathrm{N_{TE}}-1} & e_{3,\mathrm{N_{TE}}} \\ \vdots & \vdots & \vdots & \ddots & \vdots & \vdots \\ e_{\mathrm{N_w}-1,1} & e_{\mathrm{N_{TE}}-1,2} & e_{\mathrm{N_{TE}}-1,3} & \cdots & e_{\mathrm{N_w}-1,\mathrm{N_w}-1} & d_{\mathrm{N_{TE}}-1,\mathrm{N_{TE}}} \\ e_{\mathrm{N_w},1} & e_{\mathrm{N_w},2} & e_{\mathrm{N_w},3} & \cdots & e_{\mathrm{N_w},\mathrm{N_w}} & e_{\mathrm{N_w},\mathrm{N_w}} \end{bmatrix}}_{\boldsymbol{E}_\mathrm{W}} \begin{bmatrix} \Gamma_{w_1} \\ \Gamma_{w_2} \\ \Gamma_{w_3} \\ \vdots \\ \Gamma_{\mathrm{N_w}-1} \\ \Gamma_{\mathrm{N_w}} \end{bmatrix} + \cdots}_{\mathbf{RHS}} \\
\underbrace{\begin{bmatrix} a_{1,1} & a_{1,2} & a_{1,3} & \cdots & a_{1,\mathrm{N_t}-1} & a_{1,\mathrm{N_t}} \\ a_{2,1} & a_{2,2} & a_{2,3} & \cdots & a_{2,\mathrm{N_t}-1} & a_{2,\mathrm{N_t}} \\ a_{3,1} & a_{3,2} & a_{3,3} & \cdots & a_{3,\mathrm{N_t}-1} & a_{3,\mathrm{N_t}} \\ \vdots & \vdots & \vdots & \ddots & \vdots & \vdots \\ a_{\mathrm{N_t}-1,1} & a_{\mathrm{N_t}-1,2} & a_{\mathrm{N_t}-1,3} & \cdots & a_{\mathrm{N_t}-1,\mathrm{N_t}-1} & a_{\mathrm{N_t}-1,\mathrm{N_t}} \\ a_{\mathrm{N_t},1} & a_{\mathrm{N_t},2} & a_{\mathrm{N_t},3} & \cdots & a_{\mathrm{N_t},\mathrm{N_t}-1} & a_{\mathrm{N_t},\mathrm{N_t}} \end{bmatrix}}_{\boldsymbol{A}} \underbrace{\begin{bmatrix} \mu_1 \\ \mu_2 \\ \mu_3 \\ \vdots \\ \mu_{\mathrm{N_p}-1} \\ \mu_{\mathrm{N_p}} \end{bmatrix}}_{\boldsymbol{\mu}}
\end{aligned}
\tag{4.28}
$$

4.1.4 Other implementations using the Neumann boundary condition

While the preceding subsections have outlined the procedure for a body represented by constant-strength doublet panels, it is important to recognise that there are alternative implementations. The implementation which is most closely related to the constant-strength doublet panel method (using the Neumann boundary condition) is the vortex ring model.

The body panels may also be constant-strength source panels; however, with only source panels, no lift can be predicted; thus, the constant-strength source panel method (using the Neumann boundary condition) is rather limited in its applicability.

4.1.5 Numerical stability and the Neumann boundary condition

It can be shown that the matrix $\boldsymbol{A}$ for steady-flow around symmetric aerofoils (e.g. NACA 0015) is singular. This can lead to numerical instability when solving $\boldsymbol{A\mu} = \mathbf{RHS}$. In order to avoid the occurrence of singular matrices, the panelling scheme for Neumann-based methods needs to be slightly unconventional. Some degree of asymmetry must be forced into the panelling. This can be done by taking two neighbouring panels (preferably away from both the leading and trailing edges) and merging them into one as shown in figure 4.11.

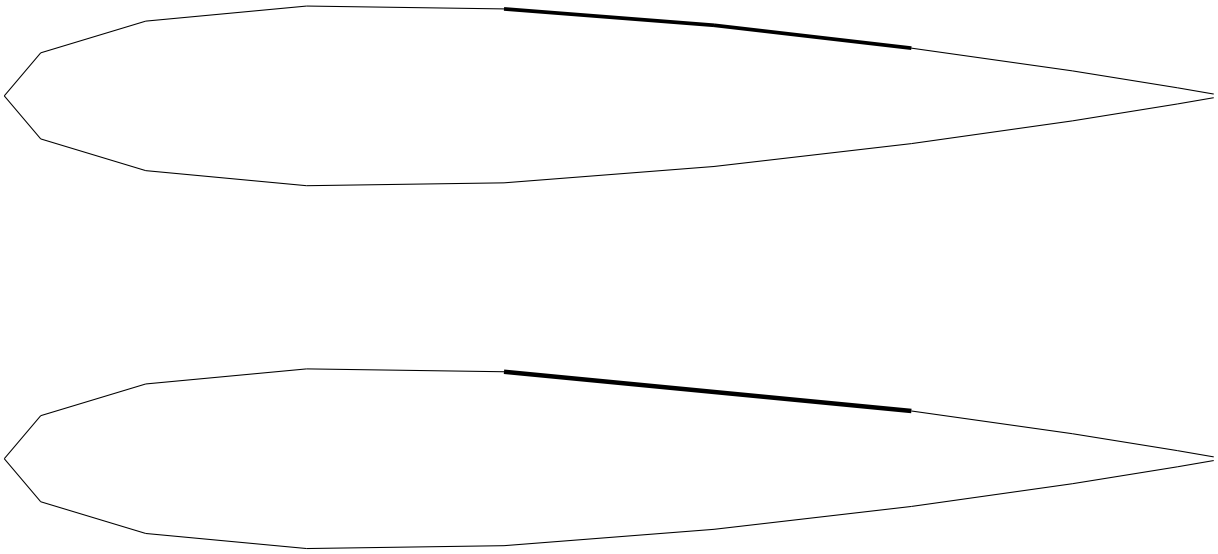

Figure 4.11: Illustration of a conventional panelling scheme and a modified panelling scheme. Through an appropriate choice of panels to merge, the effect is barely noticeable.

If the two neighbouring panels at the leading edge were to be used instead, there would be a significant change in the shape of the mapped aerofoil unless the panel number is high. Increasing the panel number is not desirable as it introduces significant costs (specifically associated with matrix algorithms).

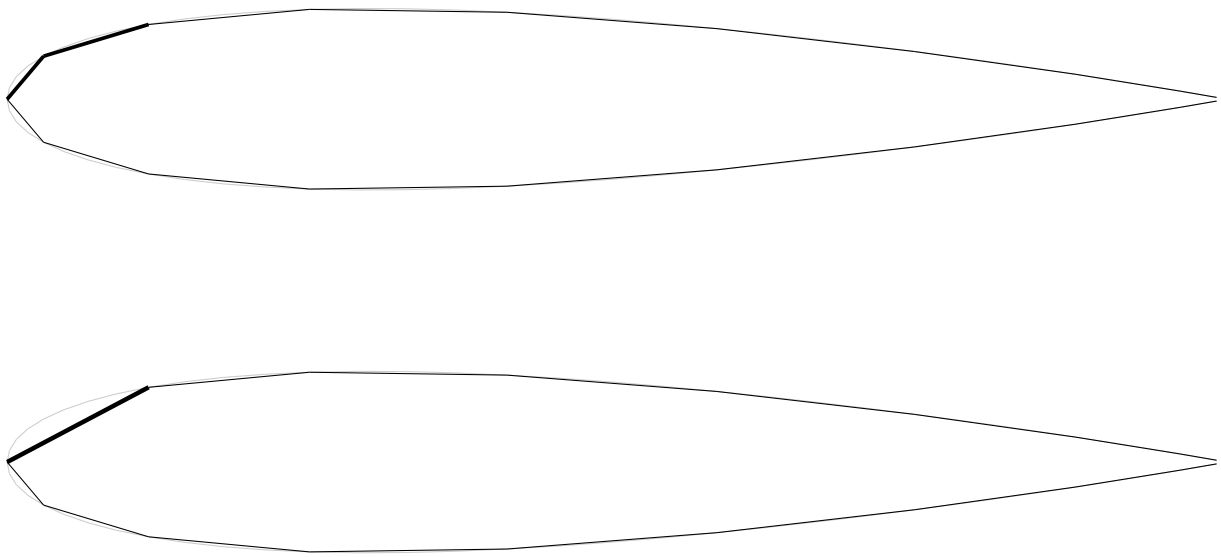

Figure 4.12: Illustration of a conventional panelling scheme and a modified panelling scheme. Through an appropriate choice of panels to merge, the effect is barely noticeable. The actual aerofoil is shown in light grey.

Alternatively, one could remove one of the rows (row 'm') and the corresponding column ('m') from $\boldsymbol{A}$. In addition, μ_{m} would be removed along with $\mathrm{RHS}_{\mathrm{m}}$. In essence, this leads to an aerofoil where, for a certain section (where there was once a collocation point), flow can enter the aerofoil. However, if the panel number is sufficiently high, the effect of enforcing the Neumann boundary condition local (at neighbouring collocation points) to the now missing collocation point should result in zero normal flow at the missing collocation point anyway. Best practice dictates that 'm' should be chosen to correspond to a panel far from the leading and trailing edges.

$$0 = \underbrace{\begin{bmatrix} \boldsymbol{u}_{\infty,1}.\hat{\boldsymbol{n}}_1 \\ \boldsymbol{u}_{\infty,2}.\hat{\boldsymbol{n}}_2 \\ \boldsymbol{u}_{\infty,3}.\hat{\boldsymbol{n}}_3 \\ \vdots \\ \boldsymbol{u}_{\infty,\mathrm{m}-1}.\hat{\boldsymbol{n}}_{\mathrm{m}-1} \\ \boldsymbol{u}_{\infty,\mathrm{m}+1}.\hat{\boldsymbol{n}}_{\mathrm{m}+1} \\ \vdots \\ \boldsymbol{u}_{\infty,\mathrm{N_p}-1}.\hat{\boldsymbol{n}}_{\mathrm{N_p}-1} \\ \boldsymbol{u}_{\infty,\mathrm{N_p}}.\hat{\boldsymbol{n}}_{\mathrm{N_p}} \end{bmatrix}}_{\mathbf{RHS}} + \underbrace{\begin{bmatrix} a_{1,1} & a_{1,2} & a_{1,3} & \cdots & a_{1,\mathrm{m}-1} & a_{1,\mathrm{m}+1} & \cdots & a_{1,\mathrm{N_p}-1} & a_{1,\mathrm{N_p}} \\ a_{2,1} & a_{2,2} & a_{2,3} & \cdots & a_{2,\mathrm{m}-1} & a_{2,\mathrm{m}+1} & \cdots & a_{2,\mathrm{N_p}-1} & a_{2,\mathrm{N_p}} \\ a_{3,1} & a_{3,2} & a_{3,3} & \cdots & a_{3,\mathrm{m}-1} & a_{3,\mathrm{m}+1} & \cdots & a_{3,\mathrm{N_p}-1} & a_{3,\mathrm{N_p}} \\ \vdots & \vdots & \vdots & \vdots & \vdots & \vdots & \vdots & \vdots & \vdots \\ a_{m-1,1} & a_{m-1,2} & a_{m-1,3} & \cdots & a_{\mathrm{m}-1,\mathrm{m}-1} & a_{\mathrm{m}-1,\mathrm{m}+1} & \cdots & a_{\mathrm{m}-1,\mathrm{N_p}-1} & a_{\mathrm{m}-1,\mathrm{N_p}} \\ a_{m+1,1} & a_{m+1,2} & a_{m+1,3} & \cdots & a_{\mathrm{m}+1,\mathrm{m}-1} & a_{\mathrm{m}+1,\mathrm{m}+1} & \cdots & a_{3,\mathrm{N_p}-1} & a_{\mathrm{m}+1,\mathrm{N_p}} \\ \vdots & \vdots & \vdots & \vdots & \vdots & \vdots & \ddots & \vdots & \vdots \\ a_{\mathrm{N_p}-1,1} & a_{\mathrm{N_p}-1,2} & a_{\mathrm{N_p}-1,3} & \cdots & a_{\mathrm{N_p}-1,\mathrm{m}-1} & a_{\mathrm{N_p}-1,\mathrm{m}+1} & \cdots & a_{\mathrm{N_p}-1,\mathrm{N_p}-1} & a_{\mathrm{N_p}-1,\mathrm{N_p}} \\ a_{\mathrm{N_p},1} & a_{\mathrm{N_p},2} & a_{\mathrm{N_p},3} & \cdots & a_{\mathrm{N_p},\mathrm{m}-1} & a_{\mathrm{N_p},\mathrm{m}+1} & \cdots & a_{\mathrm{N_p},\mathrm{N_p}-1} & a_{\mathrm{N_p},\mathrm{N_p}} \end{bmatrix}}_{\boldsymbol{A}} \underbrace{\begin{bmatrix} \mu_1 \\ \mu_2 \\ \mu_3 \\ \vdots \\ \mu_{\mathrm{m}-1} \\ \mu_{\mathrm{m}+1} \\ \vdots \\ \mu_{\mathrm{N_p}-1} \\ \mu_{\mathrm{N_p}} \end{bmatrix}}_{\boldsymbol{\mu}} \tag{4.29}$$

The same modification should be applied to three-dimensional simulations and unsteady flow simulations.

Chapter 5

Matrix solvers

Wind Panel has various algorithms for solving $\boldsymbol{Ax} = \boldsymbol{b}$ style equations. These are the LU decomposition, Gaussian elimination and Cholesky decomposition. These are explained in this chapter.

5.1 LU decomposition

Let us consider again the equation $\boldsymbol{x} = \boldsymbol{A}^{-1}\boldsymbol{b}$. Suppose that it is possible to factorize $\boldsymbol{A}$ as the product of a lower triangular matrix, $\boldsymbol{L}$, and an upper triangular matrix, $\boldsymbol{U}$. Furthermore, let the main diagonal of $\boldsymbol{L}$ contain ones. That is,

$$\begin{aligned}\boldsymbol{A} &= \boldsymbol{LU} \\ &= \begin{bmatrix} 1 & 0 & \dots & 0 \\ l_{2,1} & 1 & \dots & 0 \\ \vdots & \vdots & \ddots & \vdots \\ l_{\mathrm{n},1} & l_{\mathrm{n},2} & \dots & 1 \end{bmatrix} \begin{bmatrix} u_{1,1} & u_{1,2} & \dots & u_{1,\mathrm{n}} \\ 0 & u_{2,2} & \dots & u_{2,\mathrm{n}} \\ \vdots & \vdots & \ddots & \vdots \\ 0 & 0 & \dots & u_{\mathrm{n},\mathrm{n}} \end{bmatrix}\end{aligned} \tag{5.1}$$

Therefore, our equation of interest may be expressed as follows:

$$\boldsymbol{LUx} = \boldsymbol{b} \tag{5.2}$$

Let $\boldsymbol{y} = \boldsymbol{Ux}$. Therefore,

$$\boldsymbol{Ly} = \boldsymbol{b} \tag{5.3}$$

Given the structure of $\boldsymbol{L}$, it follows that $\boldsymbol{y}$ can be solved by forward substitution:

$$\begin{aligned} y_1 &= b_1 \\ y_2 &= b_2 - l_{2,1}y_1 \\ y_3 &= b_3 - l_{3,1}y_1 - l_{3,2}y_2 \\ &\vdots \\ y_{\mathrm{n}} &= b_{\mathrm{n}} - \sum_{i=1}^{i=n-1} l_{\mathrm{n},\mathrm{i}}y_{\mathrm{i}} \end{aligned} \tag{5.4}$$

Note, the above calculation is specific to the case of the main diagonal of $\boldsymbol{L}$ being set to ones.

To determine the unknown vector $\boldsymbol{x}$, given the structure of $\boldsymbol{U}$, backward substitution is then applied:

$$\begin{aligned} x_{\mathrm{n}} &= y_{\mathrm{n}}/u_{\mathrm{n},\mathrm{n}} \\ x_{\mathrm{n}-1} &= (y_{\mathrm{n}-1} - u_{\mathrm{n}-1,\mathrm{n}}x_{\mathrm{n}-1})/u_{\mathrm{n}-1,\mathrm{n}-1} \\ &\vdots \\ x_1 &= \left(y_1 - \sum_{j=2}^{j=n} u_{1,\mathrm{j}}x_{\mathrm{j}}\right)/u_{1,1} \end{aligned} \tag{5.5}$$

Or, generally speaking,

$$x_{\mathrm{i}} = \left(y_{\mathrm{i}} - \sum_{j=i+1}^{j=n} u_{\mathrm{i,j}} x_{\mathrm{i}} \right) / u_{\mathrm{i,i}} \tag{5.6}$$

So, if $\boldsymbol{A}$ can be factorized into $\boldsymbol{L}$ and $\boldsymbol{U}$, the system can be solved. Consequently, our goal is to develop an algorithm which can perform the decomposition/factorization. A simple but effective implementation of the LU decomposition is known as the Doolittle method.

Since only the first element of the first row of $\boldsymbol{L}$ is non-zero, it follows that all the elements of the first row of $\boldsymbol{U}$ can be determined:

$$a_{1,\mathrm{i}} = u_{1,\mathrm{i}} \tag{5.7}$$

Since only the first element of the first column of $\boldsymbol{U}$ is non-zero, it follows that all the elements of the first column of $\boldsymbol{L}$ can be determined:

$$a_{\mathrm{i},1} = l_{\mathrm{i},1} u_{1,1} \tag{5.8}$$

With all of the elements of the first column of $\boldsymbol{L}$ determined, it is then possible to go through and determine the remaining unknowns.

The next step would be to note that $l_{2,1}$ is known. By matrix multiplication, $a_{2,2} = l_{2,1} u_{1,2} + u_{2,2}$. Hence,

$$u_{2,2} = a_{2,2} - l_{2,1} u_{1,2} \tag{5.9}$$

In other words, now the entire second column of $\boldsymbol{U}$ has been determined.

At this point, the unknowns in the third row of $\boldsymbol{L}$ (only one unknown at this point) can now be determined:

$$a_{3,2} = l_{3,1} u_{1,2} + l_{3,2} u_{2,2} \tag{5.10}$$

In other words, now the entire third row of $\boldsymbol{L}$ has been determined.

Again by considering matrix multiplication, it is now possible to go through and calculate all the unknowns in the third column of $\boldsymbol{U}$:

$$\begin{aligned} a_{2,3} &= l_{2,1} u_{1,3} + u_{2,3} \\ a_{3,3} &= l_{3,1} u_{1,3} + l_{3,2} u_{2,3} + u_{3,3} \end{aligned} \tag{5.11}$$

After this, it is possible to determine all the unknowns in the fourth row of $\boldsymbol{L}$:

$$a_{4,2} = l_{4,1} u_{1,2} + l_{4,2} u_{2,2} \tag{5.12}$$

This process is then repeated i.e. solve all unknowns in column i of $\boldsymbol{U}$ and then solve all unknowns in row $i+1$ of $\boldsymbol{L}$ then proceed through i.

In short,

$$\begin{aligned} u_{1,\mathrm{j}} &= a_{1,\mathrm{j}} \\ l_{\mathrm{j},1} &= a_{\mathrm{j},1} / u_{1,1} \end{aligned} \tag{5.13}$$

and

$$\begin{aligned} u_{\mathrm{i,j}} &= a_{\mathrm{i,j}} - \sum_{t=1}^{i-1} l_{\mathrm{i,t}} u_{\mathrm{t,j}} \\ l_{\mathrm{j,i}} &= \frac{a_{\mathrm{j,i}} - \sum_{t=1}^{i-1} l_{\mathrm{j,t}} u_{\mathrm{t,i}}}{u_{\mathrm{i,i}}} \end{aligned} \tag{5.14}$$

where $i = 1 \to n$ and $j = 1 \to n$.

As can be seen from the Doolittle algorithm, matrix decompositions typically have three nested for loops (one running through i, one through j and the other being the summation parts in the above expressions). Hence, matrix inversion and decomposition goes as n^3 in terms of number of calculations where n is the size of the matrix.

5.2 Gaussian elimination

Consider again a system which may be described by the following equation:

$$\begin{bmatrix} a_{1,1} & a_{1,2} & a_{1,3} & \cdots & a_{1,\mathrm{m}} & \cdots & a_{1,\mathrm{N_p}-1} & a_{1,\mathrm{N_p}} \\ a_{2,1} & a_{2,2} & a_{2,3} & \cdots & a_{2,\mathrm{m}} & \cdots & a_{2,\mathrm{N_p}-1} & a_{2,\mathrm{N_p}} \\ a_{3,1} & a_{3,2} & a_{3,3} & \cdots & a_{3,\mathrm{m}} & \cdots & a_{3,\mathrm{N_p}-1} & a_{3,\mathrm{N_p}} \\ \vdots & \vdots & \vdots & \ddots & \vdots & \vdots & \vdots & \vdots \\ a_{m,1} & a_{m,2} & a_{m,3} & \cdots & a_{\mathrm{m,m}} & \cdots & a_{\mathrm{m,N_p}-1} & a_{\mathrm{m,N_p}} \\ \vdots & \vdots & \vdots & \vdots & \vdots & \ddots & \vdots & \vdots \\ a_{\mathrm{N_p}-1,1} & a_{\mathrm{N_p}-1,2} & a_{\mathrm{N_p}-1,3} & \cdots & a_{\mathrm{N_p}-1,\mathrm{m}} & \cdots & a_{\mathrm{N_p}-1,\mathrm{N_p}-1} & a_{\mathrm{N_p}-1,\mathrm{N_p}} \\ a_{\mathrm{N_p},1} & a_{\mathrm{N_p},2} & a_{\mathrm{N_p},3} & \cdots & a_{\mathrm{N_p},\mathrm{m}} & \cdots & a_{\mathrm{N_p},\mathrm{N_p}-1} & a_{\mathrm{N_p},\mathrm{N_p}} \end{bmatrix} \begin{bmatrix} x_1 \\ x_2 \\ x_3 \\ \vdots \\ x_{\mathrm{m}} \\ \vdots \\ x_{\mathrm{N_p}-1} \\ x_{\mathrm{N_p}} \end{bmatrix} = \begin{bmatrix} b_1 \\ b_2 \\ b_3 \\ \vdots \\ b_{\mathrm{m}} \\ \vdots \\ b_{\mathrm{N_p}-1} \\ b_{\mathrm{N_p}} \end{bmatrix} \tag{5.15}$$

Let us create an augmented matrix as shown:

$$\underbrace{\left[\begin{array}{cccccccc|c} a_{1,1} & a_{1,2} & a_{1,3} & \cdots & a_{1,\mathrm{m}} & \cdots & a_{1,\mathrm{N_p}-1} & a_{1,\mathrm{N_p}} & b_1 \\ a_{2,1} & a_{2,2} & a_{2,3} & \cdots & a_{2,\mathrm{m}} & \cdots & a_{2,\mathrm{N_p}-1} & a_{2,\mathrm{N_p}} & b_2 \\ a_{3,1} & a_{3,2} & a_{3,3} & \cdots & a_{3,\mathrm{m}} & \cdots & a_{3,\mathrm{N_p}-1} & a_{3,\mathrm{N_p}} & b_3 \\ \vdots & \vdots & \vdots & \ddots & \vdots & \vdots & \vdots & \vdots & \vdots \\ a_{m,1} & a_{m,2} & a_{m,3} & \cdots & a_{\mathrm{m,m}} & \cdots & a_{\mathrm{m,N_p}-1} & a_{\mathrm{m,N_p}} & b_{\mathrm{m}} \\ \vdots & \vdots & \vdots & \vdots & \vdots & \ddots & \vdots & \vdots & \vdots \\ a_{\mathrm{N_p}-1,1} & a_{\mathrm{N_p}-1,2} & a_{\mathrm{N_p}-1,3} & \cdots & a_{\mathrm{N_p}-1,\mathrm{m}} & \cdots & a_{\mathrm{N_p}-1,\mathrm{N_p}-1} & a_{\mathrm{N_p}-1,\mathrm{N_p}} & b_{\mathrm{N_p}-1} \\ a_{\mathrm{N_p},1} & a_{\mathrm{N_p},2} & a_{\mathrm{N_p},3} & \cdots & a_{\mathrm{N_p},\mathrm{m}} & \cdots & a_{\mathrm{N_p},\mathrm{N_p}-1} & a_{\mathrm{N_p},\mathrm{N_p}} & b_{\mathrm{N_p}} \end{array}\right]}_{\text{Augmented matrix}} \begin{bmatrix} x_1 \\ x_2 \\ x_3 \\ \vdots \\ x_{\mathrm{m}} \\ \vdots \\ x_{\mathrm{N_p}-1} \\ x_{\mathrm{N_p}} \end{bmatrix} \tag{5.16}$$

For the first column, let us find the maximum value. Whichever row that maximum exists in will be swapped with row one; that is,

$$\left[\begin{array}{cccccccc|c} a'_{1,1} & a'_{1,2} & a'_{1,3} & \cdots & a'_{1,\mathrm{m}} & \cdots & a'_{1,\mathrm{N_p}-1} & a'_{1,\mathrm{N_p}} & b'_1 \\ a'_{2,1} & a'_{2,2} & a'_{2,3} & \cdots & a'_{2,\mathrm{m}} & \cdots & a'_{2,\mathrm{N_p}-1} & a'_{2,\mathrm{N_p}} & b'_2 \\ a'_{3,1} & a'_{3,2} & a'_{3,3} & \cdots & a'_{3,\mathrm{m}} & \cdots & a'_{3,\mathrm{N_p}-1} & a'_{3,\mathrm{N_p}} & b'_3 \\ \vdots & \vdots & \vdots & \ddots & \vdots & \vdots & \vdots & \vdots & \vdots \\ a'_{m,1} & a'_{m,2} & a'_{m,3} & \cdots & a'_{\mathrm{m,m}} & \cdots & a'_{\mathrm{m,N_p}-1} & a'_{\mathrm{m,N_p}} & b'_{\mathrm{m}} \\ \vdots & \vdots & \vdots & \vdots & \vdots & \ddots & \vdots & \vdots & \vdots \\ a'_{\mathrm{N_p}-1,1} & a'_{\mathrm{N_p}-1,2} & a'_{\mathrm{N_p}-1,3} & \cdots & a'_{\mathrm{N_p}-1,\mathrm{m}} & \cdots & a'_{\mathrm{N_p}-1,\mathrm{N_p}-1} & a'_{\mathrm{N_p}-1,\mathrm{N_p}} & b'_{\mathrm{N_p}-1} \\ a'_{\mathrm{N_p},1} & a'_{\mathrm{N_p},2} & a'_{\mathrm{N_p},3} & \cdots & a'_{\mathrm{N_p},\mathrm{m}} & \cdots & a'_{\mathrm{N_p},\mathrm{N_p}-1} & a'_{\mathrm{N_p},\mathrm{N_p}} & b'_{\mathrm{N_p}} \end{array}\right] \begin{bmatrix} x_1 \\ x_2 \\ x_3 \\ \vdots \\ x_{\mathrm{m}} \\ \vdots \\ x_{\mathrm{N_p}-1} \\ x_{\mathrm{N_p}} \end{bmatrix} \tag{5.17}$$

where $a'_{1,\mathrm{k}} = a_{\mathrm{m,k}}$ and $a'_{\mathrm{m,k}} = a_{1,\mathrm{k}}$ for $k = 1, \ldots, N_{\mathrm{p}}$ and $b'_1 = b_{\mathrm{m}}$ and $b'_{\mathrm{m}} = b_1$.

The objective is to produce an upper triangular matrix. The first row of augmented matrix corresponds to the statement:

$$a'_{1,1}x'_1 + a'_{1,2}x'_2 + a'_{1,3}x'_3 + \cdots + a'_{1,\mathrm{m}} + \cdots + a'_{1,\mathrm{N_p}-1}x'_{\mathrm{N_p}-1} + a'_{1,\mathrm{N_p}}x'_{\mathrm{N_p}} = b'_1 \tag{5.18}$$

That is to say,

$$x'_1 = \frac{1}{a'_{1,1}}\left(b'_1 - \left(a'_{1,2}x'_2 + a'_{1,3}x'_3 + \cdots + a'_{1,\mathrm{m}} + \cdots + a'_{1,\mathrm{N_p}-1}x'_{\mathrm{N_p}-1} + a'_{1,\mathrm{N_p}}x'_{\mathrm{N_p}}\right)\right) \tag{5.19}$$

Using this expression, it follows that

$$a'_{\mathrm{i},1}x'_1 = \frac{1}{a'_{1,1}}\left(b'_1 - \left(a'_{1,2}x'_2 + a'_{1,3}x'_3 + \cdots + a'_{1,\mathrm{m}} + \cdots + a'_{1,\mathrm{N_p}-1}x'_{\mathrm{N_p}-1} + a'_{1,\mathrm{N_p}}x'_{\mathrm{N_p}}\right)\right) \tag{5.20}$$

Hence, all elements of column 1 below row 1 may be eliminated by substitution; that is,

$$\left[\begin{array}{ccccccccc|c} a''_{1,1} & a''_{1,2} & a''_{1,3} & \dots & a''_{1,\mathrm{m}} & \dots & a''_{1,\mathrm{N_p}-1} & a''_{1,\mathrm{N_p}} & b''_1 \\ 0 & a''_{2,2} & a''_{2,3} & \dots & a''_{2,\mathrm{m}} & \dots & a''_{2,\mathrm{N_p}-1} & a''_{2,\mathrm{N_p}} & b''_2 \\ 0 & a''_{3,2} & a''_{3,3} & \dots & a''_{3,\mathrm{m}} & \dots & a''_{3,\mathrm{N_p}-1} & a''_{3,\mathrm{N_p}} & b''_3 \\ \vdots & \vdots & \vdots & \ddots & \vdots & \vdots & \vdots & \vdots & \vdots \\ 0 & a''_{m,2} & a''_{m,3} & \dots & a''_{\mathrm{m,m}} & \dots & a''_{\mathrm{m,N_p}-1} & a''_{\mathrm{m,N_p}} & b''_{\mathrm{m}} \\ \vdots & \vdots & \vdots & \vdots & \vdots & \ddots & \vdots & \vdots & \vdots \\ 0 & a''_{\mathrm{N_p}-1,2} & a''_{\mathrm{N_p}-1,3} & \dots & a''_{\mathrm{N_p}-1,\mathrm{m}} & \dots & a''_{\mathrm{N_p}-1,\mathrm{N_p}-1} & a''_{\mathrm{N_p}-1,\mathrm{N_p}} & b''_{\mathrm{N_p}-1} \\ 0 & a''_{\mathrm{N_p},2} & a''_{\mathrm{N_p},3} & \dots & a''_{\mathrm{N_p},\mathrm{m}} & \dots & a''_{\mathrm{N_p},\mathrm{N_p}-1} & a''_{\mathrm{N_p},\mathrm{N_p}} & b''_{\mathrm{N_p}} \end{array}\right] \left[\begin{array}{c} x_1 \\ x_2 \\ x_3 \\ \vdots \\ x_{\mathrm{m}} \\ \vdots \\ x_{\mathrm{N_p}-1} \\ x_{\mathrm{N_p}} \end{array}\right] \tag{5.21}$$

where

$$\begin{aligned} a''_{\mathrm{i,j}} &= a'_{\mathrm{i,j}} - \left(\frac{a'_{\mathrm{i},1}}{a'_{1,1}}\right) a'_{1,\mathrm{j}} \\ b''_{\mathrm{k}} &= b'_{\mathrm{k}} - \left(\frac{a'_{\mathrm{i},1}}{a'_{1,1}}\right) b'_{\mathrm{k}} \end{aligned} \tag{5.22}$$

The process is then repeated whereby the row with the maximum value in column 2 (excluding the first row) is swapped with the second row.

$$\left[\begin{array}{ccccccccc|c} a'''_{1,1} & a'''_{1,2} & a'''_{1,3} & \dots & a'''_{1,\mathrm{m}} & \dots & a'''_{1,\mathrm{N_p}-1} & a'''_{1,\mathrm{N_p}} & b_1 \\ 0 & a'''_{2,2} & a'''_{2,3} & \dots & a'''_{2,\mathrm{m}} & \dots & a'''_{2,\mathrm{N_p}-1} & a'''_{2,\mathrm{N_p}} & b'''_2 \\ 0 & a'''_{3,2} & a'''_{3,3} & \dots & a'''_{3,\mathrm{m}} & \dots & a'''_{3,\mathrm{N_p}-1} & a'''_{3,\mathrm{N_p}} & b'''_3 \\ \vdots & \vdots & \vdots & \ddots & \vdots & \vdots & \vdots & \vdots & \vdots \\ 0 & a'''_{m,2} & a'''_{m,3} & \dots & a'''_{\mathrm{m,m}} & \dots & a'''_{\mathrm{m,N_p}-1} & a'''_{\mathrm{m,N_p}} & b'''_{\mathrm{m}} \\ \vdots & \vdots & \vdots & \vdots & \vdots & \ddots & \vdots & \vdots & \vdots \\ 0 & a'''_{\mathrm{N_p}-1,2} & a'''_{\mathrm{N_p}-1,3} & \dots & a'''_{\mathrm{N_p}-1,\mathrm{m}} & \dots & a'''_{\mathrm{N_p}-1,\mathrm{N_p}-1} & a'''_{\mathrm{N_p}-1,\mathrm{N_p}} & b'''_{\mathrm{N_p}-1} \\ 0 & a'''_{\mathrm{N_p},2} & a'''_{\mathrm{N_p},3} & \dots & a'''_{\mathrm{N_p},\mathrm{m}} & \dots & a'''_{\mathrm{N_p},\mathrm{N_p}-1} & a'''_{\mathrm{N_p},\mathrm{N_p}} & b'''_{\mathrm{N_p}} \end{array}\right] \left[\begin{array}{c} x_1 \\ x_2 \\ x_3 \\ \vdots \\ x_{\mathrm{m}} \\ \vdots \\ x_{\mathrm{N_p}-1} \\ x_{\mathrm{N_p}} \end{array}\right] \tag{5.23}$$

Then the elimination process is applied to produce an augmented matrix of the following form:

$$\left[\begin{array}{ccccccccc|c} a''''_{1,1} & a''''_{1,2} & a''''_{1,3} & \dots & a''''_{1,\mathrm{m}} & \dots & a''''_{1,\mathrm{N_p}-1} & a''''_{1,\mathrm{N_p}} & b''''_1 \\ 0 & a''''_{2,2} & a''''_{2,3} & \dots & a''''_{2,\mathrm{m}} & \dots & a''''_{2,\mathrm{N_p}-1} & a''''_{2,\mathrm{N_p}} & b''''_2 \\ 0 & 0 & a''''_{3,3} & \dots & a''''_{3,\mathrm{m}} & \dots & a''''_{3,\mathrm{N_p}-1} & a''''_{3,\mathrm{N_p}} & b''''_3 \\ \vdots & \vdots & \vdots & \ddots & \vdots & \vdots & \vdots & \vdots & \vdots \\ 0 & 0 & a''''_{m,3} & \dots & a''''_{\mathrm{m,m}} & \dots & a''''_{\mathrm{m,N_p}-1} & a''''_{\mathrm{m,N_p}} & b''''_{\mathrm{m}} \\ \vdots & \vdots & \vdots & \vdots & \vdots & \ddots & \vdots & \vdots & \vdots \\ 0 & 0 & a''''_{\mathrm{N_p}-1,3} & \dots & a''''_{\mathrm{N_p}-1,\mathrm{m}} & \dots & a''''_{\mathrm{N_p}-1,\mathrm{N_p}-1} & a''''_{\mathrm{N_p}-1,\mathrm{N_p}} & b''''_{\mathrm{N_p}-1} \\ 0 & 0 & a''''_{\mathrm{N_p},3} & \dots & a''''_{\mathrm{N_p},\mathrm{m}} & \dots & a''''_{\mathrm{N_p},\mathrm{N_p}-1} & a''''_{\mathrm{N_p},\mathrm{N_p}} & b''''_{\mathrm{N_p}} \end{array}\right] \left[\begin{array}{c} x_1 \\ x_2 \\ x_3 \\ \vdots \\ x_{\mathrm{m}} \\ \vdots \\ x_{\mathrm{N_p}-1} \\ x_{\mathrm{N_p}} \end{array}\right] \tag{5.24}$$

This process repeats through all $\mathrm{N_p}$ columns of the square matrix within the augmented matrix.

$$\left[\begin{array}{ccccccccc|c} a_{1,1} & a_{1,2} & a_{1,3} & \dots & a_{1,\mathrm{m}} & \dots & a_{1,\mathrm{N_p}-1} & a_{1,\mathrm{N_p}} & b_1 \\ 0 & a_{2,2} & a_{2,3} & \dots & a_{2,\mathrm{m}} & \dots & a_{2,\mathrm{N_p}-1} & a_{2,\mathrm{N_p}} & b_2 \\ 0 & 0 & a_{3,3} & \dots & a_{3,\mathrm{m}} & \dots & a_{3,\mathrm{N_p}-1} & a_{3,\mathrm{N_p}} & b_3 \\ \vdots & \vdots & \vdots & \ddots & \vdots & \vdots & \vdots & \vdots & \vdots \\ 0 & 0 & 0 & \dots & a_{\mathrm{m,m}} & \dots & a_{\mathrm{m,N_p}-1} & a_{\mathrm{m,N_p}} & b_{\mathrm{m}} \\ \vdots & \vdots & \vdots & \vdots & \vdots & \ddots & \vdots & \vdots & \vdots \\ 0 & 0 & 0 & \dots & 0 & \dots & a_{\mathrm{N_p}-1,\mathrm{N_p}-1} & a_{\mathrm{N_p}-1,\mathrm{N_p}} & b_{\mathrm{N_p}-1} \\ 0 & 0 & 0 & \dots & 0 & \dots & 0 & a_{\mathrm{N_p},\mathrm{N_p}} & b_{\mathrm{N_p}} \end{array}\right] \left[\begin{array}{c} x_1 \\ x_2 \\ x_3 \\ \vdots \\ x_{\mathrm{m}} \\ \vdots \\ x_{\mathrm{N_p}-1} \\ x_{\mathrm{N_p}} \end{array}\right] \tag{5.25}$$

For the $\mathrm{k^{th}}$ step, the elements are found according to

$$a_{\mathrm{i,j}} -= \left(\frac{a_{\mathrm{i,k}}}{a_{\mathrm{k,k}}}\right) a_{\mathrm{k,j}} \tag{5.26}$$

Remember the maximum value for column 'i' corresponds to the maximum value in the set $a_{\mathrm{i,i}}$ to $a_{\mathrm{N_p,i}}$; that is, rows above row 'i' of column 'i' are not considered.

```
    for (int i=0;i<n;i++){
                // Search for maximum in this column:
                double maxEl = abs(Ab[i][i]);
                int maxRow = i;
                for (int k=i+1;k<n;k++){
                        if (abs(Ab[k][i]) > maxEl) {
                                maxEl = abs(Ab[k][i]);
                                maxRow = k;
                        }
                }
                //Swap maximum row with current row (column by column)
                for (int k=i;k<n+1;k++) {
                        double tmp = Ab[maxRow][k];
                        Ab[maxRow][k] = Ab[i][k];
                        Ab[i][k] = tmp;
                }
                //Make all rows below this one 0 in current column
                for (int k=i+1;k<n;k++){
                        double c = -Ab[k][i]/Ab[i][i];
                        for (int j=i;j<n+1;j++) {
                                if (i==j) {
                                        Ab[k][j] = 0;
                                } else {
                                        Ab[k][j] += c*Ab[i][j];
                                }
                        }
                }
        }
```

At this point, a simple backward-substitution algorithm can be applied to determine $\boldsymbol{x}$.

5.3 Cholesky decomposition

Let us consider again the equation $\boldsymbol{x} = \boldsymbol{A}^{-1}\boldsymbol{b}$. Suppose that it is possible to factorize $\boldsymbol{A}$ as the product of a lower triangular matrix, $\boldsymbol{L}$, and an upper triangular matrix which is the transpose of L, $\boldsymbol{U} = L^{\mathrm{T}}$. That is,

$$\begin{aligned}\boldsymbol{A} &= \boldsymbol{L}\boldsymbol{L}^{\mathbf{T}} \\ &= \begin{bmatrix} l_{1,1} & 0 & \dots & 0 \\ l_{2,1} & l_{2,2} & \dots & 0 \\ \vdots & \vdots & \ddots & \vdots \\ l_{\mathrm{n},1} & l_{\mathrm{n},2} & \dots & l_{\mathrm{n,n}} \end{bmatrix} \begin{bmatrix} l_{1,1} & l_{2,1} & \dots & l_{\mathrm{n},1} \\ 0 & l_{2,2} & \dots & l_{\mathrm{n},2} \\ \vdots & \vdots & \ddots & \vdots \\ 0 & 0 & \dots & l_{\mathrm{n,n}} \end{bmatrix}\end{aligned} \tag{5.27}$$

Therefore, our equation of interest may be expressed as follows:

$$\boldsymbol{L}\boldsymbol{L}^{\mathbf{T}}\boldsymbol{x} = \boldsymbol{b} \tag{5.28}$$

Let $\boldsymbol{y} = \boldsymbol{L}^{\mathbf{T}}\boldsymbol{x}$. Therefore,

$$\boldsymbol{L}\boldsymbol{y} = \boldsymbol{b} \tag{5.29}$$

Given the structure of $\boldsymbol{L}$, it follows that $\boldsymbol{y}$ can be solved by forward substitution:

$$\begin{aligned} y_1 &= b_1/l_{1,1} \\ y_2 &= \left(b_2 - l_{2,1}y_1\right)/l_{2,2} \\ y_3 &= \left(b_3 - l_{3,1}y_1 - l_{3,2}y_2\right)/l_{3,3} \\ &\vdots \\ y_{\mathrm{n}} &= \left(b_{\mathrm{n}} - \sum_{i=1}^{i=n-1} l_{\mathrm{n,i}}y_{\mathrm{i}}\right)/l_{\mathrm{n,n}} \end{aligned} \tag{5.30}$$

To determine the unknown vector $\boldsymbol{x}$, given the structure of $\boldsymbol{L}^{\mathrm{T}}$, backward substitution is then applied:

$$\begin{aligned} x_{\mathrm{n}} &= y_{\mathrm{n}}/l_{\mathrm{n,n}} \\ x_{\mathrm{n}-1} &= (y_{\mathrm{n}-1} - l_{\mathrm{n,n}-1}x_{\mathrm{n}-1})/l_{\mathrm{n}-1,\mathrm{n}-1} \\ &\vdots \\ x_1 &= \left(y_1 - \sum_{j=2}^{j=n} l_{\mathrm{j},1}x_{\mathrm{j}}\right)/l_{1,1} \end{aligned} \tag{5.31}$$

Or, generally speaking,

$$x_{\mathrm{i}} = \left(y_{\mathrm{i}} - \sum_{j=i+1}^{j=n} l_{\mathrm{j,i}}x_{\mathrm{i}}\right)/l_{\mathrm{i,i}} \tag{5.32}$$

So, if $\boldsymbol{A}$ can be factorized into $\boldsymbol{L}$ and $\boldsymbol{L}^{\mathrm{T}}$, the system can be solved. Consequently, our goal is to develop an algorithm which can perform the decomposition/factorization.

Since only the first element of the first row of $\boldsymbol{L}$ is non-zero, it follows that all the elements of the first row of $\boldsymbol{L}$ can be determined:

$$a_{1,\mathrm{i}} = l_{\mathrm{i},1} \tag{5.33}$$

Since only the first element of the first column of $\boldsymbol{L}^{\mathrm{T}}$ is non-zero, it follows that all the elements of the first column of $\boldsymbol{L}$ can be determined:

$$a_{\mathrm{i},1} = l_{\mathrm{i},1}l_{1,1} \tag{5.34}$$

With all of the elements of the first column of $\boldsymbol{L}$ determined, it is then possible to go through and determine the remaining unknowns.

The next step would be to note that $l_{2,1}$ is known. By matrix multiplication, $a_{2,2} = l_{2,1}u_{1,2} + u_{2,2}$. Hence,

$$u_{2,2} = a_{2,2} - l_{2,1}u_{1,2} \tag{5.35}$$

In other words, now the entire second column of $\boldsymbol{U}$ has been determined.

At this point, the unknowns in the third row of $\boldsymbol{L}$ (only one unknown at this point) can now be determined:

$$a_{3,2} = l_{3,1}u_{1,2} + l_{3,2}u_{2,2} \tag{5.36}$$

In other words, now the entire third row of $\boldsymbol{L}$ has been determined.

Again by considering matrix multiplication, it is now possible to go through and calculate all the unknowns in the third column of $\boldsymbol{U}$:

$$\begin{aligned} a_{2,3} &= l_{2,1}u_{1,3} + u_{2,3} \\ a_{3,3} &= l_{3,1}u_{1,3} + l_{3,2}u_{2,3} + u_{3,3} \end{aligned} \tag{5.37}$$

After this, it is possible to determine all the unknowns in the fourth row of $\boldsymbol{L}$:

$$a_{4,2} = l_{4,1}u_{1,2} + l_{4,2}u_{2,2} \tag{5.38}$$

This process is then repeated i.e. solve all unknowns in column i of $\boldsymbol{U}$ and then solve all unknowns in row $i+1$ of $\boldsymbol{L}$ then proceed through i.

In short,

$$\begin{aligned} u_{1,\mathrm{j}} &= a_{1,\mathrm{j}} \\ l_{\mathrm{j},1} &= a_{\mathrm{j},1}/u_{1,1} \end{aligned} \tag{5.39}$$

and

$$\begin{aligned} u_{\mathrm{i,j}} &= a_{\mathrm{i,j}} - \sum_{t=1}^{i-1} l_{\mathrm{i},t}u_{t,\mathrm{j}} \\ l_{\mathrm{j,i}} &= \frac{a_{\mathrm{j,i}} - \sum_{t=1}^{i-1} l_{\mathrm{j},t}u_{t,\mathrm{i}}}{u_{\mathrm{i,i}}} \end{aligned} \tag{5.40}$$

where $i = 1 \to n$ and $j = 1 \to n$.

Chapter 6

Calculating forces, torque, moments and power

The default output for Wind Panel is to output forces in the body reference frame. The body reference frame is defined to be one which co-rotates with the low-speed shaft. If the blades are rigid and there is no pitch mechanism, the body geometry (in body reference frame coordinates) will not change with time.

An illustration of the body reference frame for a vertical axis machine is provided below:

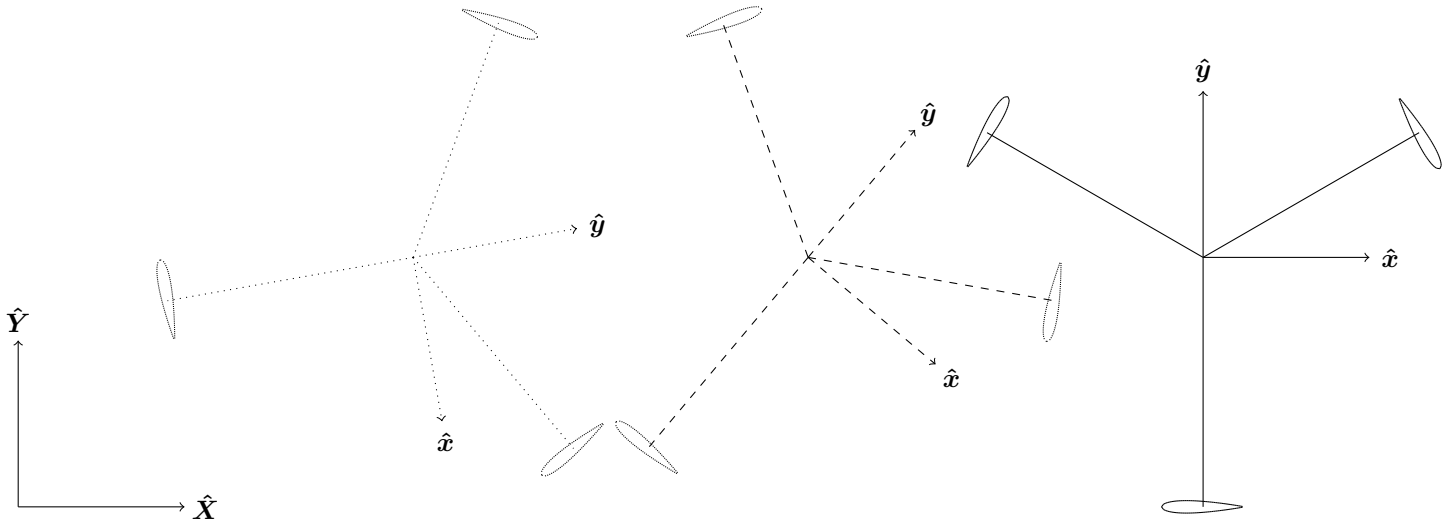

Figure 6.1: Illustration of the body reference frame for 2D simulations at three different time steps (solid, dashed and dotted). The simulation involves a steady free-stream wind speed which is aligned with $\hat{\boldsymbol{X}}$; hence, only the X component of the origin of the body reference frame changes with time.

6.1 Forces expressed in the body reference frame

Panel methods determine the 'strengths' of the body panels for each and every time step. From this, the pressure coefficient distribution across an aerofoil/blade may be determined. The equations used to calculate the pressure coefficient distributions depend on what boundary condition is being used.

6.2 Torque and power

Suppose that a time series of F_{x}, F_{y} and F_{z} are provided. These are 'instantaneous' forces. Correspondingly, the instantaneous torque and bending moments are found through equation 6.1:

$$\boldsymbol{\tau} = \boldsymbol{r} \times \boldsymbol{F} \tag{6.1}$$

For a vertical axis machine, the z-component of $\boldsymbol{\tau}$ is the driving torque. The other two components (only one for 2D simulations) are the bending moments.

For a horizontal axis machine, the x-component of $\boldsymbol{\tau}$ is the driving torque. The other two components are the bending moments.

The total torque produced over one revolution is found through integration. For example, for a vertical axis machine,

$$\tau_{\mathrm{z_{tot}}} = \int_0^{2\pi} \tau_{\mathrm{z}} \mathrm{d}\theta \tag{6.2}$$

A numerical implementation of equation 6.2 can be achieved using the trapezoidal rule:

$$\int_0^{2\pi} \tau_{\mathrm{z}} \mathrm{d}\theta \approx \sum_{k=1}^{N} \left[\frac{\tau z(\theta_{\mathrm{k}-1}) + \tau z(\theta_{\mathrm{k}})}{2} \right] \Delta\theta_{\mathrm{k}} \tag{6.3}$$

Alternatively, one could use Simpson's rule:

$$\int_0^{2\pi} \tau_{\mathrm{z}} \mathrm{d}\theta \approx \sum_{k=1}^{N} \frac{\Delta\theta_{\mathrm{k}}}{6} \left[\tau_{\mathrm{z}}(\theta_{\mathrm{k}-1}) + 4\tau_{\mathrm{z}}((\theta_{\mathrm{k}-1} + \theta_{\mathrm{k}})/2) + \tau_{\mathrm{z}}(\theta_{\mathrm{k}}) \right] \tag{6.4}$$

The power generated over one cycle is simply equation 6.5:

$$P = \int_0^{2\pi} \omega \tau_{\mathrm{z}} \mathrm{d}\theta \tag{6.5}$$

If the machine operates at a constant rotor speed, ω may be taken out of the integral.

For a horizontal axis machine, τ_{x} is used instead of τ_{z} for the power calculations.

Once the power generated over a cycled is obtained, the power coefficient can be calculated using either equation 6.6 (for a vertical axis machine) or equation 6.7 (for a horizontal axis machine):

$$C_{\mathrm{P}} = \frac{P}{\frac{1}{2}\rho A u_{\infty}^3} \tag{6.6}$$

where A is the frontal area. For a H-rotor, this is simply the diameter times the height. For a V-rotor, this is the area of a trapezium where the bottom is the radius at the base, the top is the radius at the tip and the height is the height difference between the base and the tip of a blade.

$$C_{\mathrm{P}} = \frac{P}{\frac{1}{2}\rho A u_{\infty}^3} \tag{6.7}$$

where $A = \pi r^2$ is the swept area of the rotor.

Part II

User manual

Chapter 7

Installing Wind Panel

7.1 Requirements

Wind Panel is a multi-threaded programme which uses the OpenMP (Open Multi-Processing) application programming interface (API) to use the multiple threads that are found on modern computers. Consequently, to run Wind Panel, it is necessary that the computer have the relevant files to allow OpenMP to operate successfully. These can be found in some (but not all) versions of the MinGW compiler. Alternatively, one can download the 'OpenMP files' folder, which is available from Strathcloud or by emailing Alexander Giles at alexander.giles@strath.ac.uk and then setting the PATH variable as described later.

For those given access to the source code, modifying Wind Panel will require an Integrated Development Environment (IDE) application and an appropriate compiler. It is recommended that the Code::Blocks IDE be used along with a specific MinGW compiler. Links for downloading the relevant software are provided in the following sections.

7.2 Downloading the Code::Blocks IDE

To download Code::Blocks, select the following **link**. This page has various download options:

1. codeblocks-16.01-setup.exe
2. codeblocks-16.01-setup-nonadmin.exe
3. codeblocks-16.01-nosetup.zip
4. codeblocks-16.01mingw-setup.exe
5. codeblocks-16.01mingw-nosetup.zip
6. codeblocks-16.01mingw_fortran-setup.exe

The number '16.01' will be different if a more recent version of Code::Blocks has been released.

Since the MinGW compiler will be downloaded separately, select the first option. Choose **Sourceforce.net** as the location where the IDE is to be downloaded from. Note - downloading Code::Blocks with a MinGW compiler (options 4, 5 and 6) is not recommended since the attached compiler is often inadequate.

7.2.1 Basic compiler settings

Wind Panel has been written according to the C++ 11 standard. The default standard for Code::Blocks is C++ 98. To change this, carry out the following instructions:

1. Go to Settings, search for and then select 'Compiler...'
2. Select the 'Compiler settings' tab; then from the tabs below, select 'Compiler flags'.
3. Under the 'General' section, select 'Have g++ follow the c++ ISO C++ language standard [-std=C+11]'

It is also recommended that optimizations be enabled. To achieve this, carry out the following instructions:

1. Go to Settings, search for and then select 'Compiler...'
2. Select the 'Compiler settings' tab; then from the tabs below, select 'Compiler flags'.
3. Under the 'Optimizations' section, select 'Optimize fully (for speed) [-O3]'

7.3 Downloading the MinGW compiler

To download an appropriate version of the MinGW compiler, select the following **link**. Upon arriving at the page, select '**Download mingw-get-setup.exe (86.5 kB)**'.

Setting the compiler settings in Code::Blocks

1. In Settings, search for and then select 'Compiler...'
2. Select the 'Compiler Settings' tab; then from the tabs below, select the 'Other Compiler Options' and add the phrase '-fopenmp' (without the quotation marks).
3. (a) **If Code::Blocks is in Program Files (x86)**:

   Select the 'Linker settings' tab; then click **Add**. Specify the filepath for the OpenMP DLL in the **Add library** window. The following filepath should be used:

   'C:\Program Files (x86)\CodeBlocks\MinGW\ bin\libgomp-1.dll' (without the quotation marks). Click **OK** to accept this. Click **Add** again and enter the following filepath:

   'C:\Program Files (x86)\GnuWin32\lib\libgslcblas.a' (without the quotation marks). Click **OK** to accept this. Click **Add** again and enter the following filepath:

   'C:\Program Files (x86)\GnuWin32\lib\libgsl.a' (without the quotation marks). Click **OK** to accept this.

   (b) **If Code::Blocks is in Program Files**

   Select the 'Linker settings' tab; then click **Add**. Specify the filepath for the OpenMP DLL in the **Add library** window. The following filepath should be used:

   'C:\Program Files\CodeBlocks\MinGW\ bin\libgomp-1.dll' (without the quotation marks). Click **OK** to accept this. Click **Add** again and enter the following filepath:

   'C:\Program Files\GnuWin32\lib\libgslcblas.a' (without the quotation marks). Click **OK** to accept this. Click **Add** again and enter the following filepath:

   'C:\Program Files\GnuWin32\lib\libgsl.a' (without the quotation marks). Click **OK** to accept this.

7.3.1 Setting the PATH variable

The PATH is the system variable that your operating system uses to locate needed executables (in this case those relating to OpenMP) from the command line or Terminal window. The PATH system variable can be set using **System Utility** in control panel on Windows.

Windows 8 & 10

1. In search, search for and then select 'System (Control Panel)'
2. Click the **Advanced system settings** link
3. Click **Environment Variables**. In the section **System Variables**, find the PATH environment variable and select it. Click **Edit**. If the PATH environment variable does not exist, click 'New'
4. In the **Edit System Variable** (or **New System Variable**) window, specify the value of the PATH environment variable. For those who have downloaded the MinGW, this will be either C:\Program Files (x86)\CodeBlocks\MinGW\bin or C:\Program Files \CodeBlocks\MinGW\bin depending on where the MinGW compiler has been saved. If the 'OpenMP' has been downloaded, the PATH variable needs to be set to the location of this folder.
5. Click **OK**. Close all remaining windows by clicking **OK**.

Windows 7

1. From the desktop, right click the **Computer** icon
2. Choose **Properties** from the context menu.
3. Click the **Advanced system settings** link.
4. Click **Environment Variables**. In the section **System Variables**, find the PATH environment variable and select it. Click **Edit**. If the PATH environment variable does not exist, click 'New'
5. In the **Edit System Variable** (or **New System Variable**) window, specify the value of the PATH environment variable. This will be C:\Program Files (x86)\CodeBlocks\MinGW\bin or C:\Program Files \CodeBlocks\MinGW\bin depending on where the MinGW compiler has been saved. If the 'OpenMP' has been downloaded, the PATH variable needs to be set to the location of this folder.
6. Click **OK**. Close all remaining windows by clicking **OK**.

Windows Vista

1. From the desktop, right click the **My Computer** icon.
2. Choose **Properties** from the context menu
3. Click the **Advanced** tab (**Advanced system settings** link in Vista).
4. Click **Environment Variables**. In the section **System Variables**, find the PATH environment variable and select it. Click **Edit**. If the PATH environment variable does not exist, click New.
5. In the **Edit System Variable** (or **New System Variable**) window, specify the value of the PATH environment variable. This will be C:\Program Files (x86)\CodeBlocks\MinGW\bin or C:\Program Files \CodeBlocks\MinGW\bin depending on where the MinGW compiler has been saved. If the 'OpenMP' has been downloaded, the PATH variable needs to be set to the location of this folder.
6. Click **OK**. Close all remaining windows by clicking **OK**.

Windows XP

1. Select **Start**, select **Control Panel**, double click **System**, and select the **Advanced** tab.
2. Click **Environment Variables**. In the section **System Variables**, find the PATH environment variable and select it. Click **Edit**. If the PATH environment variable does not exist, click New.
3. In the **Edit System Variable** (or **New System Variable**) window, specify the value of the PATH environment variable. This will be C:\Program Files (x86)\CodeBlocks\MinGW\bin or C:\Program Files \CodeBlocks\MinGW\bin depending on where the MinGW compiler has been saved. If the 'OpenMP' has been downloaded, the PATH variable needs to be set to the location of this folder.
4. Click **OK**. Close all remaining windows by clicking **OK**.

Chapter 8

Programme overview

This chapter outlines some of the fundamental properties of Wind Panel that need to be understood in order to know how to change or add to Wind Panel.

8.1 Basic definitions & notation

8.1.1 The global and body reference frames

Throughout the code, three types of reference frame are used: the global reference frame, the body reference frame, and the panel reference frame.

The global reference frame is denoted by capital letters. That is, velocity components in the global reference frame are denoted by U, V and U, V, W for the two and three dimensional simulations respectively. Correspondingly, coordinates are denoted by X, Y and X, Y, Z for the two and three dimensional simulations respectively.

The body reference frame is denoted by lower case letters. That is, velocity components in a body reference frame are denoted by u, v and u, v, w for two and three dimensional simulations respectively. Correspondingly, coordinates are denoted by x, y and x, y, z for two and three dimensional simulations respectively. There will be one body reference frame for each machine featured in a simulation. That is, a farm simulation comprising 'k' machines will have 'k' body reference frames. This allows the individual machines to rotate with independent angular velocities.

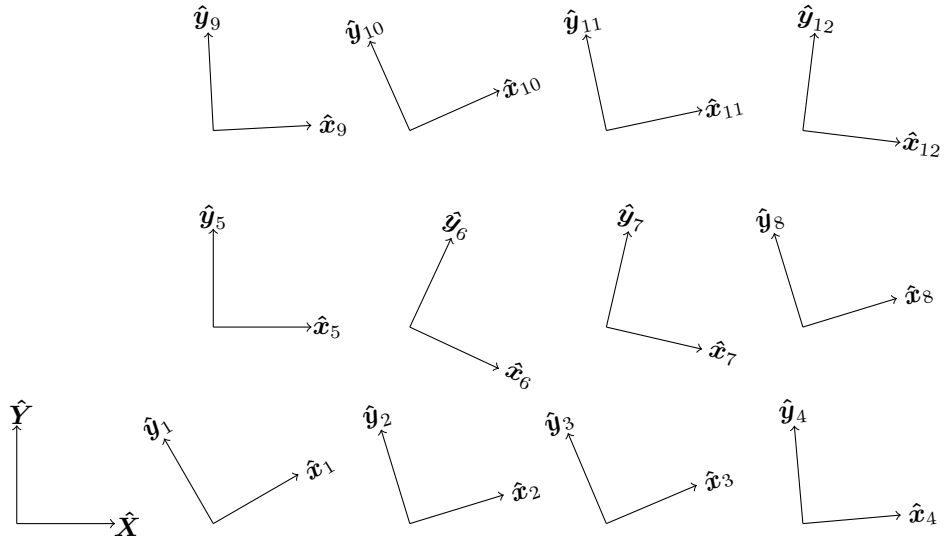

Figure 8.1: Illustration of the body reference frames for a 2D wind farm simulation comprising twelve machines

Regarding three-dimensional simulations, either horizontal or vertical axis machines can be simulated. A horizontal axis machine is defined to rotate in the yz plane of its own body reference frame. That is, rotation of the blades is about the x

axis. Hence, the x-axese of the body reference frames are parallel to the X-axis of the global reference frame.

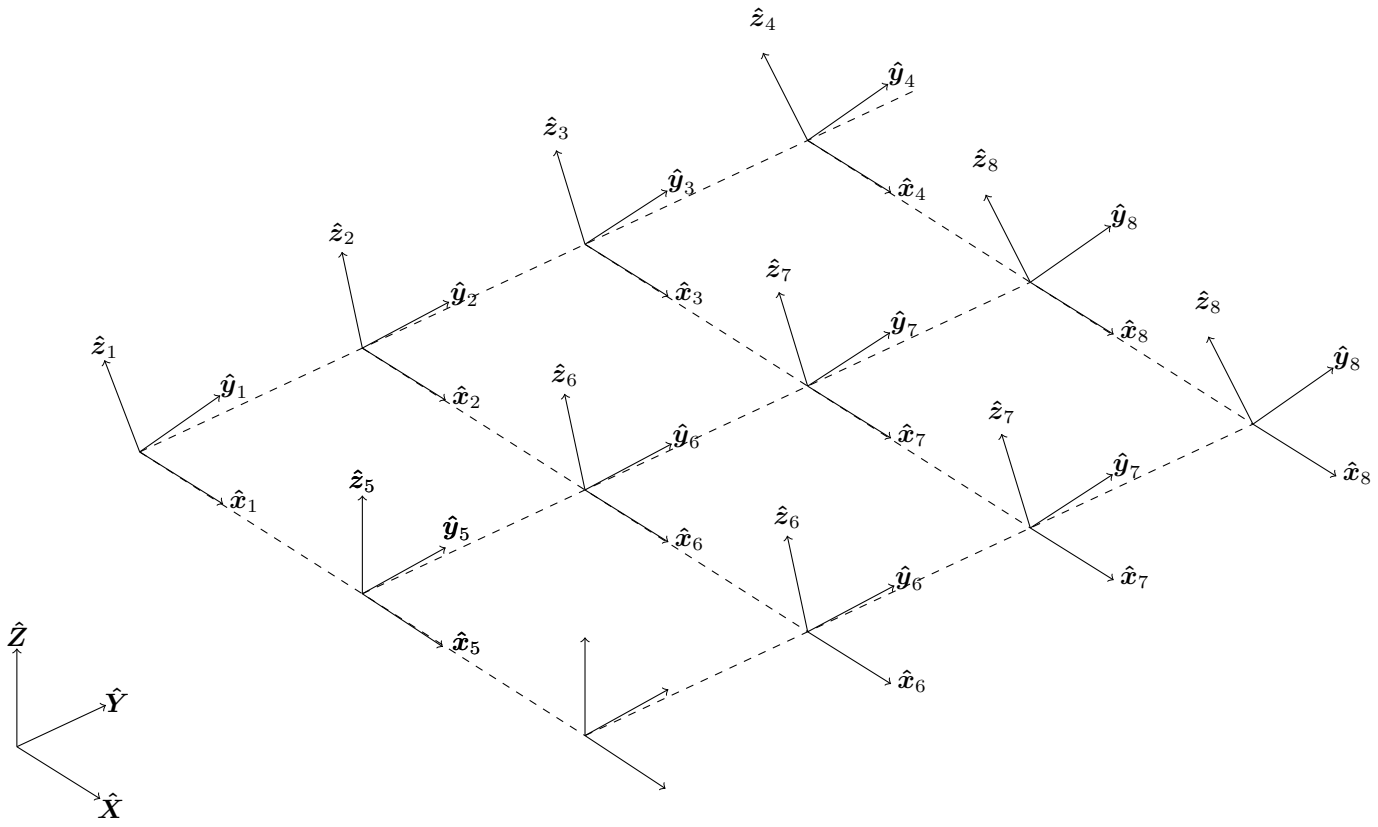

Figure 8.2: Illustration of body reference frames for a farm of horizontal axis machines

A vertical axis machines is defined to rotate in the xy plane of its own body reference frame. That is, rotation of the blades is about the z axis. Yawed and skewed flow is achieved by introducing non-zero Y and Z components (respectively) of the free-stream velocity.

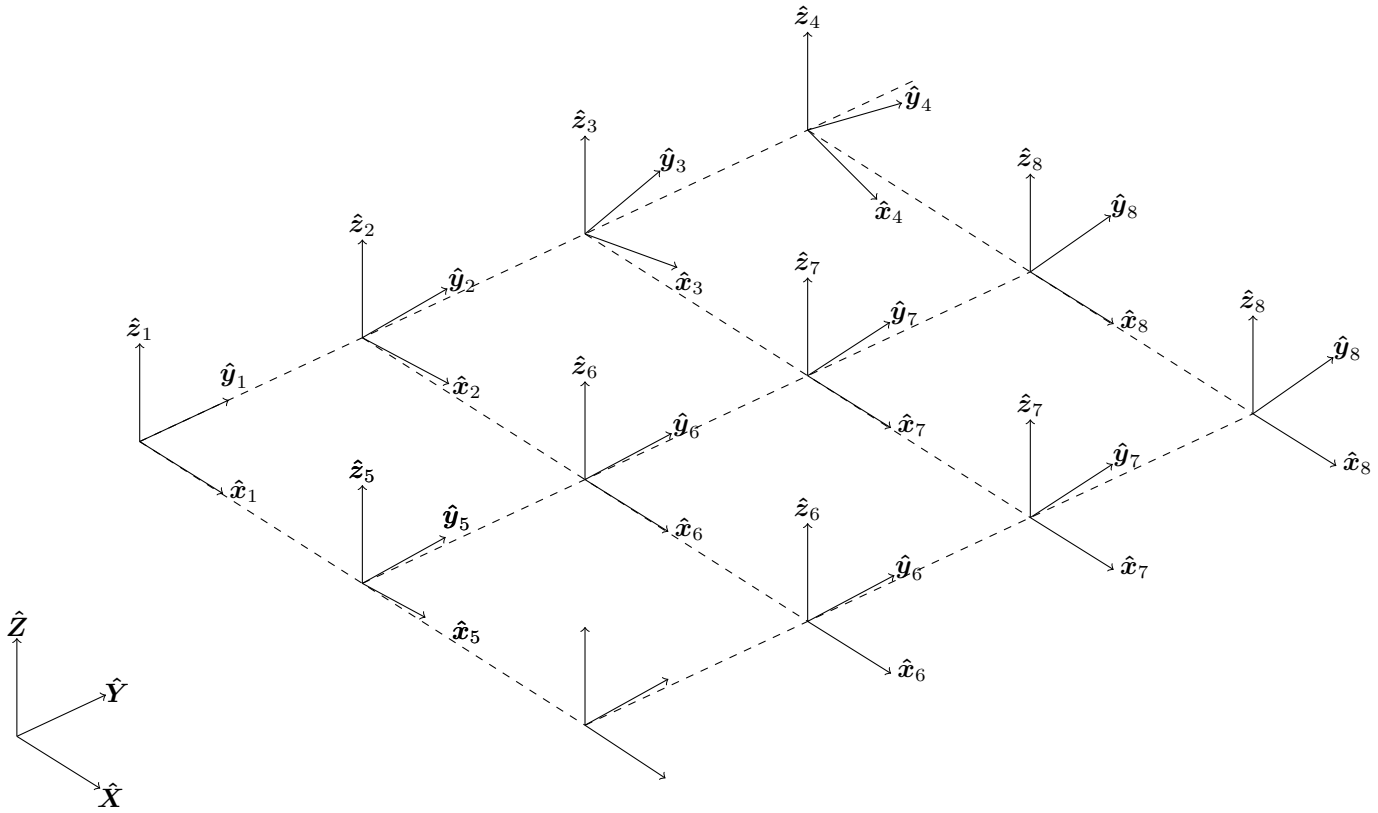

Figure 8.3: Illustration of body reference frames for a farm of vertical axis machines

8.1.2 Definitions of rotation for horizontal and vertical axis machines

As can be seen from figure 8.2, a horizontal axis machine is defined to rotate in the yz plane of its own body reference frame. That is, rotation of the blades is about the x axis. Referring to figure 8.3, a vertical axis machines is defined to rotate in the xy plane of its own body reference frame. That is, rotation of the blades is about the z axis. Yawed and skewed flow is achieved by introducing non-zero Y and Z components (respectively) of the free-stream velocity.

8.2 Programme structure

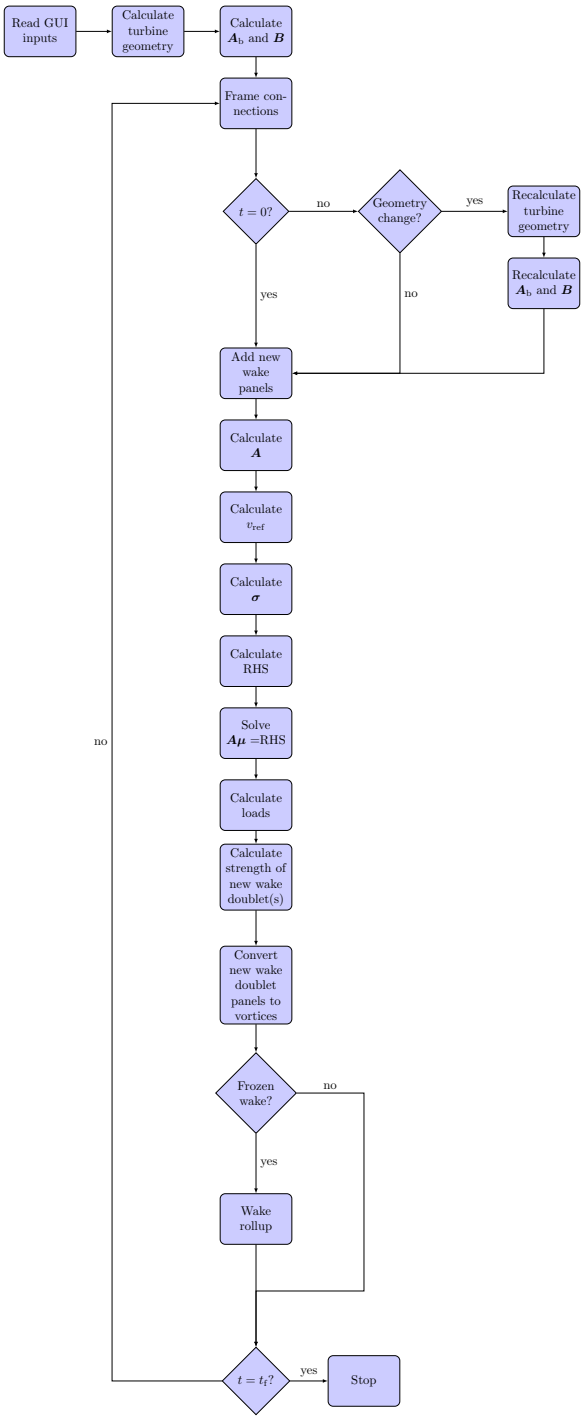

Figure 8.4: Programme structure

Chapter 9

The GUI

The Wind Panel graphical user interface (GUI) features a mixture of menu bars and textfields embedded into the main window.

9.1 Settings in the main window

The settings in the main window can be split into the following categories:

1. Mesh settings
2. Time step step settings
3. Operational settings
4. Farm settings
5. Wind settings

9.1.1 Mesh settings

Two parameters can be set in the mesh settings: number of panels per half blade element, N_{p}, and internal displacement of the collocation points.

The surface of each blade element is modelled by N_{p2} panels. The most important regions (aerodynamically speaking) of an aerofoil are the leading and trailing edges; this is also where the geometry is most likely to differ from a panel representation. The same is true for a blade element. Thus it makes sense to have a high density of panels in these regions. However, there is no need for a high density of panels in the middle of an aerofoil. Having such would yield a limited increase in accuracy at the expense of a significant increase in computational cost. Therefore, a panelling scheme based on the 'semi-circle' concept is applied to ensure that the panel density is highest at the leading and trailing edges, keeping the total number of panels within reasonable limits. The scheme is illustrated by figure 9.1.

If the aerofoil is to represented by N_{p2} panels, then there will be N_{p2} angular values split evenly over the interval $0 \rightarrow 2\pi$. The formula for calculating the x coordinates from the angular values is as follows:

$$x = \frac{c}{2}(1 - \cos\beta) \tag{9.1}$$

where β is the angle and c is the chord. The corresponding y values may then be calculated easily. For a NACA XXXX-aerofoil, the corresponding y values are calculated through equation :

$$y = 5tc\left[0.2969\sqrt{\frac{x}{c}} - 0.1260\left(\frac{x}{c}\right) - 0.3516\left(\frac{x}{c}\right)^2 + 0.2843\left(\frac{x}{c}\right)^3 - 0.1036\left(\frac{x}{c}\right)^4\right] \tag{9.2}$$

where t is the maximum thickness as a fraction of the chord.

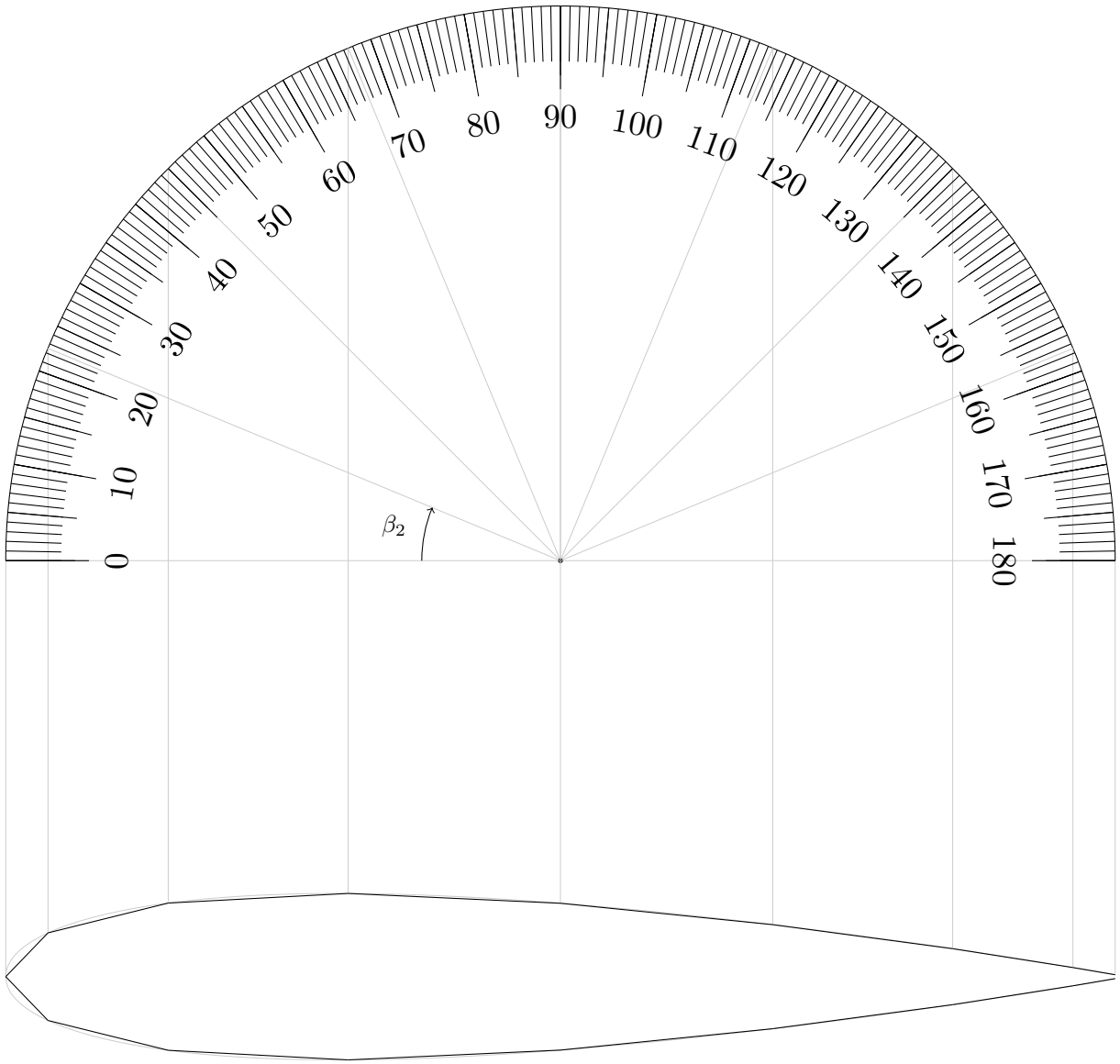

Figure 9.1: Panelling scheme for an aerofoil. The panel approximation is given by the black line while the actual aerofoil shape is given by the faint grey line. Only the second angle, β_2, is explicitly shown.

It is stressed that the body coordinates are expressed using the body reference frame(s).

The standard convention, which is adopted in Wind Panel, is to number the panels clockwise from the underside of the trailing edge as shown.

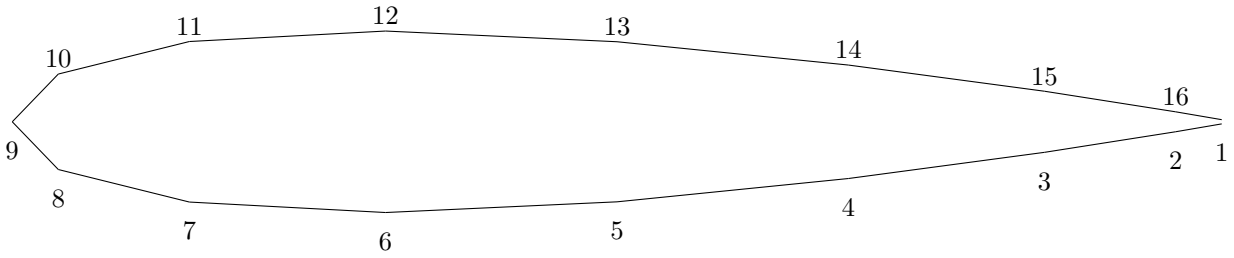

Figure 9.2: Panel numbering scheme for an aerofoil. The numbers coincide with the panel origins.

For both Dirichlet and Neumann panel methods, the collocation points are chosen to lie somewhere in the vicinity of the midpoints of the panels as shown in figure 4.2. For numerical stability reasons, it is often preferable to apply a small inward displacement so that the the collocation point does not lie on the surface of a panel. According to Katz & Plotkin, an

internal displacement of 0.05 panel lengths is appropriate. However, Wind Panel allows the user to choose what the internal displacement should be. Note that, in keeping with Katz & Plotkin, the internal displacement is expressed as a fraction of the panel length. That is an entry of 0.0125 corresponds to an internal displacement of 0.0125 panel lengths. It should also be pointed out that this approach also means that collocation points for panels of different lengths have different internal displacements. Since the trailing edge involves two sides coming close together, only a small internal displacement can be applied; hence, the chosen variation of internal displacement (which complements the panelling scheme used in Wind Panel).

It should be noted that the number of panels should be kept as low as possible in order to minimise the computational cost.

9.1.2 Wake modelling settings

Two parameters can be set in the time step settings: the number of time steps per revolution, N_{one}, and the number of revolutions, N_{rev}. Correspondingly, the total number of time steps is $N_{\text{one}}N_{\text{rev}}$.

Ferreira recommends 72 time steps per revolution with 20 - 30 revolutions for 2D VAWT simulations. Generally speaking, for a 2D VAWT system with N_t machines, each having N_{b} blades, the total number of wake vortex blobs at the final step is given as follows:

$$N_{\text{wake}-\text{vor}} = N_{\text{t}}N_{\text{b}}(N_{\text{one}}N_{\text{rev}} + 1) \tag{9.3}$$

For 3D simulations, the recommended time step depends on whether a VAWT or HAWT is being simulated. For HAWTs, as low an amount as 40 time steps per revolution can be used. For VAWTs, as with the 2D simulations, a relative fine time step is recommended; this is mainly due to the inherent unsteadiness associated with a VAWT.

Care must be taken to ensure that the number of wake vortex blobs/line segments does not become excessive, particularly if the wake is modelled as a free-vortex system (for frozen wakes controlling the size of the wake is not as important).

The current implementation of Wind Panel allows the user to freeze the wake. By that, it is meant that the wake vortices are uninfluenced by each other and by the body singularity elements. This significantly reduces the computational cost; however, it comes at the cost of decreased accuracy. If the double-wake concept is to be applied, it is recommended that the wake be unfrozen. This is to allow accurate prediction of the angle of attack (which is required to prescribe the separation location). To have an unfrozen wake simulation, select **On**. To have a frozen wake simulation, select **Off**.

9.1.3 Operational settings

Four parameters can be set in the operational settings: nominal tip-speed ratio, initial pitch angle, amplitude of time-varying pitch, and frequency of time-varying pitch.

The nominal tip-speed ratio is defined as the ratio of the rotor speed (at the tip of the blade) at which the turbine would operate without any active effort by the controller (to change the rotor speed) to the mean x-component of the wind speed. That is,

$$\lambda_{\text{nom}} = \frac{\Omega_0 R}{u_\infty} \tag{9.4}$$

where R is the perpendicular (to the axis of rotation) distance from the axis of rotation to the blade tip. For a HAWT this is simply the blade length plus the radius of the hub.

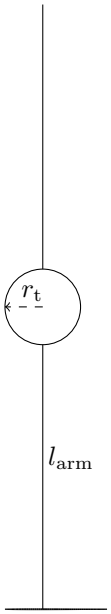

Figure 9.3: Simple illustration of a 2D VAWT. The radius of the tower is denoted by r_t; the length of the arm attaching the blade to the tower is l_arm. Hence, the radius is given by $R = r_\mathrm{t} + l_\mathrm{arm}$. The axis of rotation, $\hat{\boldsymbol{z}}$, is coming out of the page and is centred on the rotor centre.

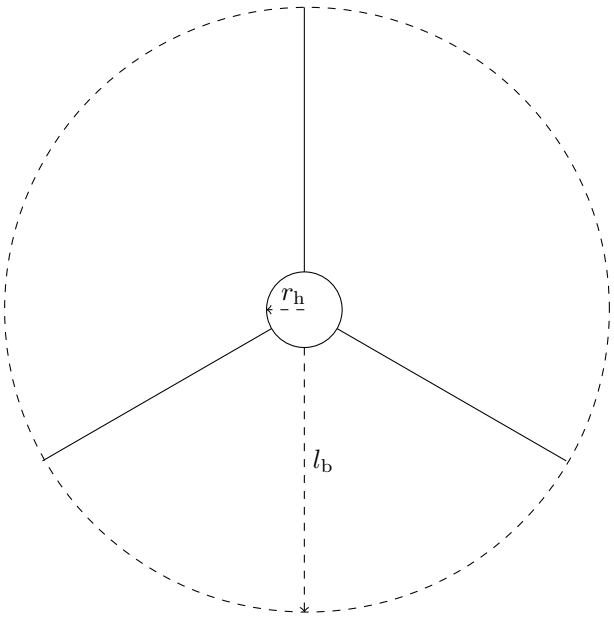

Figure 9.4: Simple illustration of a HAWT. The radius of the hub is denoted by r_h; the blade length is denoted by l_b. The axis of rotation, $\hat{\boldsymbol{x}}$, is going into the page and is centred on the rotor centre.

The pitch angle convention is that positive angles correspond to the leading edge pointing out and away from the centre of rotation for vertical axis machines while negative angles correspond to the leading edge pointing in and towards the centre of rotation for vertical axis machines. Examples are shown below:

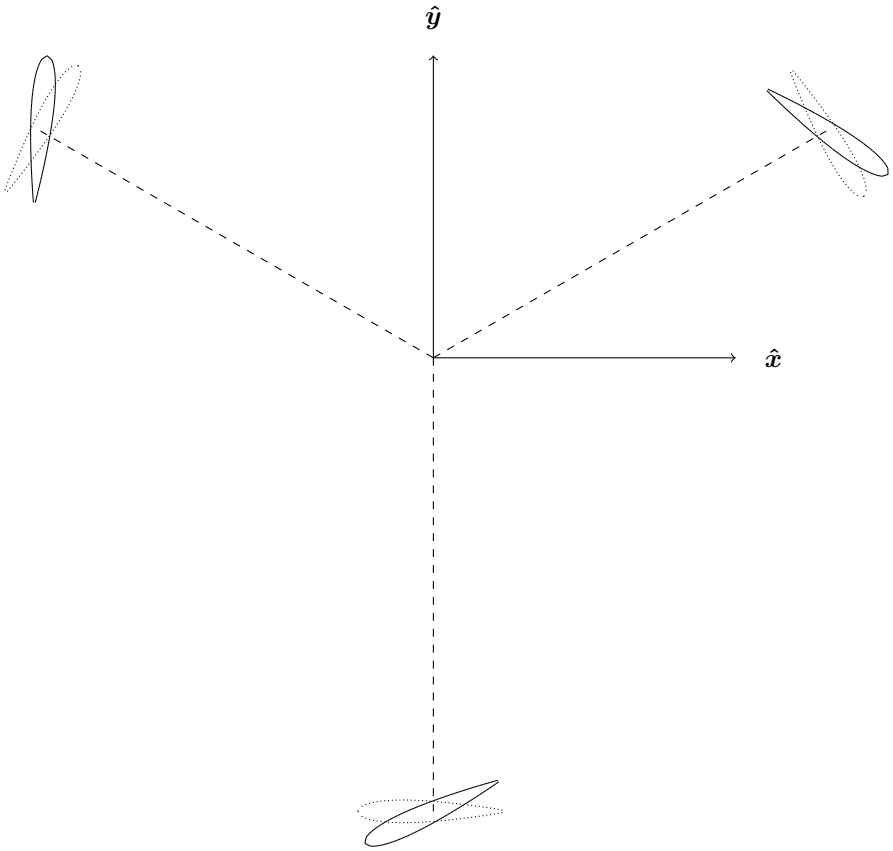

Figure 9.5: Illustration of the pitch angle conventions for 2D simulations (positive pitch angle). The dotted blades are unpitched blades for reference.

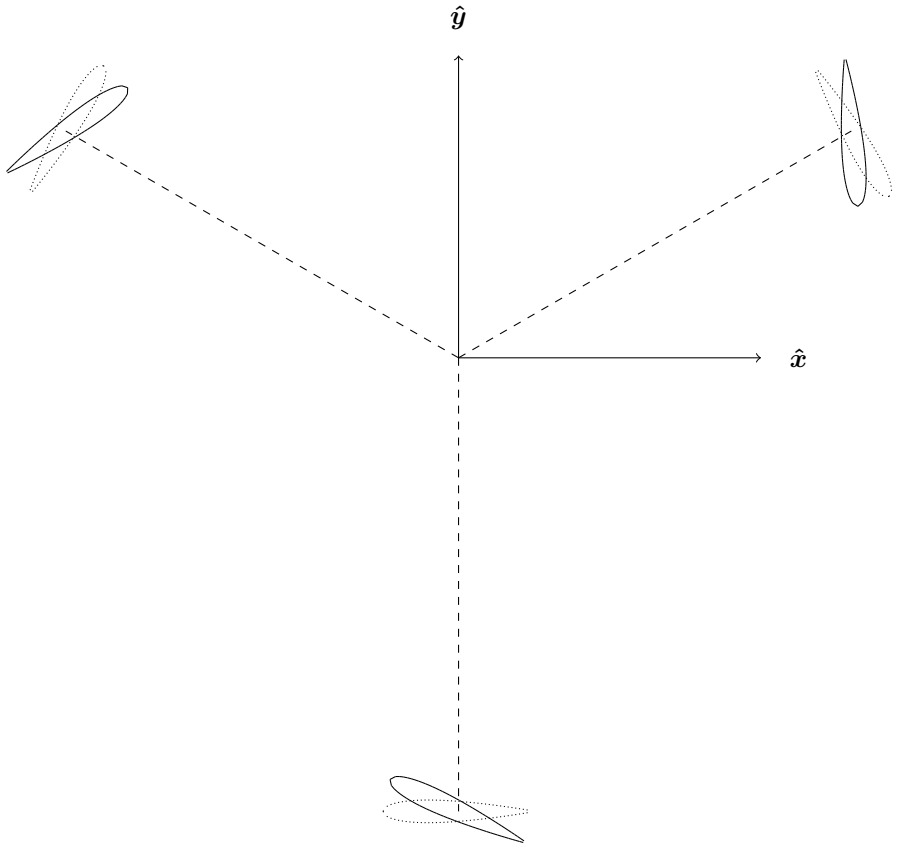

Figure 9.6: Illustration of the pitch angle conventions for 2D simulations (negative pitch angle). The dotted blades are unpitched blades for reference.

9.1.4 Farm settings

Three parameters can be set in farm settings: numbers of rows, number of columns and spacing between wind turbines.

For single turbine simulations, the number of rows and columns should both be set to one. In this case, the spacing between wind turbines is an unused variable.

For multiple turbine simulations, the number of rows corresponds to the number of turbines parallel to the X axis (global reference frame), while the number of columns corresponds to the number of turbines parallel to the Y axis (global reference frame). The spacing between wind turbines is expressed as an multiple of the rotor diameter of the turbines (all will have the same rotor diameter).

9.1.5 Wind settings

Three parameters can be set in wind settings: mean X-component of the free stream wind speed, mean Y-component of the free stream wind speed, and mean Z-component of the free stream wind speed. These components are expressed in terms of the global reference frame.

For HAWT simulations, non-yawed flow is simulated when the latter two components' values are zero. For VAWT simulations, skewed flow is obtained by having a non-zero value for the mean Z-component of the free stream wind speed.

9.1.6 Simulation type (2D or 3D)

To perform any simulation, the number of dimensions needs to be specified. When selecting 2D or 3D, the user will be prompted to provide a rotor geometry .csv file. These must be correctly formatted. A .csv file may be generated from the Excel files found in the 'Excel files' folder.

3D rotor profile .csv files

Two types of 3D rotors can be simulated: horizontal axis and vertical axis machines.

Blade	Radius	Chord	Twist (degrees)	Pitch axis location	Aerofoil
1	4.50	1.63	20.00	0.82	15
1	5.50	1.60	16.30	0.80	15
1	6.50	1.54	13.00	0.77	15
1	7.50	1.48	10.05	0.74	15
1	8.50	1.42	7.45	0.71	15
1	9.50	1.36	5.85	0.68	15
1	10.50	1.29	4.85	0.65	15
1	11.50	1.23	4.00	0.61	15
1	12.50	1.16	3.15	0.58	15
1	13.50	1.10	2.60	0.55	15
1	14.50	1.03	2.02	0.51	15
1	15.50	0.96	1.36	0.48	15
1	16.50	0.88	0.77	0.44	15
1	17.50	0.81	0.33	0.40	15
1	18.50	0.71	0.14	0.35	15
1	19.50	0.55	0.05	0.27	15
1	20.30	0.27	0.02	0.13	15
2	4.50	1.63	20.00	0.82	15
2	5.50	1.60	16.30	0.80	15
2	6.50	1.54	13.00	0.77	15
2	7.50	1.48	10.05	0.74	15
2	8.50	1.42	7.45	0.71	15
2	9.50	1.36	5.85	0.68	15
2	10.50	1.29	4.85	0.65	15
2	11.50	1.23	4.00	0.61	15
2	12.50	1.16	3.15	0.58	15
2	13.50	1.10	2.60	0.55	15
2	14.50	1.03	2.02	0.51	15
2	15.50	0.96	1.36	0.48	15
2	16.50	0.88	0.77	0.44	15
2	17.50	0.81	0.33	0.40	15
2	18.50	0.71	0.14	0.35	15
2	19.50	0.55	0.05	0.27	15
2	20.30	0.27	0.02	0.13	15

Table 9.1: Illustration of a correctly formatted .csv file for HAWT simulations

The header for the vertical axis rotor geometry file is as follows: To represent a blade by N_z blade elements, there must be $N_z + 1$ entries for each of the above. This is to cover the end tops and bottoms of all blade elements.

For a rotor with N_b blades, with each blade being represented by N_z blade elements, there must be $N_b(N_z + 1)$ entries for each of the above, $N_z + 1$ for each blade. This is to allow variations from blade to blade.

For blade one, the first $N_z + 1$ entries under 'Blade' are 1. For the second $N_z + 1$ entries, the entries under 'Blade' are 2; this is for the second blade. This process is continued for the N_b blades. A sample is shown in table 9.2.

The second column is for the height of the blade element top/bottom. The height is the z value as defined in the body reference (xyz) frame. The third column is the radius, r; this is the distance from a height h along the z axis to the pitch axis location of the blade element top/bottom located at a height h. Mathematically, $r = \sqrt{x^2 + y^2}$. The chord values are specified in the fourth column. The twist is the internal pitch about the pitch axis; positive angles refer to . The seventh column is for the coning angle. The coning angle is the angle beween the blade and $\hat{\boldsymbol{z}}$. For H-rotors, this angle is zero; for V-rotors, this angle is a constant; and for egg-beaters, this will be a function of height. The eighth column is the phase; this refers to the rotation of the blade element about $\hat{\boldsymbol{z}}$. This makes it possible for twisted turbines to be modelled.

An illustration of a twisted blade on a vertical axis machine is presented in figure 9.7:

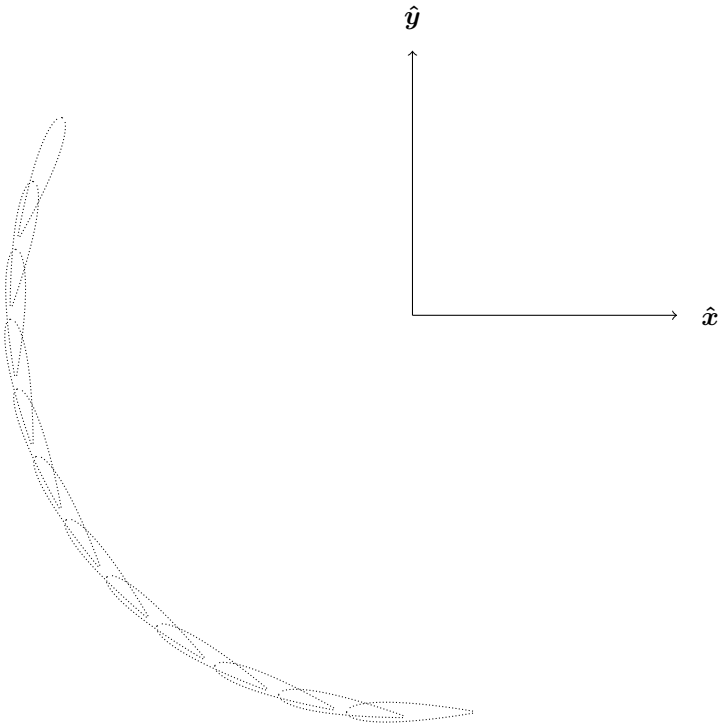

Figure 9.7: Plan view of the first blade of a Gorlov/helical/twisted turbine

The phase of each blade at the root, ψ_{n} is set according to equation 9.5

$$\psi_{\mathrm{n}} = \frac{2\pi n}{N_{\mathrm{n}}} \tag{9.5}$$

Thus, for a machine with four blades, if they are to form an X-rotor, the phase column should be non-zero as shown in the following table:

Blade	Height	Radius	Chord	Twist (degrees)	Pitch axis location	Coning angle (degrees)	Phase (see manual)	Aerofoil
1	0.00	25.00	3.75	0.00	0.94	15.00	0.00	15
1	20.00	30.18	4.53	0.00	1.13	15.00	0.00	15
1	40.00	35.35	5.30	0.00	1.33	15.00	0.00	15
1	60.00	40.53	6.08	0.00	1.52	15.00	0.00	15
1	80.00	45.71	6.86	0.00	1.71	15.00	0.00	15
1	100.00	50.88	7.63	0.00	1.91	15.00	0.00	15
2	0.00	25.00	3.75	0.00	0.94	15.00	0.00	15
2	20.00	30.18	4.53	0.00	1.13	15.00	0.00	15
2	40.00	35.35	5.30	0.00	1.33	15.00	0.00	15
2	60.00	40.53	6.08	0.00	1.52	15.00	0.00	15
2	80.00	45.71	6.86	0.00	1.71	15.00	0.00	15
2	100.00	50.88	7.63	0.00	1.91	15.00	0.00	15
3	0.00	25.00	3.75	0.00	0.94	15.00	0.00	15
3	-20.00	19.82	2.97	0.00	0.74	15.00	0.00	15
3	-40.00	14.65	2.20	0.00	0.55	15.00	0.00	15
3	-60.00	9.47	1.42	0.00	0.36	15.00	0.00	15
3	-80.00	4.29	0.64	0.00	0.16	15.00	0.00	15
3	-100.00	-0.88	-0.13	0.00	-0.03	15.00	0.00	15
4	0.00	25.00	3.75	0.00	0.94	15.00	0.00	15
4	-20.00	19.82	2.97	0.00	0.74	15.00	0.00	15
4	-40.00	14.65	2.20	0.00	0.55	15.00	0.00	15
4	-60.00	9.47	1.42	0.00	0.36	15.00	0.00	15
4	-80.00	4.29	0.64	0.00	0.16	15.00	0.00	15
4	-100.00	-0.88	-0.13	0.00	-0.03	15.00	0.00	15

Table 9.2: Illustration of the a correctly formatted .csv file for VAWT simulations.

Once Wind Panel has read the data in from the .csv files (assuming they are properly formatted), Wind Panel will create the wind turbine object. For a vertical axis machine, the arm which links the first blade to the tower is anti-parallel to $\hat{\boldsymbol{y}}$ as shown in figure 9.8. Subsequent blades are introduced at regular angular intervals going in a clockwise fashion.

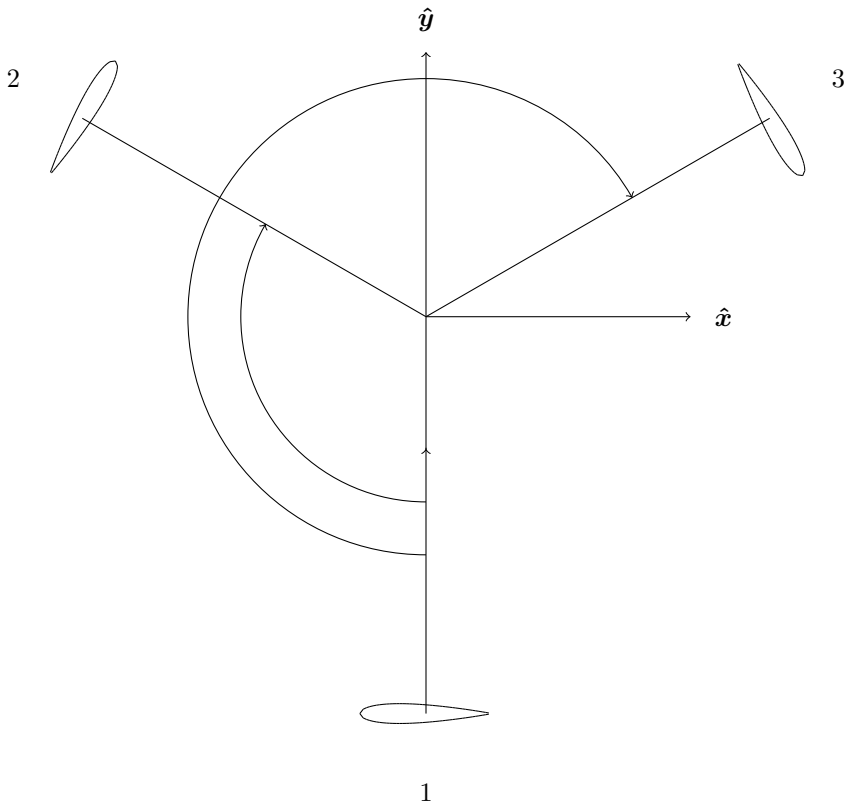

Figure 9.8: Blade numbering convention for a VAWT

9.2 The 'File' tab

The 'File' tab is where data may be loaded or saved. Data which can be loaded into Wind Panel includes the following: rotor profile, body coordinates, wake data, operational settings, turbulent wind field, and stiffness matrices.

9.3 The 'settings' tab

The 'settings' tab is where settings additional to those in the main GUI are set. Under this tab, the following properties can be set:

1. Solver
2. Singularity element
3. Vortex settings

9.3.1 Solver

Wind Panel features three matrix solvers: LU decomposition, LUP decomposition, Cholesky decomposition and Gaussian elimination. Full details of each can be found in section 5.

For simulations involving vertical axis machines, the distance covered by the trailing edge(s) of the blade(s) varies around the azimuth. As a result, the 'lengths' of the most recently shed doublet wake panels vary around the azimuth. This means that the $\boldsymbol{A}$ matrices in equations ... and ... vary with each time step. Since each call of Gaussian elimination is less costly than each call of LU, LUP or Cholesky (all coupled to forward-backward substitution functions), simulations involving vertical axis machines should employ Gaussian elimination.

For simulations involving horizontal axis machines, if the geometry of the machine (from the perspective of the body reference frame) is time invariant, LU or LUP decomposition should be used. Otherwise, Gaussian elimination should be selected.

9.3.2 Vortex settings

Under the 'Vortex settings', the core model and core growth model can be set. The following core model options are available:

1. **Basic**: in this method, the velocity induced by a vortex segment at a point inside the core is zero. The core size is set to half the thickness of the aerofoil. Outside of the core, velocity calculations follow the standard approach.
2. **Rankine**: the velocity induced by a vortex blob is defined as follows:

$$u_\theta = \begin{cases} \Gamma r/(2\pi R^2) & \text{if } r \leq R \\ \Gamma/(2\pi r) & \text{if } r > R \end{cases}$$

   where R is the radius of the vortex core. An equivalent modification is applied to the 'K' factor (see equation 3.22) for vortex segment calculations.
3. **Lamb-Oseen**: this model is based on an exact solution of the Navier-Stokes equations in two dimensions. The azimuth velocity component is found to be

$$u_\theta(r,t) = \frac{\Gamma}{2\pi r}\left(1 - \exp\left(-\frac{r^2}{r_c^2(t)}\right)\right) \tag{9.6}$$

   where r_c is the size of the vortex core, which in this model can change with time. The evolution of the vortex core size is calculated using equation 9.7

$$r_c(t) = \sqrt{4\nu t + r_c(0)^2} \tag{9.7}$$

   where ν is the dynamic viscosity of the fluid, t is the time (since the vortex was created), and $r_c(0)$ is the initial size of the vortex core.

   An equivalent modification is applied to the 'K' factor (see equation 3.22) for vortex segment calculations.

9.4 Saving the results

Under the 'File' tab, there is a drop down menu called 'Save'. Under 'Save', select 'Forces Data (Body Reference Frame)'. This will save the forces acting on each blade element to a .csv file.

The format of this .csv file is as follows: column 1 is the time step, columns two to $Nz+1$ are the x-components of the forces acting on the blade elements of blade 1, the next Nz columns are for the y-components of the forces acting on the blade elements of blade 1, the next Nz columns for the z-components of the forces acting on the blade elements of blade 1. The next Nz are for the x-components of the forces acting on the blade elements of blade 2 etc.